

USAAMRDL-TR-76-14

WEAR-INDICATING ROD END BEARING



**Kaman Aerospace Corporation
Old Windsor Road
Bloomfield, Conn. 06002**

September 1976

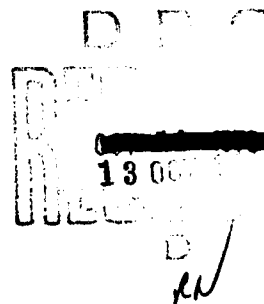
Final Report for Period June 1975 - May 1976

AD A030641

Approved for public release;
distribution unlimited.

Prepared for

**EUSTIS DIRECTORATE
U. S. ARMY AIR MOBILITY RESEARCH AND DEVELOPMENT LABORATORY
Fort Eustis, Va. 23604**



EUSTIS DIRECTORATE POSITION STATEMENT

This investigation is one of a series being conducted by the Eustis Directorate, U. S. Army Air Mobility Research and Development Laboratory, to improve inspection and maintenance techniques on current and future helicopter designs.

This Directorate concurs with the findings of this program that conclude that the wear-indicating rod end (WIRE) is capable of functioning in an operational helicopter environment. The results of the test program indicated that a standard rod end modified to incorporate the indicating device did not show any degradation in wear life, fatigue strength, and Teflon liner condition. The correlation between the actual measured wear and the indicating pin wear was within .001 inch, which indicates great potential for the WIRE concept. Although several deficiencies were discovered during the testing program, none are considered to be serious or to preclude the successful application of the WIRE concept.

Field evaluation of the WIRE concept is planned as a follow-on effort. A limited-life rod end will be selected and modified to incorporate the indicating device. Field monitoring of this evaluation will be collectively accomplished by the Directorate of Maintenance, AVSCOM, and this Directorate.

Mr. John Ariano, Military Operations Technology Division, served as technical monitor for this contract.

DISCLAIMERS

The findings in this report are not to be construed as an official Department of the Army position unless so designated by other authorized documents.

When Government drawings, specifications, or other data are used for any purpose other than in connection with a definitely related Government procurement operation, the United States Government thereby incurs no responsibility nor any obligation whatsoever; and the fact that the Government may have formulated, furnished, or in any way supplied the said drawings, specifications, or other data is not to be regarded by implication or otherwise as in any manner licensing the holder or any other person or corporation, or conveying any rights or permission, to manufacture, use, or sell any patented invention that may in any way be related thereto.

Trade names cited in this report do not constitute an official endorsement or approval of the use of such commercial hardware or software.

DISPOSITION INSTRUCTIONS

Destroy this report when no longer needed. Do not return it to the originator.

Unclassified

SECURITY CLASSIFICATION OF THIS PAGE (When Data Entered)

REPORT DOCUMENTATION PAGE		READ INSTRUCTIONS BEFORE COMPLETING FORM
1. REPORT NUMBER USAAMRL-TR-76-14	2. GOVT ACCESSION NO.	3. RECIPIENT'S CATALOG NUMBER
4. TITLE (and Subtitle) WEAR-INDICATING ROD END BEARING.	5. TYPE OF REPORT & PERIOD COVERED Technical Report, June 1975 - May 1976	6. PERFORMING ORG. REPORT NUMBER R-1455
7. AUTHOR(s) Edward J. Nagy	8. CONTRACT OR GRANT NUMBER(s) DAAJ02-75-C-0031	9. PROGRAM ELEMENT, PROJECT, TASK AREA & WORK UNIT NUMBERS 62209A 1F262209AH76 00 062 EK
10. PERFORMING ORGANIZATION NAME AND ADDRESS Kaman Aerospace Corporation Old Windsor Road Bloomfield, Connecticut 06002	11. CONTROLLING OFFICE NAME AND ADDRESS Eustis Directorate, U.S. Army Air Mobility Research and Development Laboratory, Fort Eustis, Virginia 23604	12. REPORT DATE Sep 1976
13. MONITORING AGENCY NAME & ADDRESS (if different from Controlling Office) DA-1-F-262209-AH-76	14. SECURITY CLASS. (of this report) Unclassified	15. NUMBER OF PAGES 131
16. DISTRIBUTION STATEMENT (of this Report) Approved for public release; distribution unlimited.		17. SECURITY CLASS. (of this report) Unclassified
18. DECLASSIFICATION/DOWNGRADING SCHEDULE		
19. DISTRIBUTION STATEMENT (of the abstract entered in Block 20, if different from Report)		
20. SUPPLEMENTARY NOTES		
21. KEY WORDS (Continue on reverse side if necessary and identify by block number) Rod End Wear Measurement Bearing Teflon-Fabric Wear Dry Lubricated Helicopters Self-Lubricated UH-1		
22. ABSTRACT (Continue on reverse side if necessary and identify by block number) The purpose of this program was to design, analyze, and test a wear-indicating device which will provide a practical, efficient method for the in-place measurement of wear on rod end bearings, commonly called rod ends.		

DD FORM 1 JAN 73 1473 EDITION OF 1 NOV 65 IS OBSOLETE

Unclassified
SECURITY CLASSIFICATION OF THIS PAGE (When Data Entered)

404 362

Unclassified

SECURITY CLASSIFICATION OF THIS PAGE(When Data Entered)

20. ABSTRACT (Continued)

Preliminary design concepts were investigated. Then the chosen design was modified as a result of manufacturing experience and preliminary tests. The final configuration uses a pin entrapped within a bushing which is welded in place in the rod end.

Twenty-six wear-indicating rod end (WIRE) test specimens were fabricated from Government-furnished rod ends, FSN 3120-269-4453, Bell Helicopter Part No. 47-140-252-3. This rod end is used on the damper link on the UH-1 helicopter.

The test program included wear testing in sanitary and hostile environments, fatigue testing, and static testing. The objective was to determine the ability of the WIRE device to function in the helicopter environment and to assess the effect of the device on a standard rod end.

It was found that the WIRE device functions properly in the wear conditions tested, that the wear endurance of the rod end has not been reduced by incorporation of the WIRE device, that the fatigue strength of the standard rod end has not been reduced, and that the ultimate static strength of the standard rod end has been reduced somewhat, which is not considered to be significant because the rod end static strength greatly exceeds that of the mounting bolt.

Service evaluation by ground and flight test in helicopters is recommended.

ACCESSION for	
NTIS	White Section <input checked="" type="checkbox"/>
DOC	Bull Section <input type="checkbox"/>
UNANNOUNCED	<input type="checkbox"/>
JUSTIFICATION	
BY	
DATE	
A	

OCT 13 1976

Unclassified

SECURITY CLASSIFICATION OF THIS PAGE(When Data Entered)

PREFACE

The U.S. Army Air Mobility Research and Development Laboratory (USAAMRDL) supervises research programs aimed at improving helicopter reliability and maintainability. Measurement of rod end bearing wear has been identified as a serious problem by the users of all makes of Army helicopters. A device which adapts the proven flush pin gage technique to the measurement of the rod end internal clearance was invented during Kaman participation in Contract DAAJ02-72-C-0052, "Helicopter Inspection Design Requirements Study". The device was described in USAAMRDL Technical Report 73-221, pages 66, 67, and 68. A patent application was filed on 22 June 1973 entitled, "Apparatus for Measuring Wear of Rod End Bearings", File No. 372666. U.S. Patent 3,845,735 was issued on 5 November 1974. The official report of the invention was submitted to Eustis Directorate via Form DD 882, Report on Inventions and Sub-contracts, on 8 August 1973.

Work on improving helicopter inspection continued under Contract DAAJ02-73-C-0059, Investigation of Inspection Aids, with Kaman participation as reported in USAAMRDL Technical Report 74-442. The Inspection Aids program was addressed to the identification of inspection aids and the experimental evaluation of a specific inspection aid was outside the scope of the Inspection Aids contract. Accordingly, the wear-indicating rod end (WIRE) has been investigated under USAAMRDL Contract DAAJ02-75-C-0031. Technical direction was provided by Mr. John Ariano, Aerospace Engineer, Eustis Directorate, USAAMRDL.

-
- 1 Blake, D. O., Hohn, F. W. and Stareses, Helicopter Inspection Design Requirements, USAAMRDL Technical Report 73-22, Eustis Directorate, U.S. Army Air Mobility Research and Development Laboratory, Fort Eustis, Virginia, May 1973.
 - 2 Cahoon, R. L., Hohn, F. W., McNamee, J. A., Wierenga, B. B., Cook, T. N., Stareses, F. E., Investigation of Inspection Aids, USAAMRDL Technical Report 74-44, Eustis Directorate, U.S. Army Air Mobility Research and Development Laboratory, Fort Eustis, Virginia, July 1974.

This report covers some design considerations, analyses, and bench tests of the WIRE. The test specimens were manufactured at Kaman from Government-furnished rod ends. The program reported herein was accomplished during the period from 6 May 1975 to 19 December 1975. The work was conducted at Kaman Aerospace Corporation, Bloomfield, Connecticut, under the technical supervision of Mr. Edward J. Nagy, Project Engineer. Overall cognizance of the program was maintained by Mr. Robert B. Bossler, Jr., Chief of Mechanical Systems Research.

TABLE OF CONTENTS

	<u>Page</u>
PREFACE	3
LIST OF ILLUSTRATIONS.....	8
LIST OF TABLES.....	12
INTRODUCTION.....	13
DESCRIPTION OF THE WEAR-INDICATING ROD END.....	15
OPERATION.....	15
ADVANTAGES.....	15
WORTH OF SIMPLIFIED ROD END WEAR INSPECTION.....	17
DESIGN AREAS REQUIRING INVESTIGATION.....	17
PRELIMINARY DESIGN AND ANALYSIS.....	18
FINAL DESIGN.....	19
INTRODUCTION.....	19
MATERIAL SELECTION.....	19
A. WEAR-INDICATING PIN.....	19
B. BUSHING.....	20
TEST PROGRAM.....	22
INTRODUCTION.....	22
OBJECTIVE.....	22
TEST SPECIMEN.....	22
TEST PARAMETERS.....	24
A. WEAR TESTS.....	24
1. SANITARY WEAR TESTS.....	25

TABLE OF CONTENTS (Continued)

	<u>Page</u>
2. ENVIRONMENTAL WEAR TESTS.....	25
B. FATIGUE TEST.....	28
C. STATIC TEST.....	28
WEAR TEST RIG.....	28
FATIGUE TEST RIG.....	34
TEST RESULTS.....	37
INTRODUCTION.....	37
PRELIMINARY RESULTS.....	37
FINAL RESULTS.....	40
A. WEAR TEST.....	40
B. FATIGUE TEST.....	65
C. STATIC TEST.....	69
METALLURGICAL EVALUATION OF TESTED BEARINGS.....	73
LINER CONDITION AND BOND INTEGRITY.....	73
DEBRIS RETENTION AND PIN HANG-UP.....	73
OUTWARD MOVEMENT OF WELDED BUSHING ASSEMBLIES.....	75
FAILURE OF WEAR-INDICATING PIN FROM BEARING W18...	75
FATIGUE FAILURES.....	81
ANALYSIS OF STATIC TEST AND FATIGUE TEST RESULTS.....	83
INTRODUCTION.....	83
STATIC TEST RESULTS.....	83
FATIGUE TEST RESULTS.....	83
A. DETERMINATION OF MEAN LOAD-CYCLE CURVE...	83

TABLE OF CONTENTS (Continued)

	<u>Page</u>
B. ENDURANCE LIMIT.....	90
C. DISCUSSION.....	90
D. COMPARISON OF TEST RESULTS AND MEASURED LOADS.....	90
CONCLUSIONS.....	91
CONCLUSIONS.....	92
RECOMMENDATIONS.....	93
APPENDIXES	
A. EVALUATION OF SEVEN PRELIMINARY DESIGNS.....	94
B. WIRE MANUFACTURE.....	109
C. FLIGHT TEST LOADS.....	120
D. WEAR MEASUREMENTS.....	126

LIST OF ILLUSTRATIONS

<u>Figure</u>		<u>Page</u>
1	Wear-Indicating Rod End Bearing.....	16
2	Corrosion Potentials in Flowing Sea Water.....	21
3	Pylon Assembly, Upper Section, UH-1 Helicopter.	23
4	Sanitary and Environmental Test Plan Parameters	26
5	Bearings Before Immersion in Comtaminants a Through f.....	27
6	Wear Test Rig (Plan View).....	29
7	Wear Test Rig (Elevation View).....	30
8	Wear Test Rig (Front).....	31
9	Wear Test Rig (End View).....	32
10	Wear Test Rig (Top).....	33
11	Fatigue Test Rig Schematic.....	35
12	Fatigue Test Rig.....	36
13	Total Liner Wear Vs. Rig Time - WIRE Test Specimen W13.....	39
14	Radial Play Vs. Rig Time - WIRE Test Specimens W1 and W2.....	43
15	Radial Play Vs. Rig Time - WIRE Test Specimens W3 and W4.....	44
16	Radial Play Vs. Rig Time - WIRE Test Specimens W5 and W6.....	45
17	Radial Play Vs. Rig Time - WIRE Test Specimens W7 and W8.....	46
18	Radial Play Vs. Rig Time - WIRE Test Specimens W9 and W10.....	47
19	Radial Play Vs. Rig Time - WIRE Test Specimens W11 and W12.....	48

LIST OF ILLUSTRATIONS (Continued)

<u>Figure</u>		<u>Page</u>
20	Radial Play Vs. Rig Time - WIRE Test Specimen W13.....	49
21	Radial Play Vs. Rig Time - WIRE Test Specimens W14 and W15.....	50
22	Radial Play Vs. Rig Time - WIRE Test Specimens W16 and W17.....	51
23	Radial Play Vs. Rig Time - WIRE Test Specimens W18 and W19.....	52
24	Radial Play Vs. Rig Time - Standard Rod Ends W20 and W21.....	53
25	Liner Wear Vs. Rig Time - WIRE Test Specimens W1 and W2.....	54
26	Liner Wear Vs. Rig Time - WIRE Test Specimens W3 and W4.....	55
27	Liner Wear Vs. Rig Time - WIRE Test Specimens W5 and W6.....	56
28	Liner Wear Vs. Rig Time - WIRE Test Specimens W7 and W8.....	57
29	Liner Wear Vs. Rig Time - WIRE Test Specimens W9 and W10.....	58
30	Liner Wear Vs. Rig Time - WIRE Test Specimens W11 and W12.....	59
31	Liner Wear Vs. Rig Time - WIRE Test Specimen W13.....	60
32	Liner Wear Vs. Rig Time - WIRE Test Specimens W14 and W15.....	61
33	Liner Wear Vs. Rig Time - WIRE Test Specimens W16 and W17.....	62
34	Liner Wear Vs. Rig Time - WIRE Test Specimens W18 and W19.....	63

LIST OF ILLUSTRATIONS (Continued)

<u>Figure</u>		<u>Page</u>
35	Liner Wear Vs. Rig Time - Standard Rod Ends W20 and W21.....	64
36	Load Vs. Deflection - Standard Rod End S3.....	70
37	Load Vs. Deflection - WIRE Test Specimen Sl....	71
38	Photograph of Static Test Failures.....	72
39	Displaced Bushing From Bearing W15.....	76
40	Cross Section of W1.....	78
41	Enlarged View of Electron Beam Weld on Bearing W1	78
42	Cross-Sectional View of Failure of Bearing W18.	79
43	Abnormal Wear Pattern on Pin From W18.....	80
44	Failed Pin on Bearing W18.....	80
45	Fatigue Test Failure Locations.....	82
46	Load Vs. Cycles.....	85
47	Weibull Probability Chart for Bearings F3, F5, and F6.....	89
C-1	Damper Rod Installation on a UH-1H Helicopter..	121
C-2	Main Rotor Slip Ring Installation on Rotor Shaft.....	122
C-3	Onboard Instrumentation Package as Seen From Left Side of Helicopter.....	123
C-4	Damper Rod Load Vs. Bank Angle and Airspeed....	124
C-5	Damper Rod Load Vs. Rate of Climb (Descent)....	125
D-1	Kamatics Wear-Measuring Fixture (KWMF).....	127

LIST OF ILLUSTRATIONS (Continued)

<u>Figure</u>		<u>Page</u>
D-2	Close-up of KWMF, Showing Wire Test Specimen Installed for Measurement.....	128
D-3	Depth Micrometer Measuring System.....	131

LIST OF TABLES

<u>Table</u>		<u>Page</u>
1	Wear Test Summary.....	41
2	Fatigue Test Summary.....	66
3	Pin Hang-up Summary.....	74
4	Measurements of Weld Penetration.....	77
5	Fatigue Test Load-Cycle Summary.....	84
6	Data from Cumulative Damage Analysis.....	87
7	Weibull Analysis.....	88

INTRODUCTION

Rod end bearings are used extensively in helicopters. The conventional rod end bearing consists of a spherical ball mounted in an equatorial band which has a spherical internal surface. The ball is attached to one structural element and the mount to another. The spherical rod end bearing allows limited relative rotation of the two structural elements about the center of the ball. Thus, the device is useful for applications where limited relative rotation about one, two, or three axes must be accommodated. Such locations in a helicopter include control systems, engine mounts, landing gear linkages, door hinges, and other similar applications.

The ball must have internal clearance with respect to its mount so that rotation can take place. However, the internal clearance must remain small to limit control system travel losses and to minimize component damage from shock loads which can develop if excessive free play is present in a system subjected to rapid load reversals. The internal clearance is increased by wear, which can be rapid in some circumstances. Thus, the internal clearance of the rod ends in critical applications must be monitored frequently and accurately. The rod end must be replaced when the allowable limit of internal clearance is approached. On the control systems of Army helicopters, the maximum allowable internal clearance is on the order of 0.020 inch to 0.030 inch. The present method of measurement is by feel or shake while the rod end is installed in the helicopter, or by dial indicator measurement after the rod end is removed from the helicopter. The former is inaccurate; the latter is difficult and time consuming.

A measuring device made by tool and die makers for use by production workers appeared adaptable to the measurement of the internal clearance of rod end bearings. The measuring device is known as a flush pin gage. An example of a flush pin gage application would be to find if the depth of a slot below a reference surface fell within a required tolerance. A block would rest on the reference surface. The block would contain a hole with a sliding pin which can rest on the bottom of the slot. The top of the pin is stepped by the amount of the maximum and minimum tolerance for the depth measurement. For the slot depth to be acceptable, the lower flat on the top of the pin must be below the surface of the block and the upper flat must be above the surface of the block. The pin is read by rubbing the top of the block and pin with a fingertip. A flush pin gage is customarily read to an accuracy of ± 0.001 inch by production workers. Thus, an adaptation of

the flush pin gage technique to standard rod end design could be expected to be sufficiently accurate to monitor the desired maximum internal clearance of the bearing (0.020 to 0.030 inch).

A device which adapts the proven flush pin gage technique to the measurement of the rod end internal clearance is illustrated and discussed immediately following. This report describes the design, analysis and experimental evaluation of the device shown.

DESCRIPTION OF THE WEAR-INDICATING ROD END

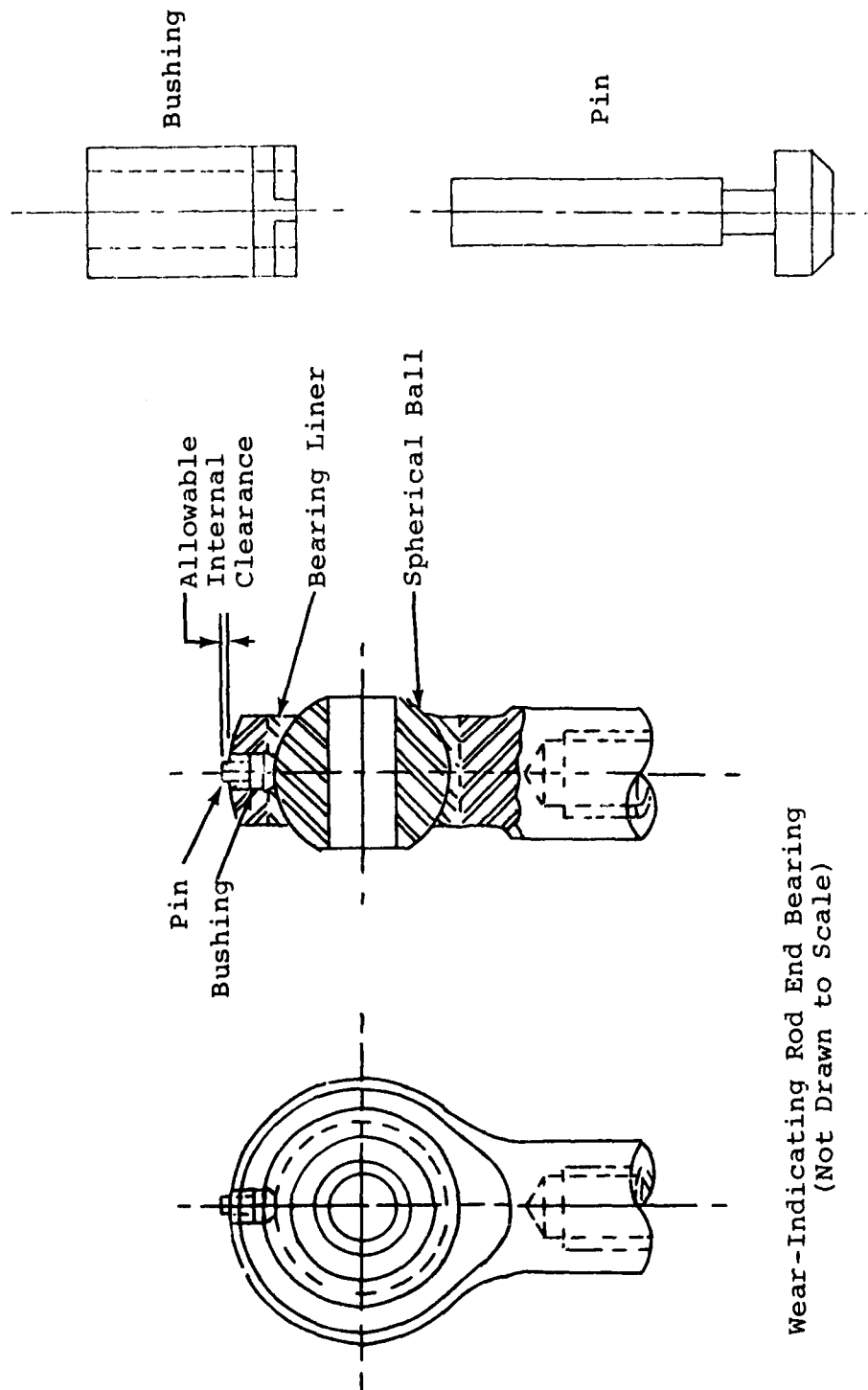
The wear-indicating rod end is illustrated in Figure 1. Greater detail is given in Appendix B, WIRE Manufacture. A measuring pin is permanently trapped in a bushing which is welded in place in the bearing outer race. The pin is restricted from moving outward by a shoulder which contacts the welded bushing. The pin is restricted from moving inward by contact with the spherical ball. The inner surface of the pin coincides with the inner surface of the bearing liner. The pin will be worn the same amount as the bearing liner. The top of the pin protrudes above the adjacent outer surface of the rod end bearing. The long axis of the pin coincides with the long axis of the rod end bearing, which is the axis of applied load and greatest wear. At the time of manufacture the ball is loaded into intimate contact with its spherical seat on the side toward the pin. The protruding portion of the pin is machined off until the pin height above the adjacent surface is equal to or slightly less than the allowable internal clearance.

OPERATION

A mechanic measures rod end bearing wear in the helicopter. The rod end is loaded so that the ball is forced into intimate contact with the spherical seat on the side opposite the pin. The pin is depressed by the mechanic with a bolt, a steel scale, a screwdriver blade or the like. The allowable wear has been exceeded if the pin sinks below the adjacent surface of the rod end.

ADVANTAGES

1. Rod end wear can be measured in place on the helicopter with greater accuracy than present practice.
2. Measurement can be made after simple instruction and does not require skill, training or practice.
3. The measuring device accompanies the rod end and is always ready for use.
4. Wear is measured by feel, so inspection in unlighted areas is not a problem.
5. No change in control system design practice is required by this device.



Wear-Indicating Rod End Bearing
(Not Drawn to Scale)

Figure 1. Wear-Indicating Rod End Bearing.

6. The ability of the device to function can be easily tested by rotating the ball until the bolt hole aligns with the pin. The pin is then depressed below the adjacent surface of the rod end to test freedom of motion. The ball is then rotated to cam the pin back to its normal wear-indicating position.
7. The measuring device does not add weight to conventional rod end bearings.
8. With automated manufacture, the cost of the measuring device should not be significant.
9. Investigation with Army training instructors showed that rod end bearings with this device could be inspected in the most difficult rod end bearing inspection areas on the UH-1, AH-1, OH-6, OH-58 and CH-47 helicopters.

WORTH OF SIMPLIFIED ROD END WEAR INSPECTION

Difficulty of inspection can mean that rod ends are replaced either too soon or too late. Consistently replacing rod ends too soon, which is Kaman's experience with Navy fleet use, carries a cost penalty, which is the installed cost of the rod end prorated to reflect the wasted portion of the rod end life. The cost of not replacing a worn rod end is not easily identified but could be very high. Excess bearing slop in key rod ends results in increased vibration, which reduces the life of many other helicopter components, thus incurring a cost penalty which is large and unknown. Also, safety of flight is jeopardized. An example would be worn rod ends in an engine mount, resulting in excessive drive shaft coupling misalignment, coupling failure, and loss of the complete helicopter.

DESIGN AREAS REQUIRING INVESTIGATION

Some areas were identified that required analytical and experimental investigation.

The pin and/or the hole may require a chamfer to provide space for debris to accumulate if the pin gives a false reading by resting on an accumulation of material trapped in the pin hole between the pin and the spherical ball. The protruding pin must be big enough and tough enough to be not easily worn off or broken. The rod end may require a thicker section around the pin hole if the pin hole were found to increase stress beyond acceptable limits.

PRELIMINARY DESIGN AND ANALYSIS

Seven design concepts were evaluated. These concepts are shown in Appendix A. Included for each concept is a description of the design plus listings of advantages and disadvantages for each. The final two pages of the appendix include a summary of the seven designs and a rating table which was used to evaluate the relative merits of each design concept. The six evaluation factors used were:

1. Relative Difficulty of Machining.
2. Effect on Banjo Strength.
3. Murphy-proof Pin Retention.
4. Debris Cavity Adjacent to the Pin/Ball Contact.
5. Possible Mechanical Failure.
6. Possible Misinterpretation.

A numerical rating system was used wherein equal weight was used for all six factors, and the numerical rates assigned to each concept for each evaluation factor could range from a minimum of 2 to a maximum of 10 in steps of 2. The lowest score denotes the best design.

Design Number 7 was chosen to be the candidate for the final design phase, even though this particular design entails the most difficulty in machining.

FINAL DESIGN

INTRODUCTION

A series of preliminary designs was drawn and analyzed. This work is reported in the Preliminary Design section and Appendix A of this report. The design selected for the final design phase was refined by detail design, preliminary test, manufacturing investigation, and experience gained in the initial phases of the test program. The final design is reported in Appendix B, WIRE Manufacture, and the information given therein is believed to be sufficient for future WIRE production.

MATERIAL SELECTION

A. Wear-Indicating Pin

Material selection for the pin was based on the following requirements:

1. The pin material must be removed by sliding wear on an AISI 440C stainless steel ball with a hardness of Rockwell C58.
2. The pin material must machine well.
3. The pin material must be tough and durable.
4. The pin material must have good bending and shear strength.
5. The pin material must not gall or seize when sliding under load on an AISI 440C stainless steel ball.
6. The pin material must be corrosion resistant.
7. The pin material must have a low galvanic corrosion potential with respect to AISI 4130 steel (rod end banjo) and stainless steel (AISI 440C ball, AISI 410C race, AMS5613, 410 cres. bushing).

The material selected was beryllium copper, CA 173 Condition H. This material has good wear characteristics. It provides differential material with respect to the ball, which is a known method of avoiding seizing and galling. The material was heat treated to 112,000 psi minimum tensile strength, which provides good strength characteristics. At this hardness level (Rockwell C20), the beryllium copper is softer than

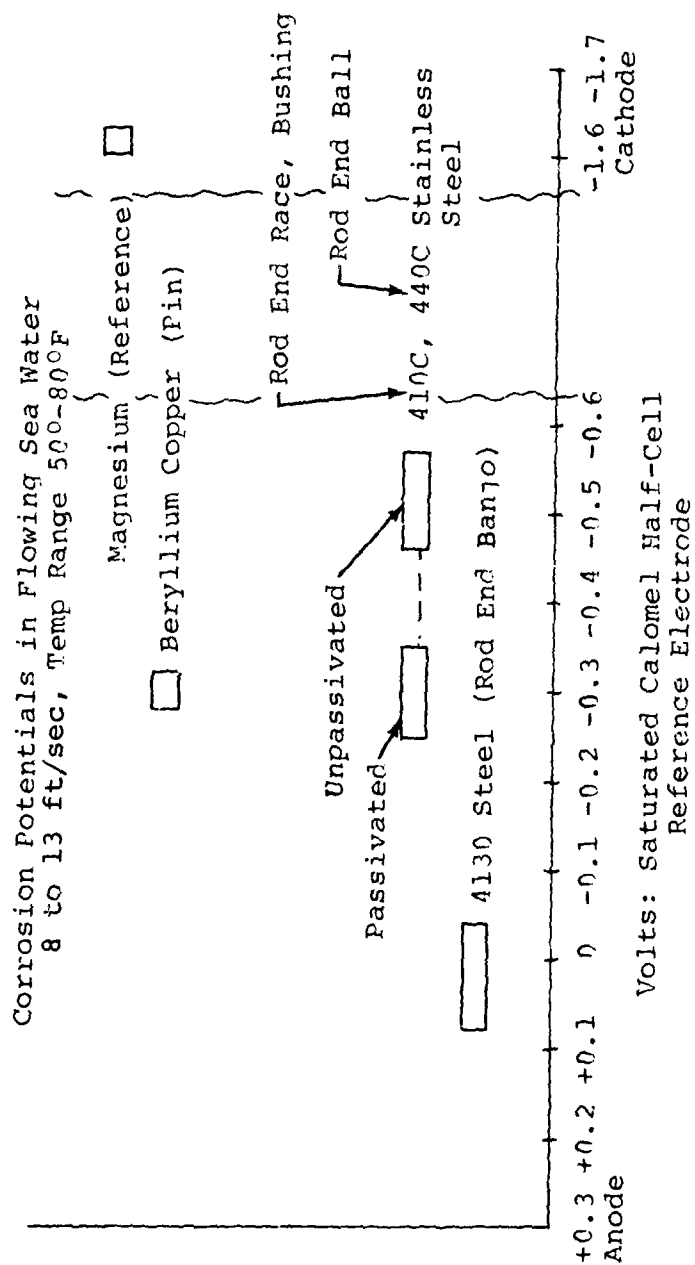
the ball and is the sacrificial wearing member. Also, the beryllium copper machines freely and is corrosion resistant.

In the galvanic series, the beryllium copper is slightly anodic to the encapsulating bushing, the bearing race, and the ball. It is slightly cathodic to the rod end banjo. The galvanic relationship between beryllium copper and the adjacent bearing component materials is shown in Figure 2, Corrosion Potentials in Flowing Sea Water.

B. Bushing

The material selected for the bushing was 410 corrosion resistant stainless steel per AMS 5613, heat treated to 133,000 psi minimum tensile strength (Rockwell C28-36). This material has good bending and shear strength, is a different material from the pin which avoids seizing and galling, machines freely, is corrosion resistant, and has low galvanic corrosion potential with respect to adjacent materials.

This bushing material also has an additional important characteristic. It provides a very compatible combination for electron beam welding with the AISI 4130 steel rod end banjo.



Note: In this figure, beryllium copper has been added to data taken from Nickel Topics, volume 23, No. 3, Marine Materials, page 7.

Figure 2. Corrosion Potentials in Flowing Sea Water.

TEST PROGRAM

INTRODUCTION

In order to investigate the feasibility of the wear-indicating rod end device and to evaluate its applicability to installation on standard GFE rod ends, wear-indicating rod ends were manufactured, a test plan was developed, and tests were conducted.

OBJECTIVE

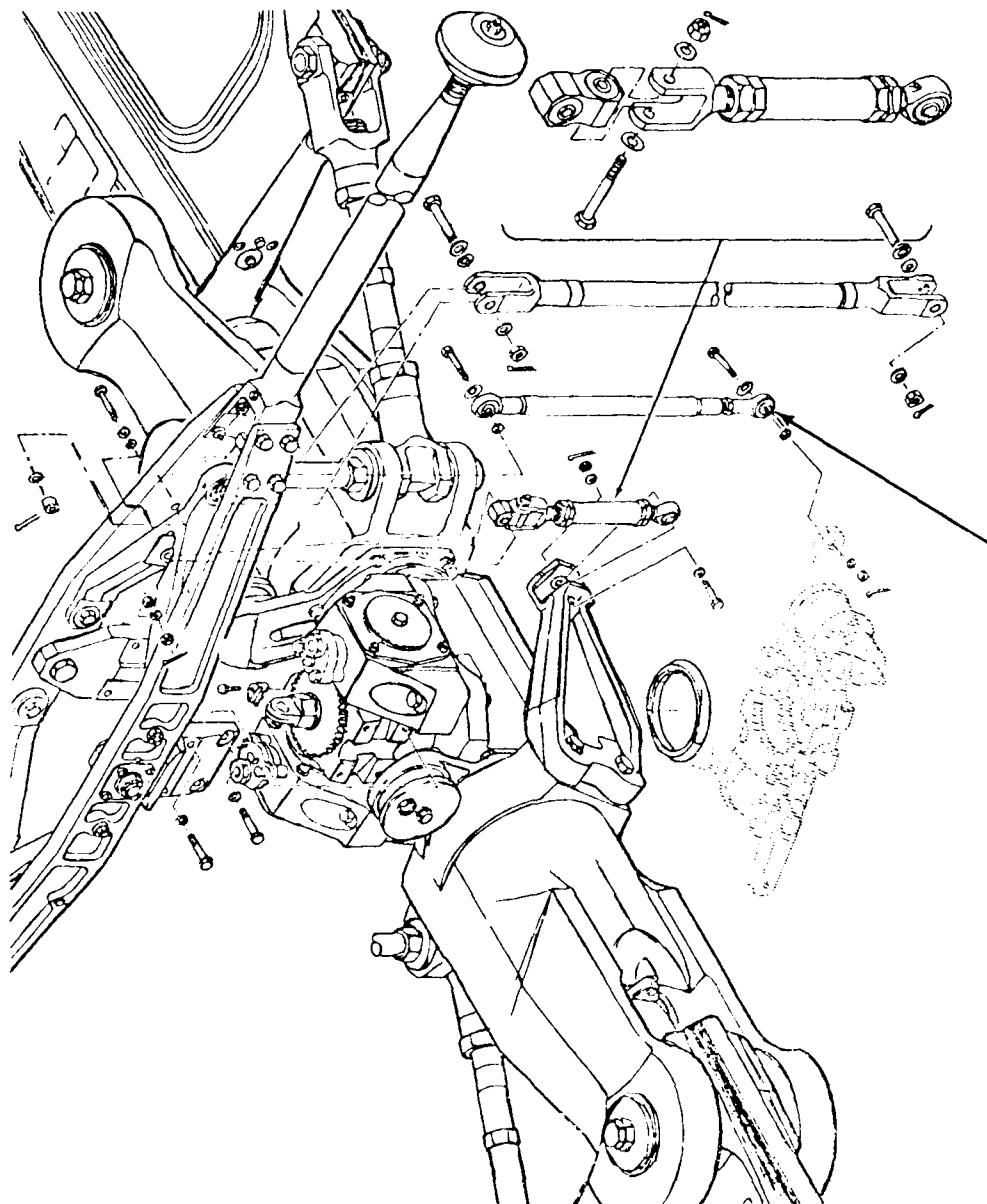
The overall test objective was to determine the ability of the wear-indicating device to function in the helicopter environment and to assess the effect of the device on a standard rod end. Specific test objectives were:

1. Comparison of indicated wear versus actual wear in a sanitary environment.
2. Measurement of effective performance in hostile environments.
3. Determination of the fatigue strength of the rod ends with the wear-measuring device installed.
4. Comparison of the ultimate static strength of the wear-indicating rod end with a standard rod end.

TEST SPECIMEN

The test specimens were 26 wear-indicating rod ends (WIRE). These test specimens were fabricated from 30 Government-furnished rod ends, FSN 3120-269-4453, Bell Helicopter Part No. 47-140-252-3. This rod end is used on the lower end of the damper link assembly as shown on Figure 165 from TM-55-1520-210-34P, a copy of which is reproduced in Figure 3. This rod end was chosen as the GFE test specimen for the following reasons:

1. The test program will qualify the WIRE concept for experimental flight test. Therefore, a rod end with an actual helicopter application should be selected so that a flight test program can follow immediately.
2. The selected rod end is visible from the ground and can be inspected from the outside of the helicopter.



Selected Test Specimen

Figure 3. Pylon Assembly, Upper Section, UH-1 Helicopter.

No disassembly is required.

3. The allowable internal clearance (0.012 in.) is smaller than the allowable internal clearance for many other rod ends (0.020 to 0.030 in.), representing a more difficult application.
4. The operating load is fully reversed so that both sides of the rod end should wear equally. This application tests the ability of the device to measure true internal clearance regardless of the wear zone.
5. The measured load on the rod end in service (± 5 to 10 pounds, transients to ± 33 to 38 pounds) is much lower than the test load (± 600 pounds), providing a very high factor of safety. The derivation of the test load is discussed elsewhere.
6. The damper link application is believed to be not critical to survival, i.e., loss of a rod end in experimental flight test would not necessarily mean loss of an aircraft.

TEST PARAMETERS

The test specimens were tested for sanitary wear, environmental wear, fatigue strength, and static strength. Each of these four major categories of testing is discussed in detail in the following subparagraphs.

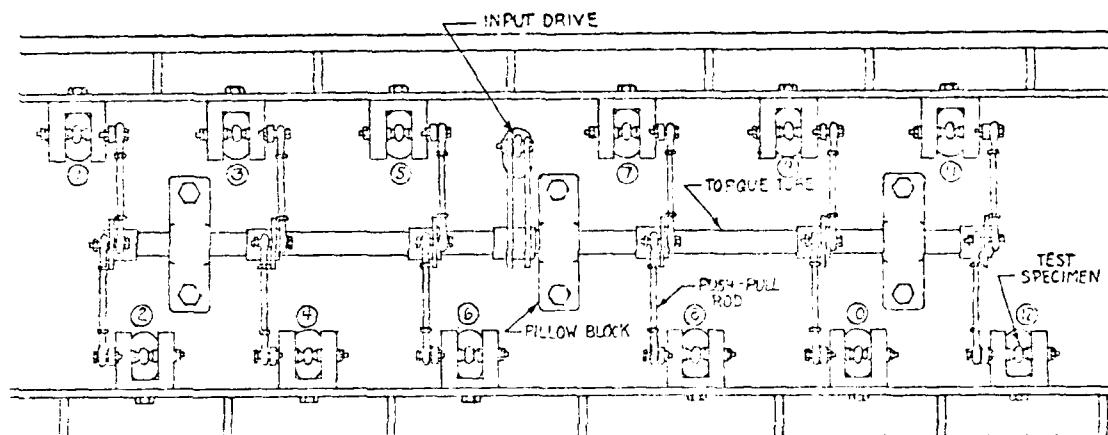
A. Wear Tests - The wear tests consisted of both sanitary wear tests and environmental wear tests. The wear test rig, described later, was utilized for all these tests. All sanitary and environmental wear testing basically consisted of in-plane oscillation of the ball with a constant radial load maintained for 4 hours in tension, then 4 hours in compression, and continually reversed every 4 hours for the duration of the testing. The ball was oscillated through an angle of $\pm 10^\circ$ minimum (a total of 40° minimum angular travel per cycle of oscillation). The radial wear test load was 600 pounds tension or compression. The wear test load was calculated by the formula in Table II, MIL-B-81819 Proposed, revision of February 1974. Therein the dynamic test load = (2000 psi) (ball diameter) (outer race width) = (2000) (0.688) (0.42) = 578 pounds, rounded off to 600 pounds. This load also met the WIRE wear test requirement of causing wearout in 400 hours or less. The

frequency of oscillation was 5.4 hertz, which is the oscillating frequency of the damper link in service. Figure 4 presents a summary of the sanitary and environmental wear test parameters. The number of bearings tested is discussed below.

1. Sanitary Wear Tests - Seven WIRE test specimens were tested for a total of 400 test rig hours each or to malfunction. Rod ends which wore to tolerance limit or malfunction were replaced. Two standard rod ends were tested for a total of 200 test rig hours.
2. Environmental Wear Tests - Twelve WIRE test specimens were exposed to environmental condition and contaminants as follows:

	<u>Number of WIRE Test Specimens</u>
a. Skydrol 500A Hydraulic Fluid	1
b. TT-S-735 Type VII Standard Test Fluid	1
c. MIL-L-7808 Lubricating Oil	1
d. MIL-H-5606 Hydraulic Oil	1
e. MIL-A-8243 Anti-Icing Fluid	1
f. P-D-680 Type I Dry Cleaning Solvent	1
g. Salt Water, 5% by Weight	2
h. Arizona Road Dust (AC Spark Plug P/N 1543094)	2
i. Temperature Extremes + Distilled Water	2

For testing with (a) Skydrol 500A Hydraulic Fluid, (c) MIL-L-7808 Lubricating Oil, (d) MIL-H-5606 Hydraulic Oil, (e) MIL-A-8243 Anti-Icing Fluid, and (f) P-D-680 Type I Dry Cleaning Solvent, the particular test specimen was immersed in the corresponding fluid for 24 hours at 160° ± 5°F. For contaminant (b), TT-S-735 Type VII Standard Test Fluid, the test specimen was immersed for 24 hours at 110° ± 5%. For contaminants (a) through (f), the wear test was started within 1/2 hour after removal from the fluid and continued for 200 hours without any additional contamination. Figure 5 shows the bearings before immersion in contaminants (a) through (f).



LOADS

600 pounds tension or compression load reversed every 4 hours

SPEED OF OSCILLATION

5.4 hertz

ANGLE

$\pm 10^\circ$ minimum

DURATION

Sanitary wear tests: failure or 400 hours

Environmental tests: failure or 200 hours

MICROMETER INSPECTIONS

100 hr measure $\pm .001$, clean, remeasure

400 hr measure $\pm .001$, clean, remeasure (one specimen)

ENVIRONMENT

Sanitary wear tests: Bay 1 - 6 room ambient (7) + 2 standard
 Bays 7 & 8 skydrol (1) and TT-S-735(1)
 salt water (2)
 Bays 9 & 10 MIL-L-7808(1) & MIL-H-5606(1)
 Arizona Road Dust (2)
 Bays 11 & 12 MIL-A-8243(1) and P-D-680(1)
 Temperature Extremes +
 Water (2)

STEADY COMPRESSION OR TENSION LOAD REVERSED AT 4-HOUR
 INTERVALS - VISUALLY INSPECT FOR FAILURE

Figure 4. Sanitary and Environmental Test Plan Parameters.



Figure 5. Bearings Before Immersion in Contaminants a through f.

For contamination (g), salt water, the WIRE test specimens were contaminated by spraying both sides of the specimen every hour of the test run and while the balls were being oscillated. For contaminant (h), Arizona Road Dust, the WIRE test specimens were contaminated by dusting both sides of the specimens every hour of the test run while the balls were being oscillated.

For condition (i), temperature extremes plus distilled water, the WIRE test specimens were soaked in an air circulating oven at or above 160°F for 4 hours, then soaked for an additional 4 hours at or below -65°F, and finally sprayed with distilled water on each side at every hour of the test run while the ball was being oscillated.

B. Fatigue Test - Six WIRE test specimens, F1 through F6, were tested in the fatigue test rig at a frequency of 70 hertz. The alternating radial load was to be ± 600 pounds or the highest load measured in flight, whichever was higher. As shown in Appendix C, the loads measured in flight were considerably lower than ± 600 pounds. Each bearing was to be removed from the test rig after failure or completion of 30 million fatigue cycles. As discussed later in this report, the ± 600 -pound load proved to be too low, and all six bearings were eventually tested at higher loadings for the purpose of failure mode determination.

C. Static Test - One standard rod end, FSN 3120-269-4453, Part NO. 47-140-252-3, specimen S3, and one WIRE test specimen, S1, were each tested to failure in tension loading in a Tinius Olsen testing machine.

WEAR TEST RIG

As shown in Figures 6 through 10, the wear test rig consisted of twelve individual test stations. Each test station had provisions for testing one WIRE test specimen. The WIRE test specimens were positioned midway between two heavy-duty rig bearings. A suitable-length NAS 464-4 bolt was used to clamp two bushings against the ball of the bearing and to provide the radial load path.

Radial load (either tension or compression) was provided by a deadweight (one for each test station) which applied the constant radial load through a compound mechanical multiplication

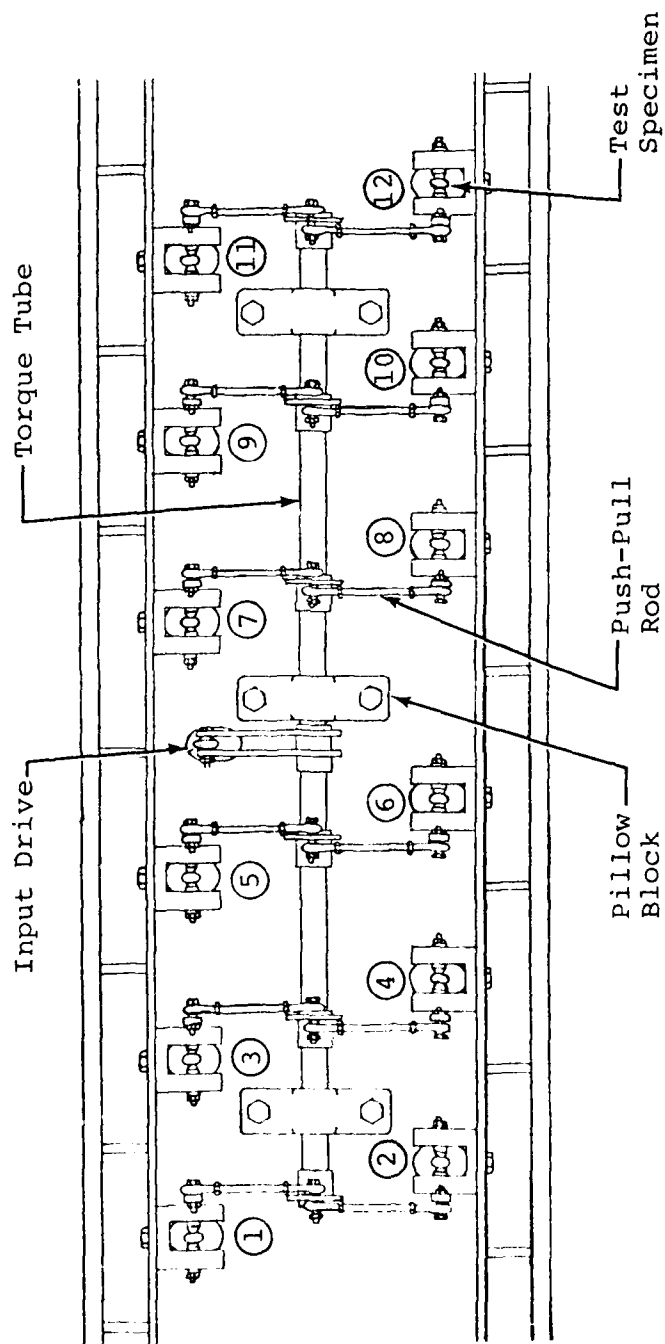


Figure 6. Wear Test Rig (Plan View).

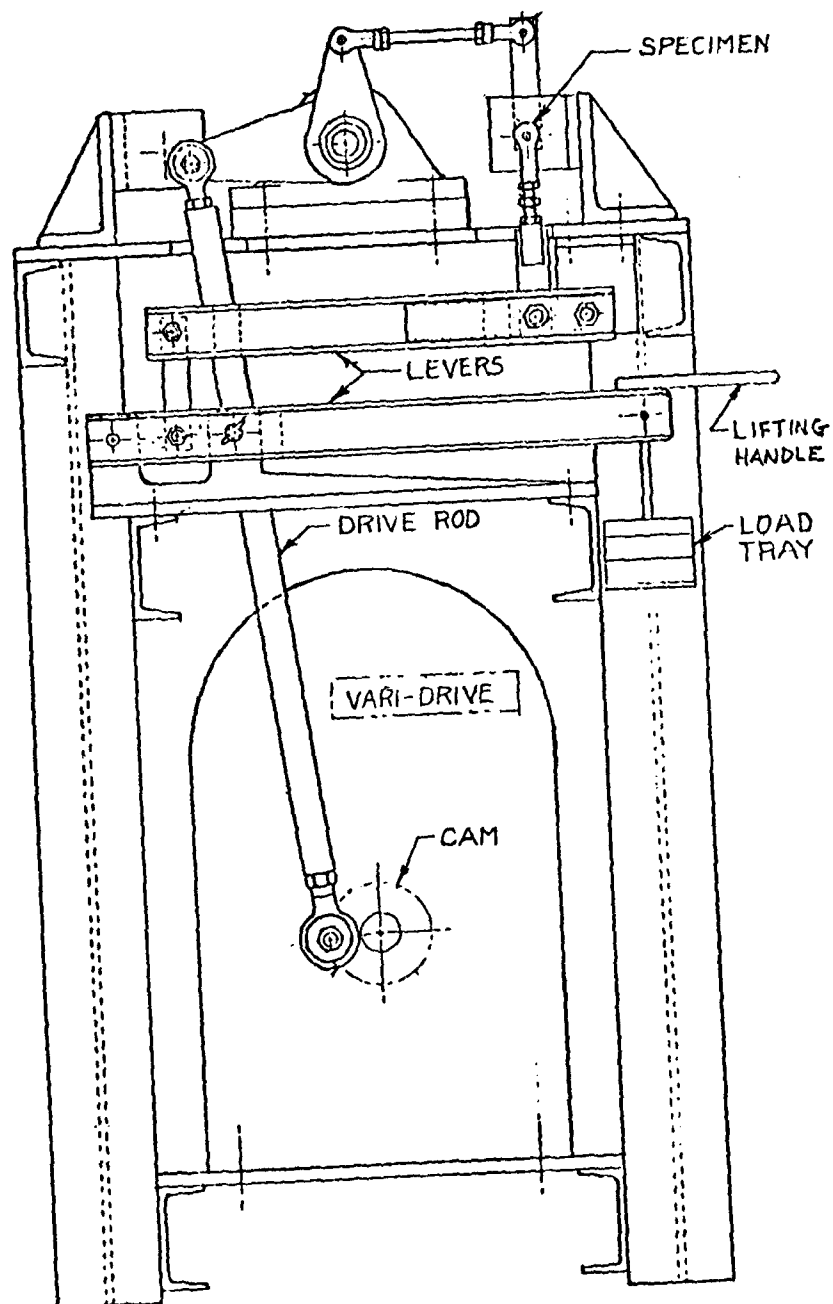


Figure 7. Wear Test Rig (Elevation View).

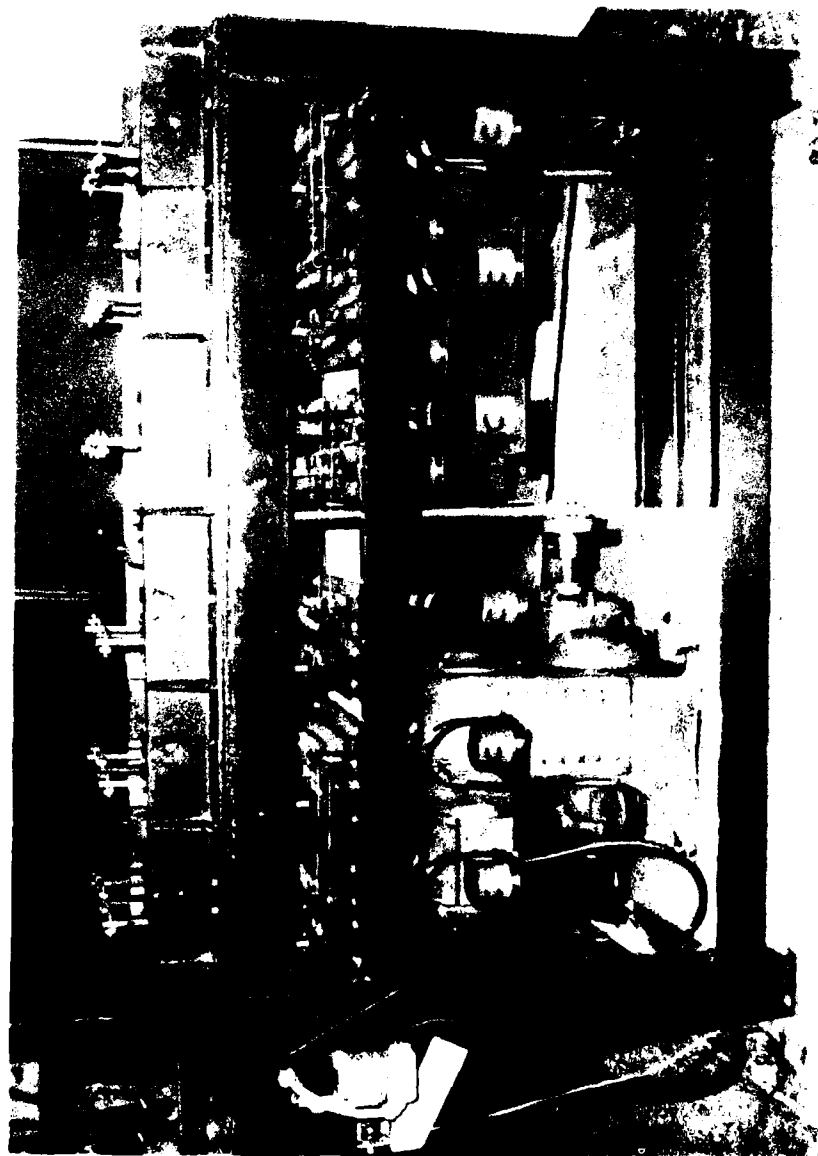


Figure 8. Wear Test Rig (Front).

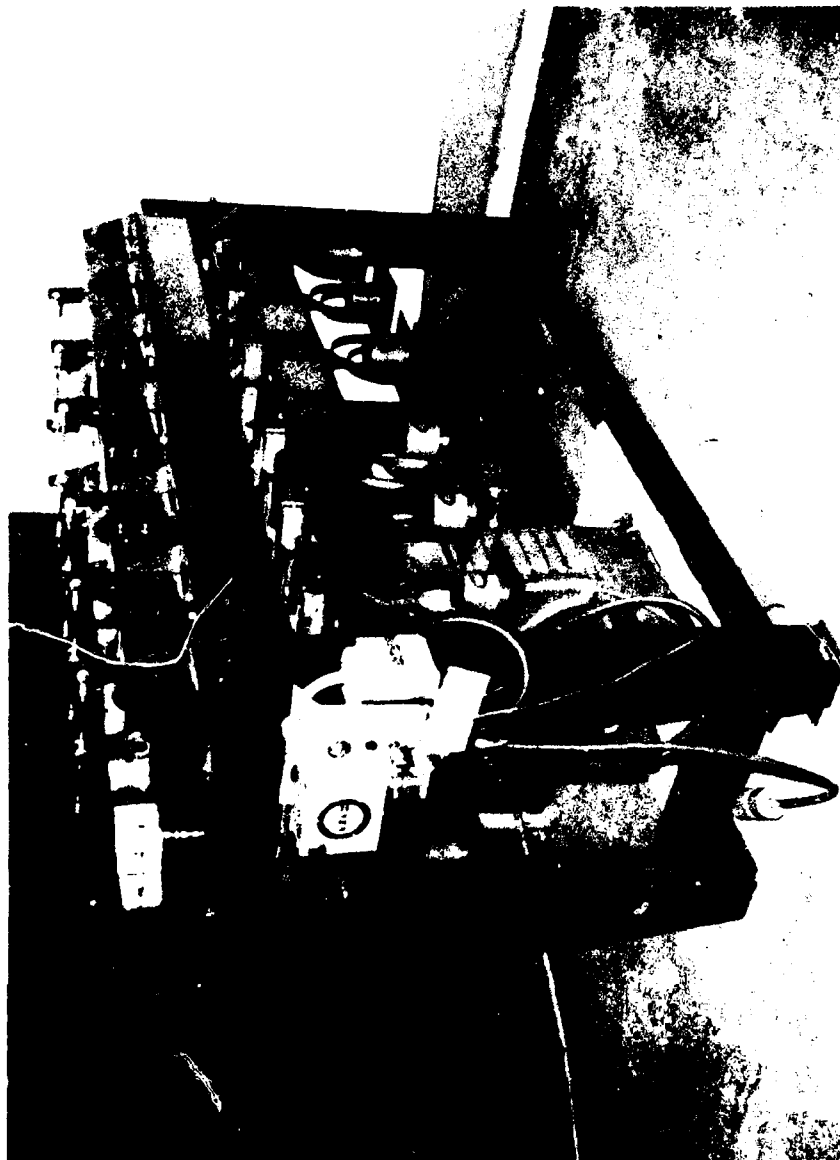


Figure 9. Wear Test Rig (End View).

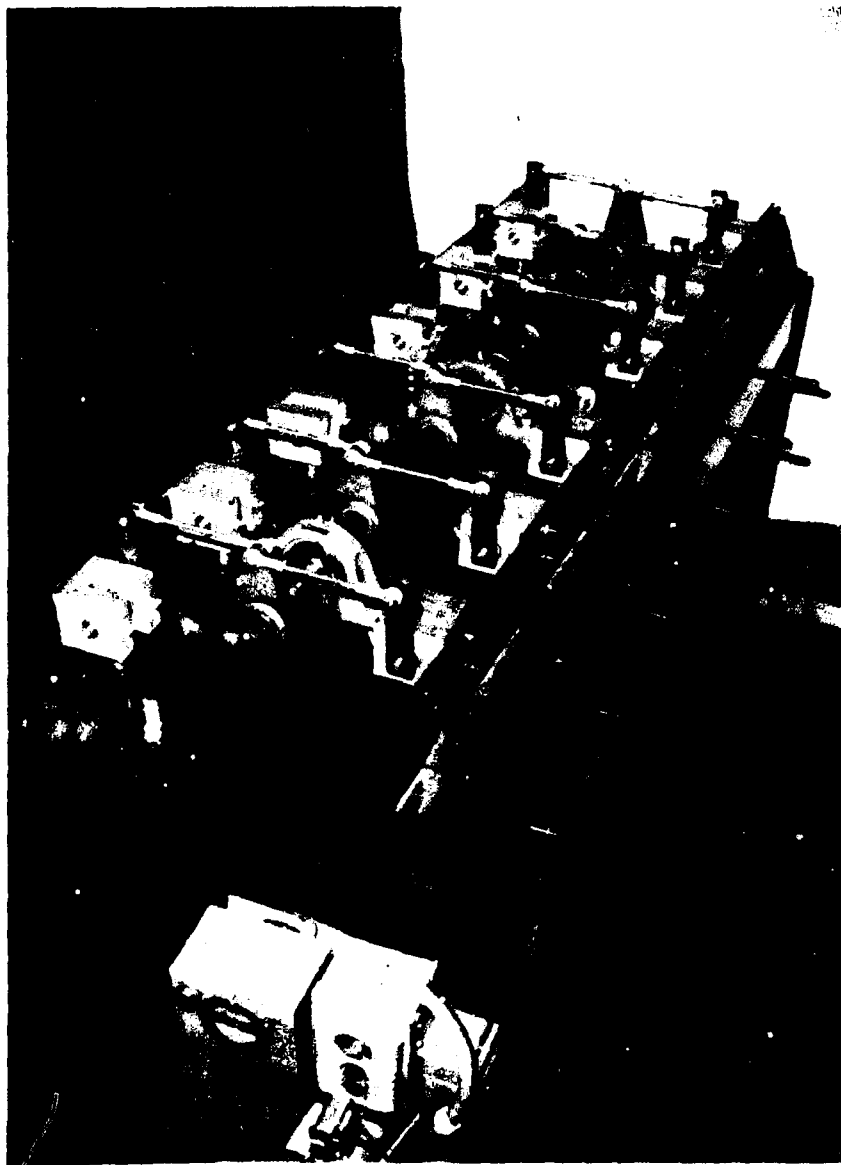


Figure 10. Wear Test Rig (Top).

linkage. A pip pin arrangement allowed easy reversal of the direction of the constant radial load.

The WIRE test specimen at each test station was thus radially loaded and held stationary while the ball was oscillated through the required angle by a torque arm which was also part of the aforementioned bolt-bushing-ball stackup. Each torque arm was attached to a common oscillating shaft which was driven by one power source. Thus, the oscillating motion for all 12 test stations was derived from one vari-drive electric motor.

FATIGUE TEST RIG

The fatigue test rig was mounted above a conventional electromagnetic shaker and utilized the oscillatory vertical motion of the exciter head to provide the necessary vibratory radial loading to the WIRE test specimens. Two WIRE test specimens were tested simultaneously, with one WIRE attached to the loading head of the exciter and the second WIRE attached to the stationary load reaction structure. Linear bearings were utilized to retain the entire loading path in a coincident straight loading line. See Figures 11 and 12 for further details.

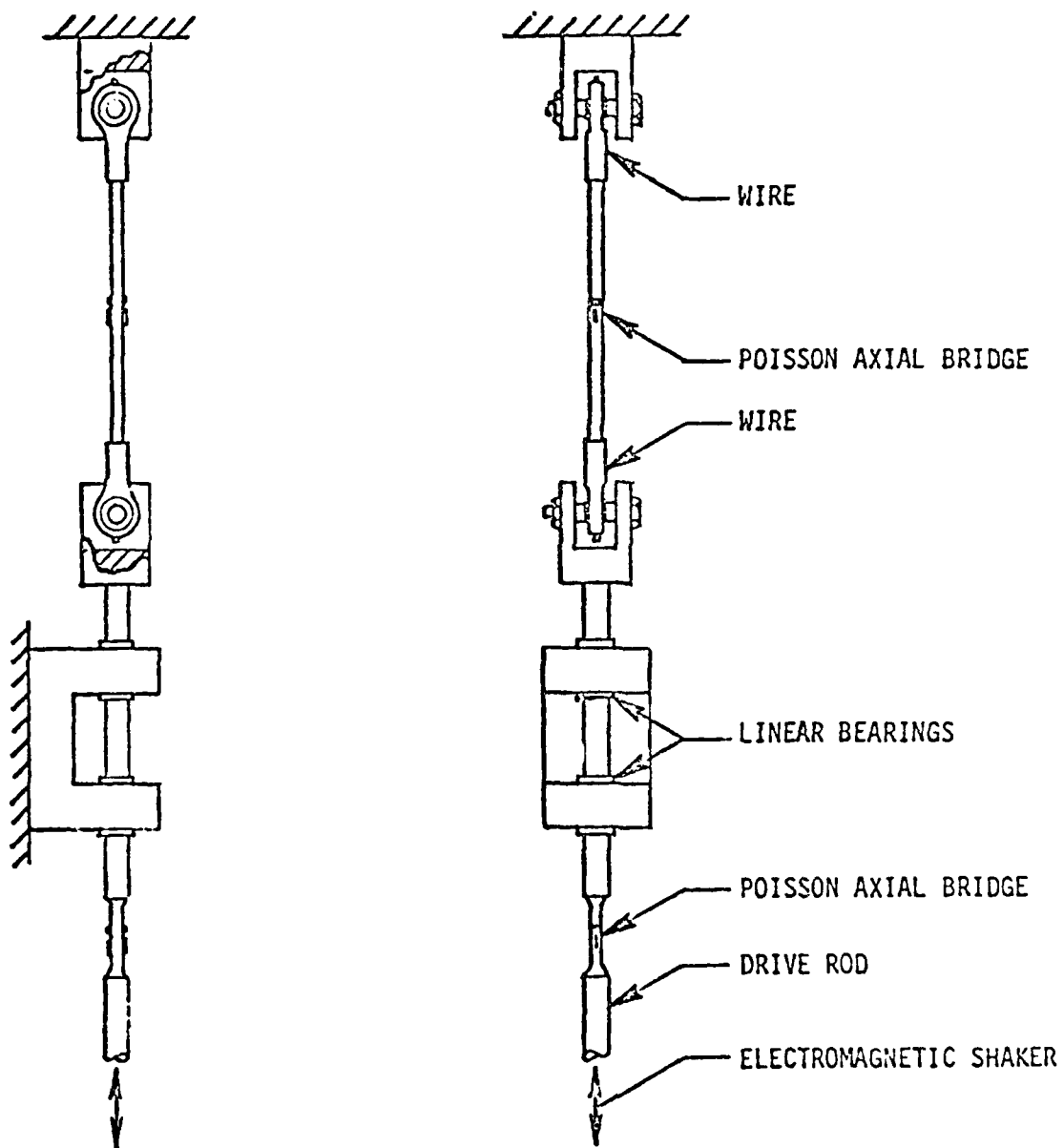


Figure 11. Fatigue Test Rig Schematic.

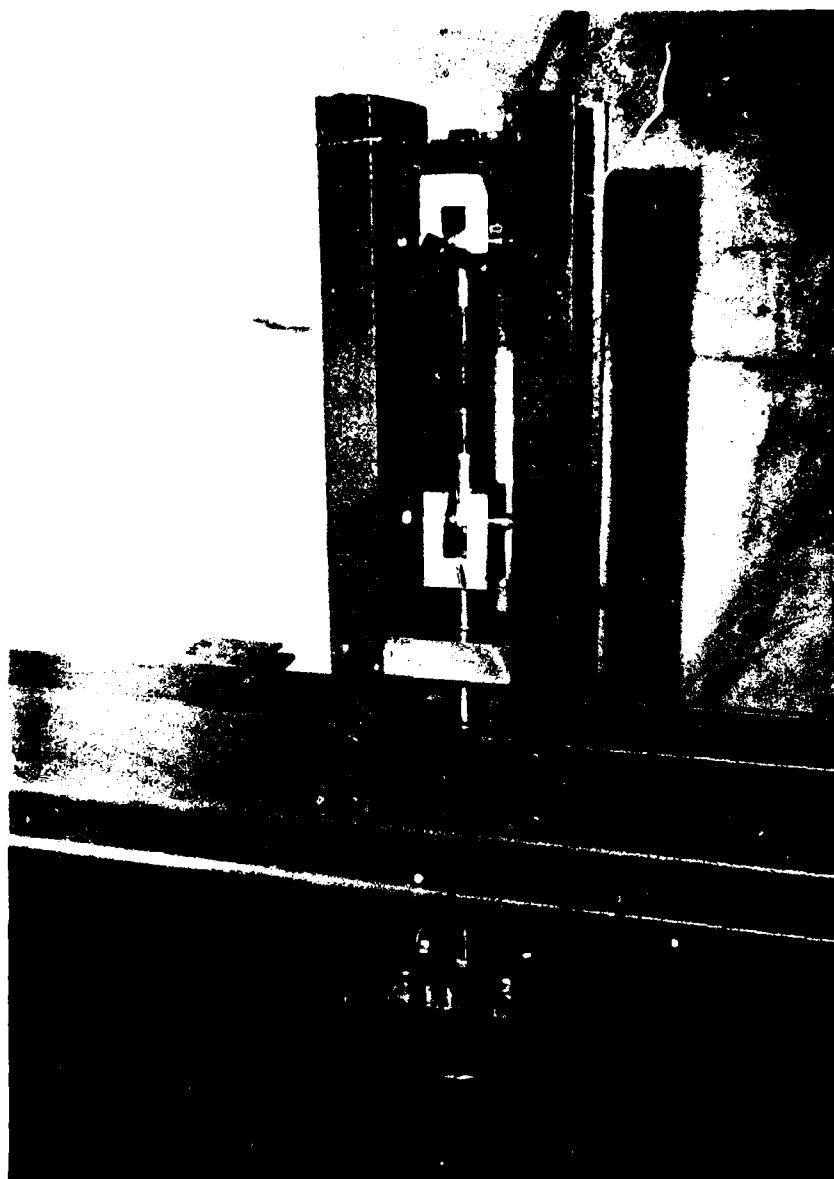


Figure 12. Fatigue Test Rig.

TEST RESULTS

INTRODUCTION

Twenty six WIRE test specimens were manufactured. Six of these specimens were assembled without a wear measuring pin and were reserved for fatigue test. Two of these six bearings, F1 and F2, were installed in the fatigue test rig, and testing at ± 600 pounds and 70 hertz was started. Almost immediately, it was noticed that the bushing assemblies were moving outward with respect to the rod end banjo. Testing was continued because it was decided that bushing movement would not detract from the prime target of determination of rod end fatigue strength.

Twelve of the remaining bearings, W1 through W12, were prepared for installation in the wear test rig. Sanitary wear test specimens W1, W2, W3, W4, W5, and W6 were installed in bays 1, 2, 3, 4, 5, and 6, respectively. Contaminated wear test specimens W7, W8, W9, W10, W11, and W12 were installed in bays 7, 8, 9, 10, 11, and 12, respectively. All twelve bearings were tested for 4 hours in tension and 4 hours in compression using a radial load of 600 pounds with an oscillatory angle of $\pm 10^\circ$ at a frequency of 5.4 hertz.

PRELIMINARY RESULTS

After completion of the above-mentioned testing, all bearings except bearing W12 exhibited outward movement of the wear-indicating bushing assembly from the rod end. This outward movement has the effect of negating indicator pin wear and results in nonconservative indications of wear from the wear-indicating device. The outward movement of the bushing was a direct result of lack of positive mechanical retainment of the bushing. The interference fit of the bushing in the drilled hole plus the use of Loctite retaining compound was not adequate to react 600 pounds of radial load. The 600 pounds of radial load can conceivably be applied to the pin when the Teflon liner elastically deforms in its normal manner under the tension loading. Bushing pushout tests had shown that approximately 200 pounds was the maximum load that this type of retention would sustain.

Preliminary results from test bearings W1 through W12 indicated that the wear-indicating pin wear may have been less than the Teflon liner wear and, if true, would result in incorrect

function of the wear-indicating system. These results were not conclusive because of the bushing movement. There was also some concern as to the validity of the testing condition being used for the wear testing. The intent was to have a testing condition which would develop approximately 0.012 inch of wear for 400 hours of sanitary wear testing.

It was suggested that adequate bushing retainment could be obtained by electron beam welding the bushing in the rod end. Therefore, the decision was made to electron beam weld WIRE specimen W13 and to wear test the bearing in order to determine the following:

- a. If the electron-beam-welded bushing assembly could withstand the 600-pound radial load.
- b. If the indicating pin would wear properly.
- c. If the testing condition of 600 pounds, $\pm 10^\circ$, and 5.4 hertz produced adequate wear in 400 hours.

WIRE test specimen W13 was tested in bay 11 for a total of 44 hours in tension and 44 hours in compression, a total of 88 hours. Values of total liner wear (which is a summation of the liner wear occurring on the indicating pin side of the bearing and the liner wear occurring on the side opposite the indicating pin) were plotted versus test hours as shown in Figure 13. This plot indicated that the expected high initial wear rate occurred in the first 30 hours of running, and a constant wear rate of .0022 inch per 100 hours prevailed for the remaining 58 test hours. Also, extrapolating the wear curve to 100 hours as shown on Figure 13 resulted in a predicted total wear of 0.00505 inch for the first 100 hours of running; assuming .0022 inch per 100 hours constant wear rate for an additional 300 hours, the total wear on bearing W13 would be 0.0116 inch for a test run of 400 hours. Since 0.0120 inch was the specified radial play on this particular bearing, it followed that the 600-pound radial load, 5.4-hertz oscillation frequency condition was reasonable for the 400-hour sanitary wear testing to be performed on bearings W1 through W6.

The results of test specimen W13 indicated that the electron beam welding of the wear-indicating bushing was adequate and that the beryllium copper wear-indicating pin was functioning properly. The decision was then made to rework test bearings W1 through W12 to incorporate an electron-beam-welded wear-indicating bushing assembly and to electron beam weld the bushings

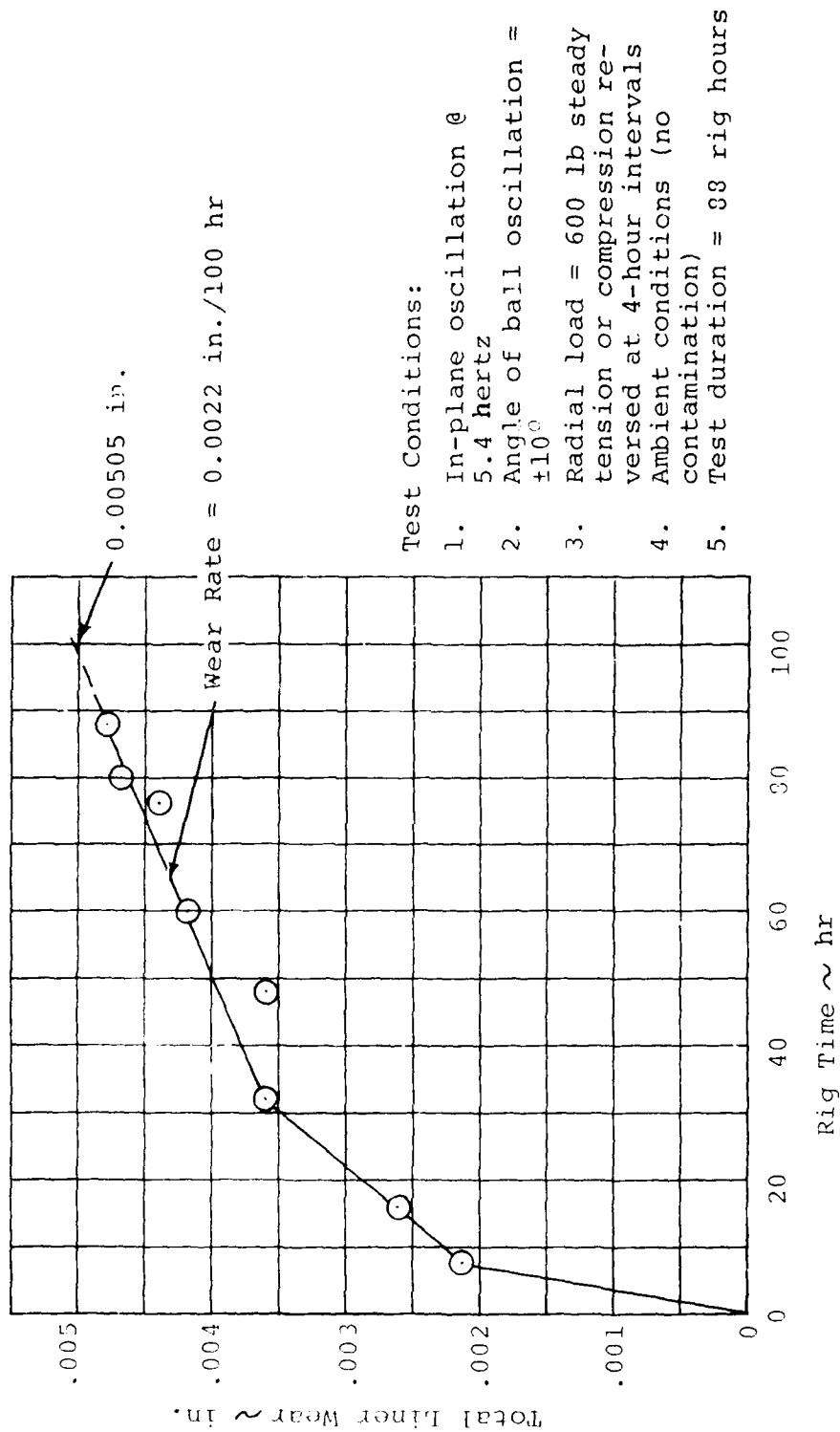


Figure 13. Total Liner Wear vs. Rig Time - WIRE Test Specimen W13.

in bearings W14, W15, F3, F4, F5, F6, and S1. This was done.

After ultrasonically cleaning, each of the WIRE wear test specimens, W1 through W12, was installed in the Kamatics wear measuring fixture for determination of the new initial wear tare readings. WIRE specimens W7 through W12 were immersed in their respective contaminating fluids, and 24 hours later wear testing of sanitary bearings W1 through W6 and environmental bearings W7 through W12 was restarted. (Note that it was decided to reset the test hour clock back to zero and measure all future test time from this new zero reference.)

FINAL RESULTS

A. Wear Test

A total of 19 WIRE test specimens and 2 standard test specimens were tested in the wear test rig. Table 1 is a summary of the bearings tested, the test conditions, and the total number of hours each bearing was tested. Figures 14 through 23 are plots of radial play in inches versus rig time in hours for each of the 19 WIRE wear test specimens, W1 through W19. The plots for each of the 19 bearings present a comparison of the radial play readings as determined from the Kamatics wear measuring fixture (KWMF) to the indicated radial play as determined from the wear-indicating device. Figure 24 presents plots of KWMF radial play readings in inches versus rig time in hours for standard rod ends, W20 and W21.

It is significant to note that in almost all 19 plots, the wear-indicating device tends to give nonconservative play readings. (In other words, the wear-indicating device has a tendency to register lower play than the KWMF radial play.) This discrepancy can be on the order of 0.002 inch at the worst and is usually closer to 0.001 inch.

This is not true for the initial reading at zero rig hours. For all bearings except W11, which had exact agreement between indicated and KWMF play, the wear-indicating device indicated more play before testing began by approximately 0.001 inch. This was caused by the use of 600 pounds for obtaining wear readings with the wear-indicating device, while only using 50 pounds for obtaining wear readings with the Kamatics wear measuring fixture. (Appendix D describes the wear-measuring methods and the measuring loads used.)

TABLE 1. WEAR TEST SUMMARY

<u>DESIGNATION</u>	<u>BEARING TYPE</u>	<u>TEST CONDITION (CONTAMINANT)</u>	<u>CLEANED</u>	<u>TOTAL HOURS TESTED</u>
W1	WIRE	Room Ambient	After 400 Hr	400
W2	"	" "	Every 100 Hr	"
W3	"	" "	" " "	"
W4	"	" "	" " "	200
W5	"	" "	" " "	400
W6	"	" "	" " "	"
W7	"	Skydrol 500A	No	200
W8	"	TT-S-735, Type VII	"	"
W9	"	MIL-L-7808	"	"
W10	"	MIL-H-5606	"	"
W11	"	MIL-A-8243	"	"
W12	"	P-D-680, Type I	"	"
W13	"	Room Ambient	Every 100 Hr	400
W14	"	Arizona Road Dust	No	148
W15	"	" " "	"	152
W16	"	Temp. Extremes and Distilled Water	"	200
W17	"	Salt Water	"	"
W18	"	Temp. Extremes and Distilled Water	"	"
W19	"	Salt Water	"	"
W20	Standard	Room Ambient	Every 100 Hr	"
W21	"	" "	" " "	"

For the unworn Teflon liner, the difference in deflection of the liner at 50 pounds and 600 pounds is significant. After the first 100 hours of testing, the Teflon liner had worn sufficiently to negate any major deflection differences of the liner between 50 pounds and 600 pounds.

Figures 25 through 35 are plots of liner wear in inches versus rig time in hours for bearings W1 through W21. Each plot is for one bearing and presents the wear of the liner on the pin side of the liner, the liner wear on the side opposite the wear-measuring pin, and the total liner wear. For sanitary wear test bearings W1 through W6, the wear on the side opposite the pin was higher for all bearings.

For the six bearings contaminated with the fluids, W7, W9, and W12 had higher liner wear readings on the side opposite the pin. Bearing W8 had equal wear on both sides. For the bearings with Arizona Road Dust, salt, and distilled water, W17 and W19 (salt contaminated) had higher liner wear on the side opposite the pin. W18 had practically equal wear.

For the standard rod ends, W20 and W21, W20 experienced higher wear on the side normally opposite the wear-indicating pin, and W21 exhibited approximately equal wear.

The conclusion can be drawn that the introduction of the wear-indicating device has not caused any drastic reduction in wear capability.

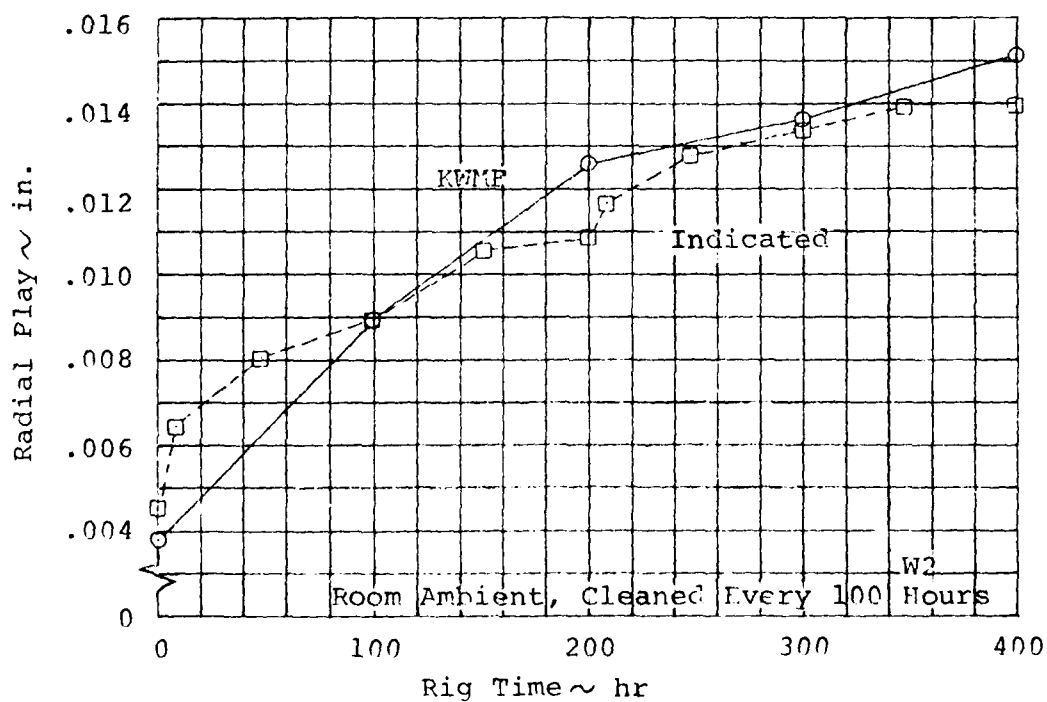
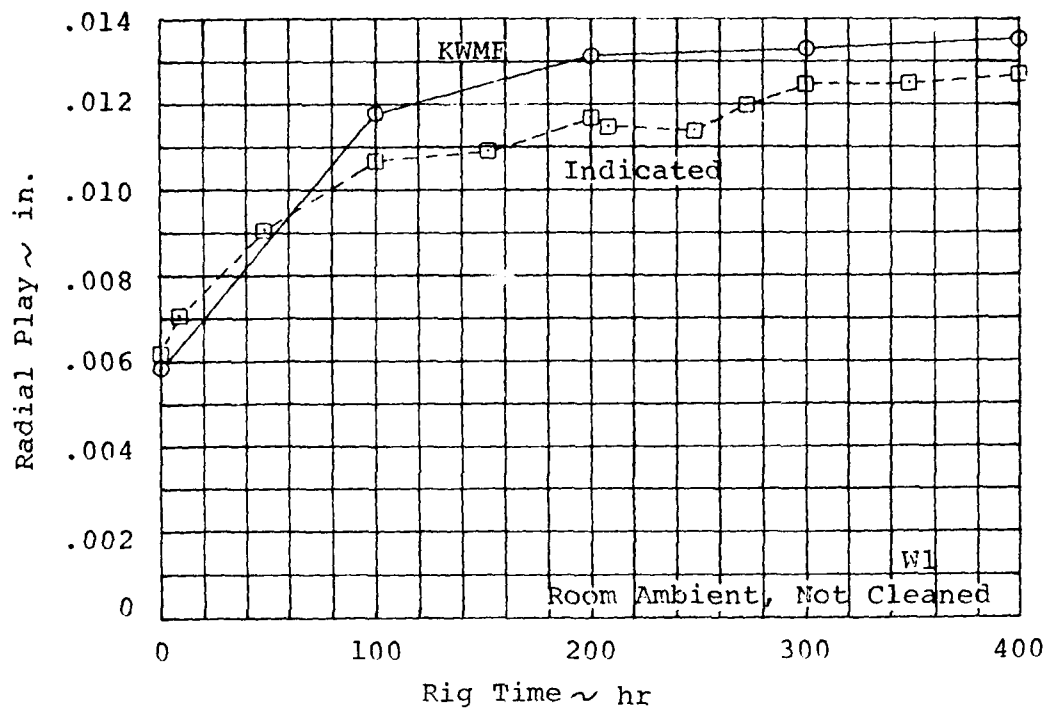


Figure 14. Radial Play vs. Rig Time - WIRE Test Specimens W1 and W2.

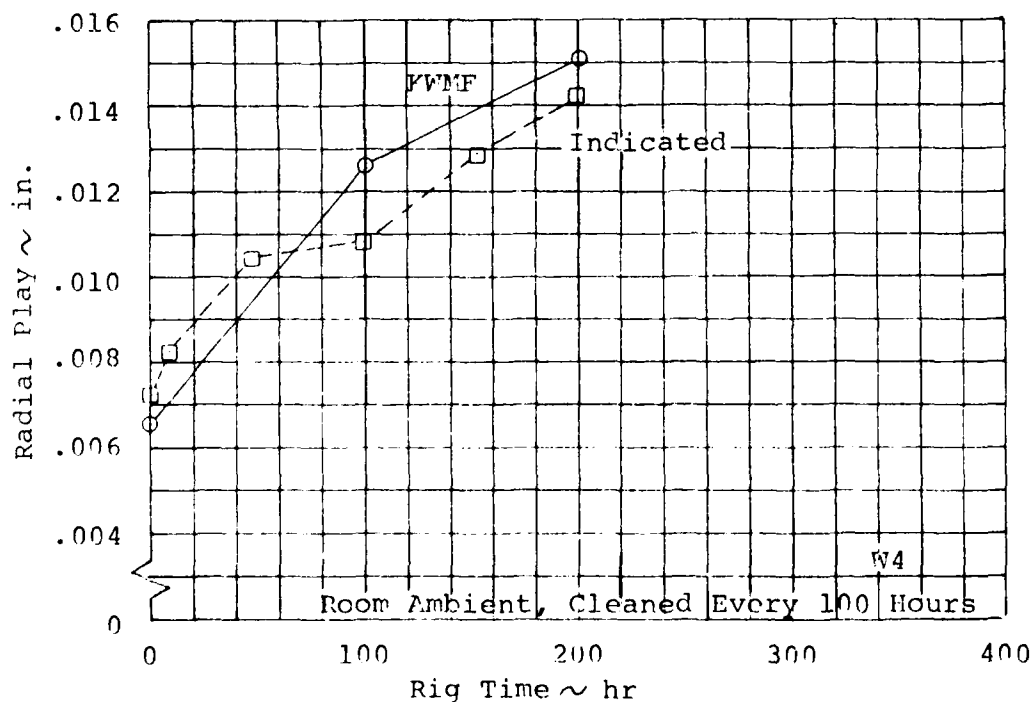
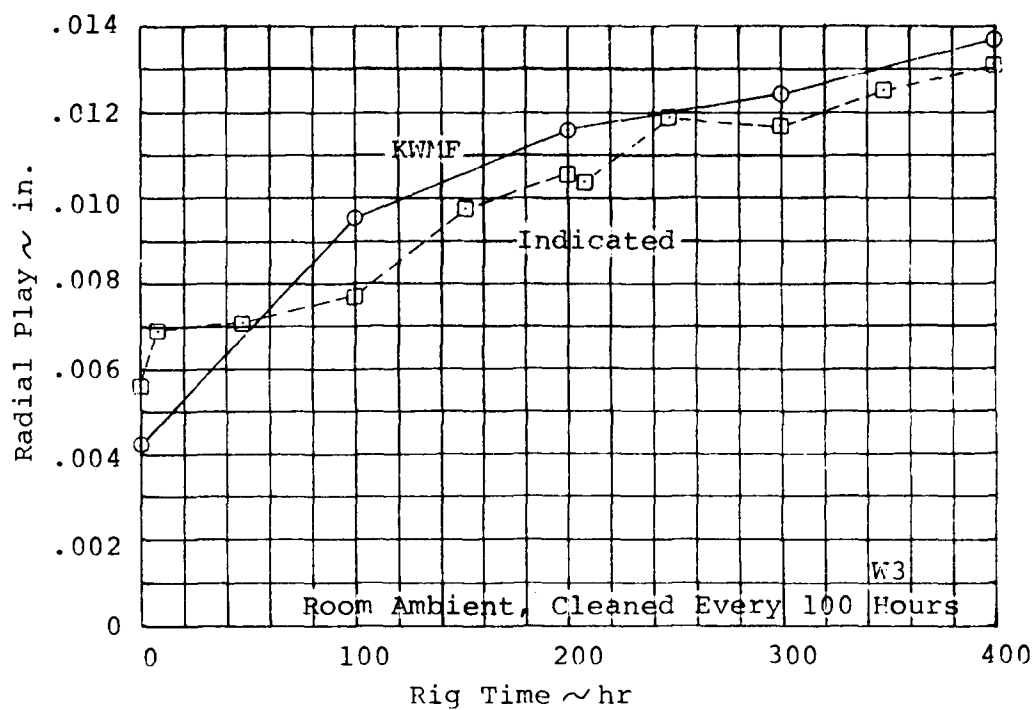


Figure 15. Radial Play vs. Rig Time -WIRE
Test Specimens W3 and W4.

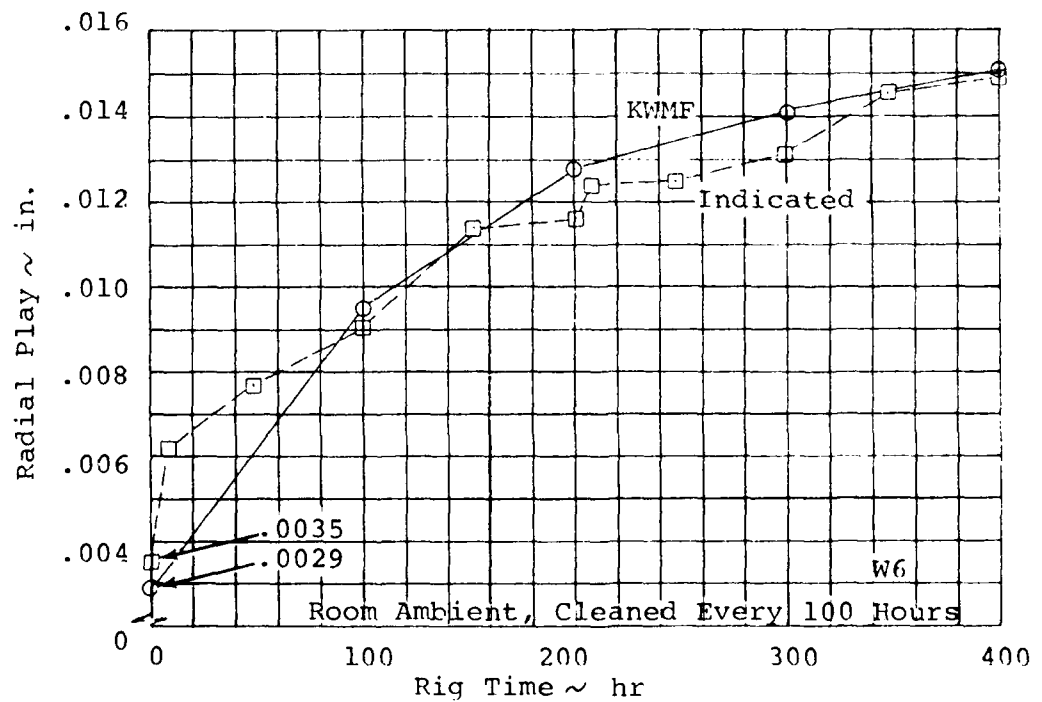
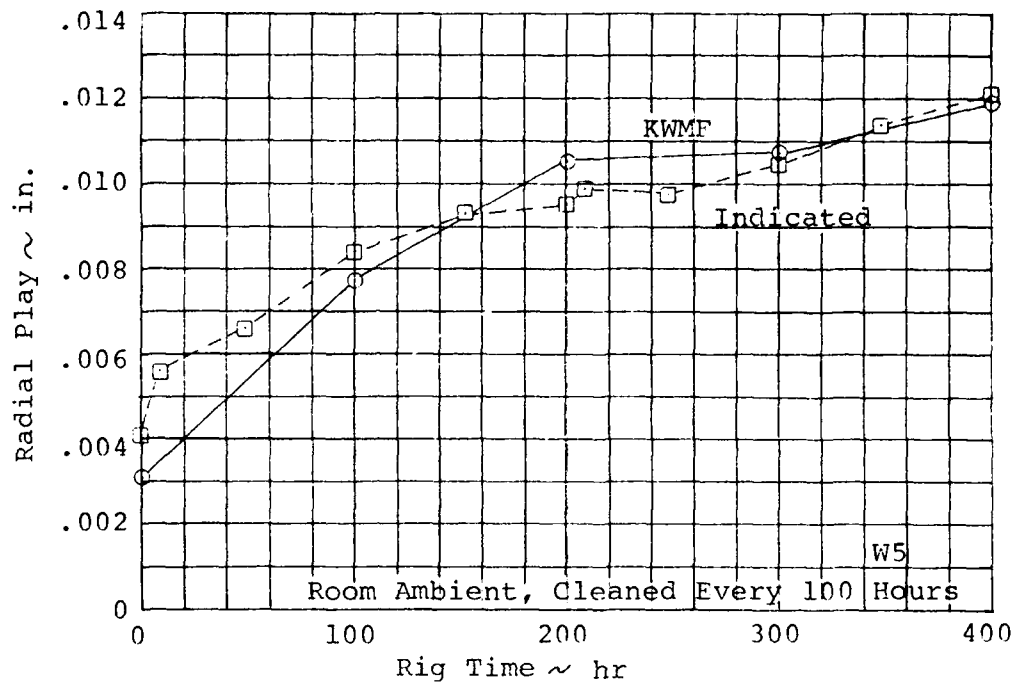


Figure 16. Radial Play vs. Rig Time - WIRE Test Specimens W5 and W6.

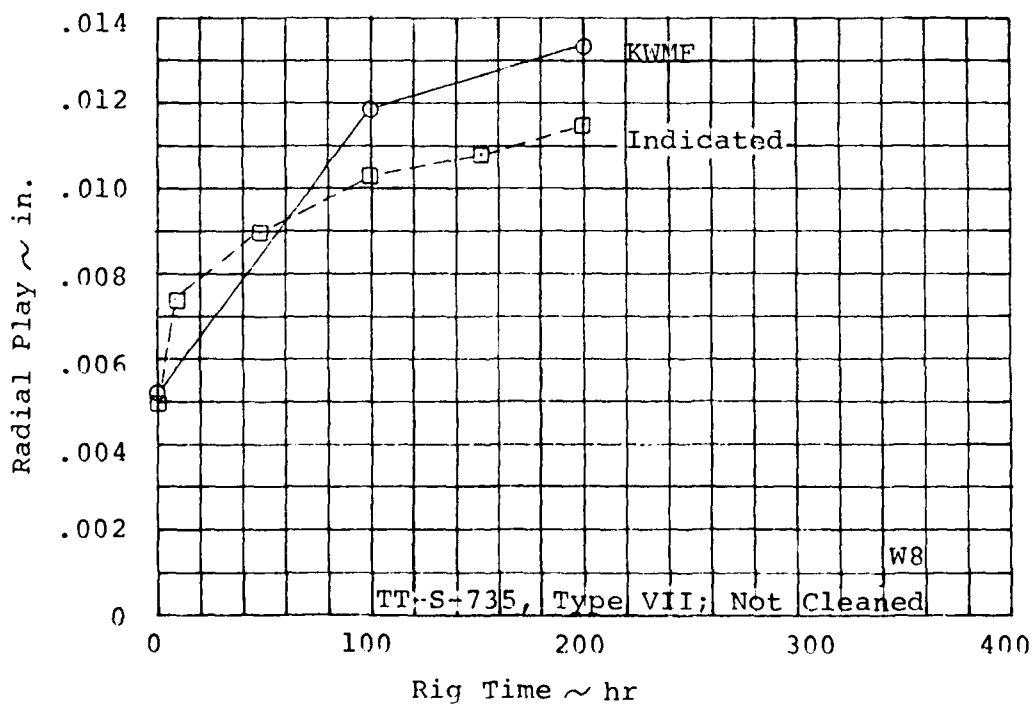
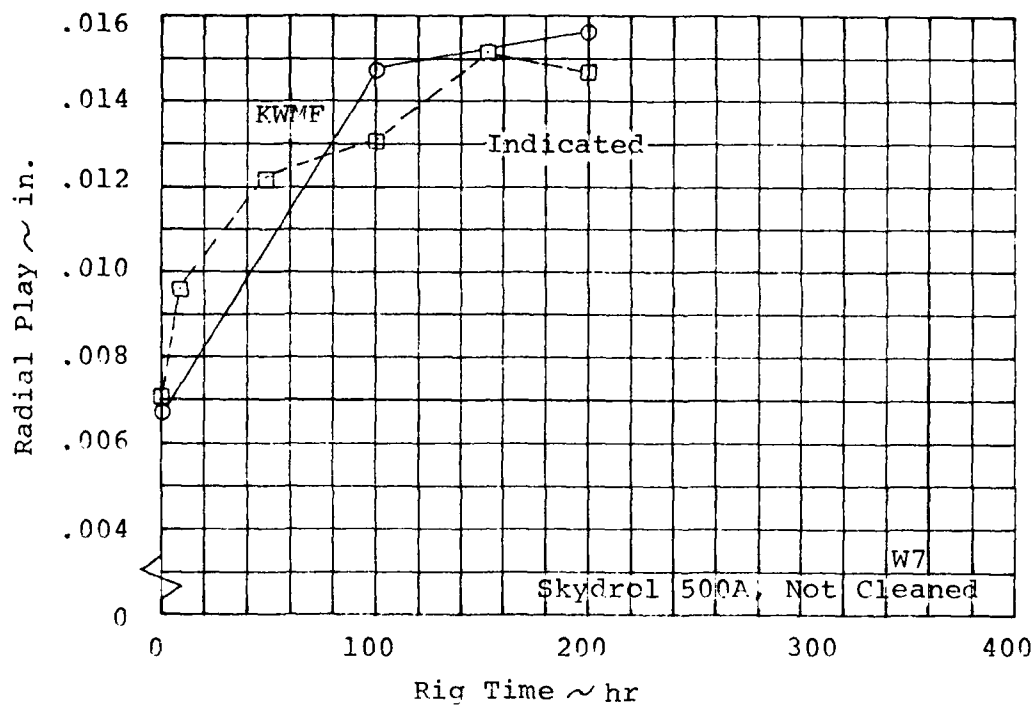


Figure 17. Radial Play vs. Rig Time - WIRE Test Specimens W7 and W8.

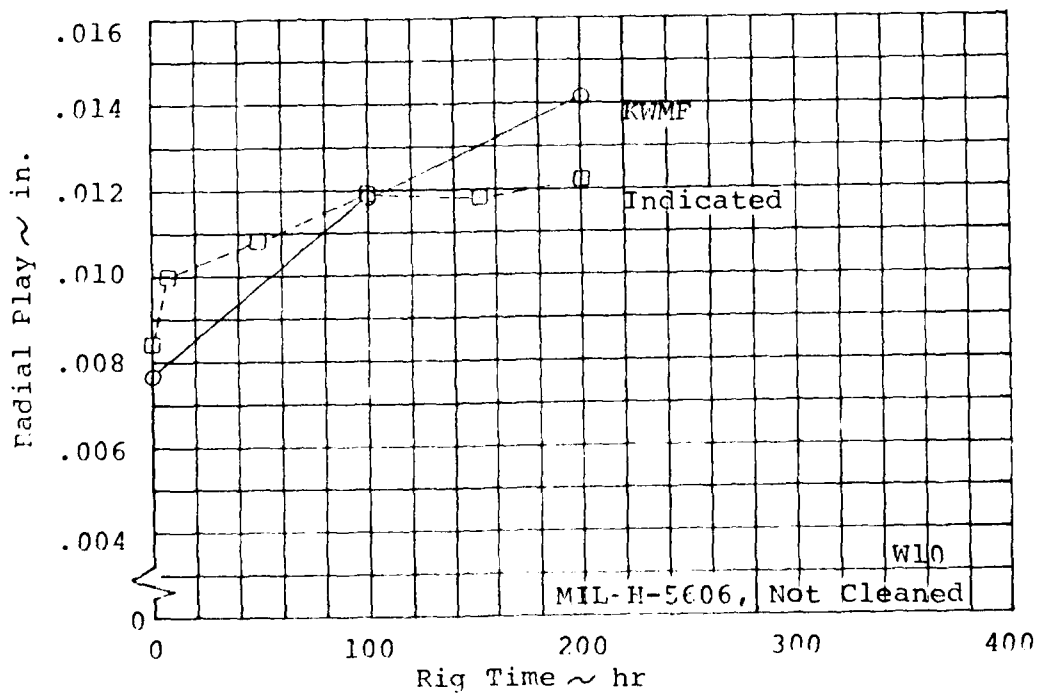
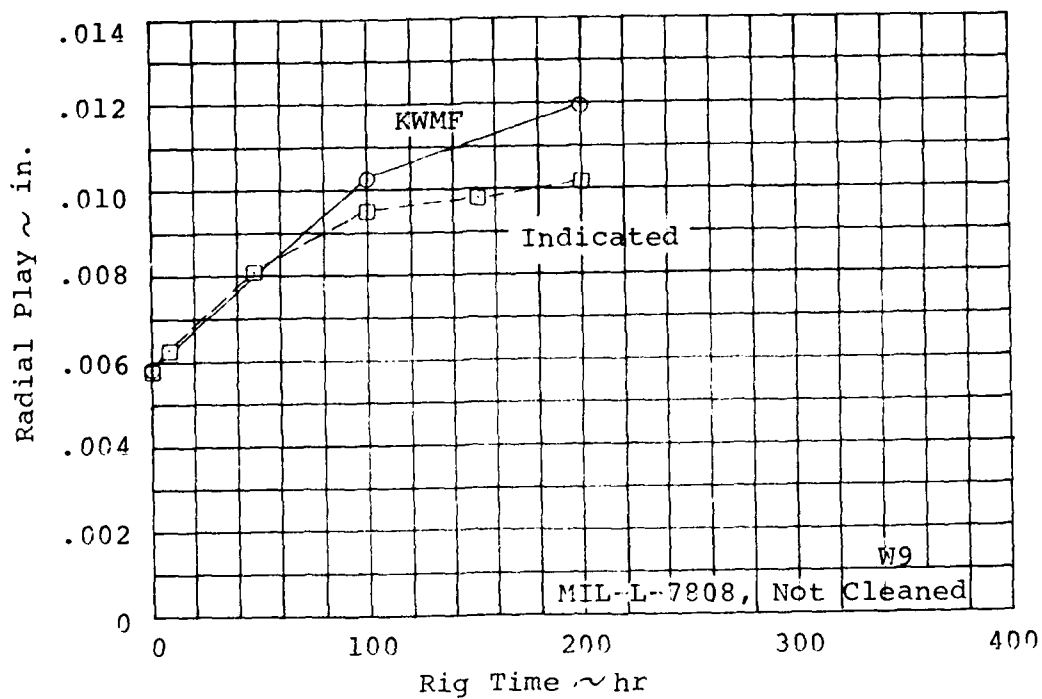


Figure 18. Radial Play vs. Rig Time - WIRE
Test Specimens W9 and W10.

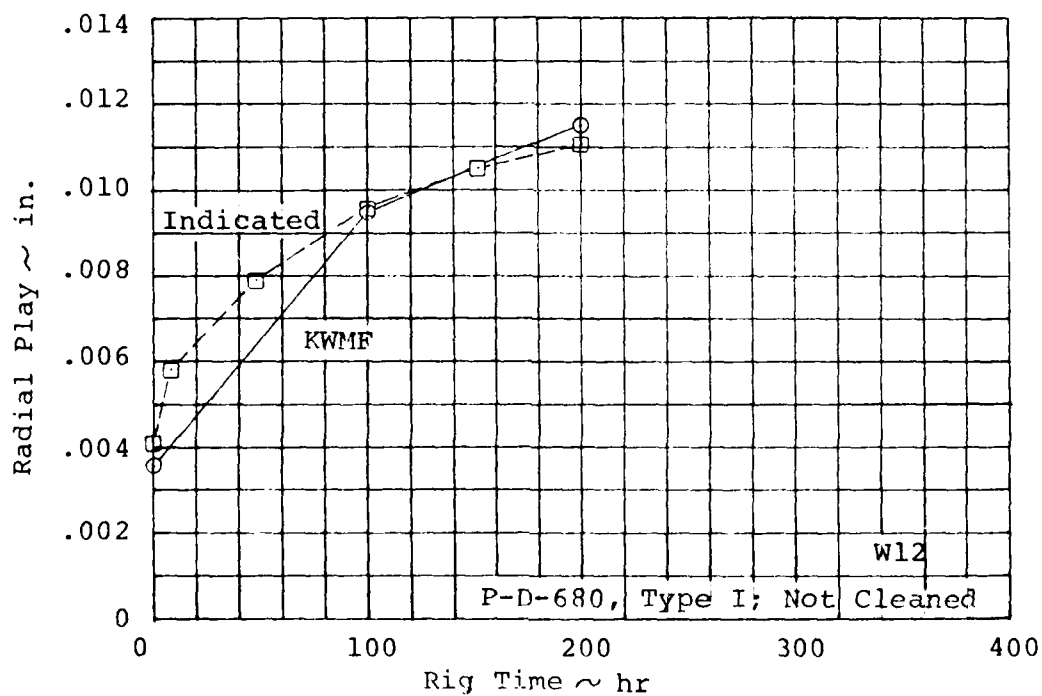
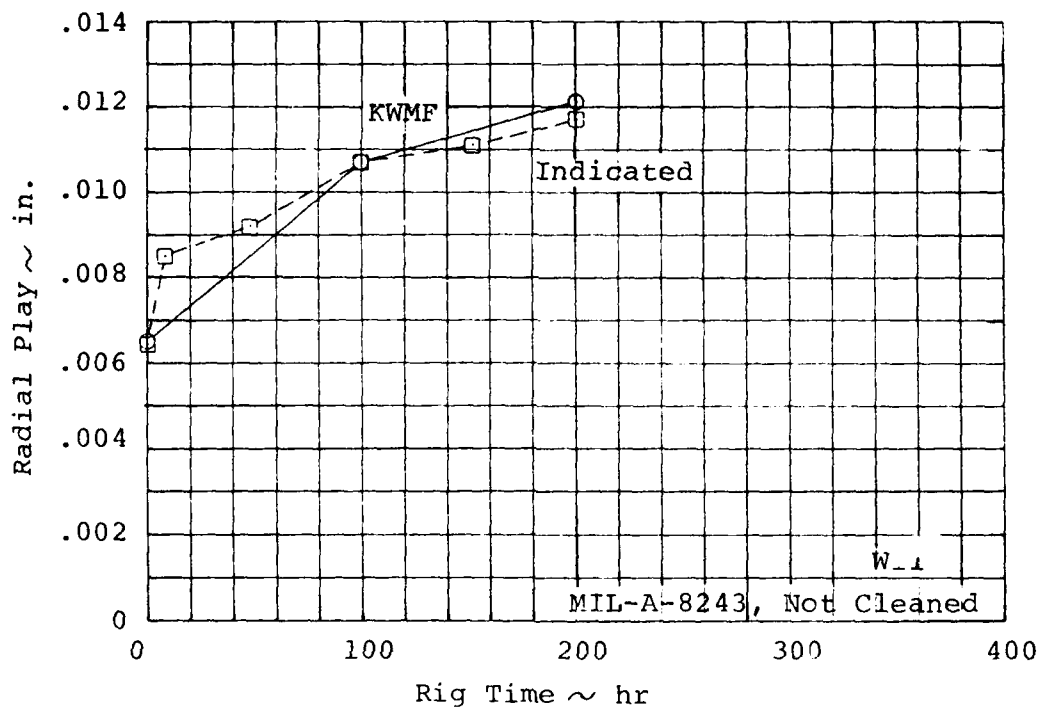


Figure 19. Radial Play vs. Rig Time - WIRE Test Specimens W11 and W12.

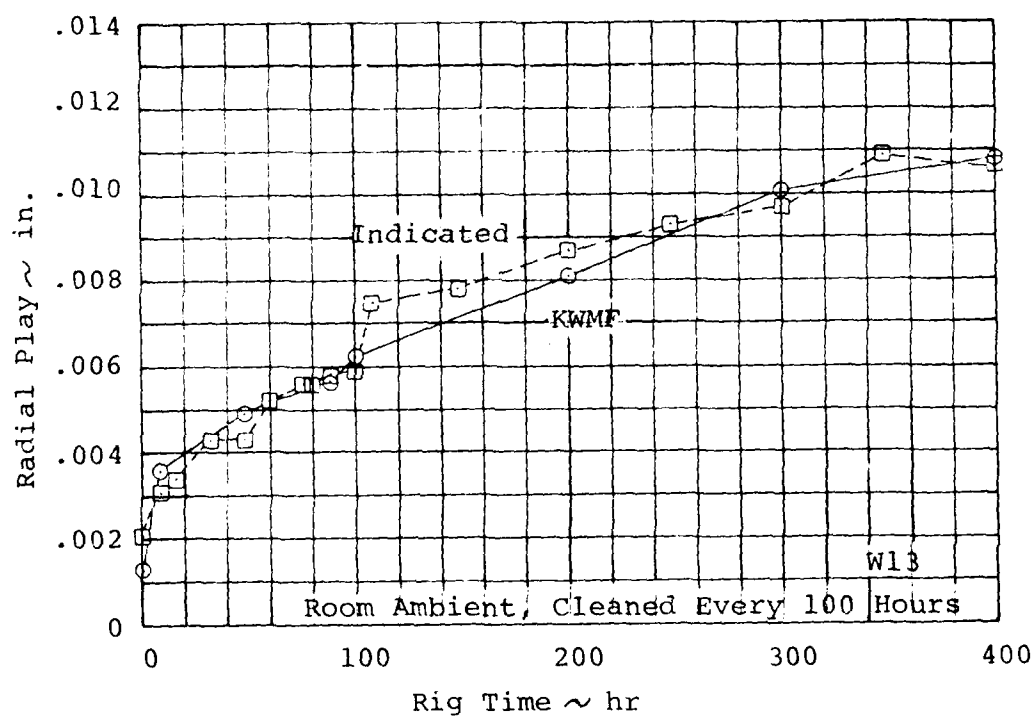


Figure 20. Radial Play vs. Rig Time - WIRE Test Specimen W13.

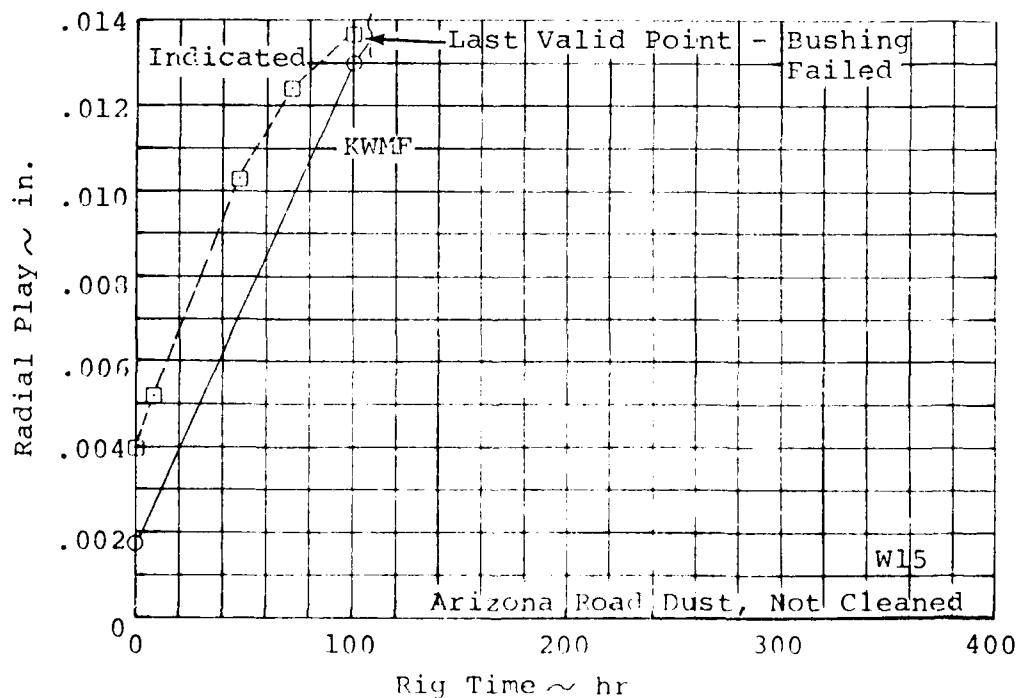
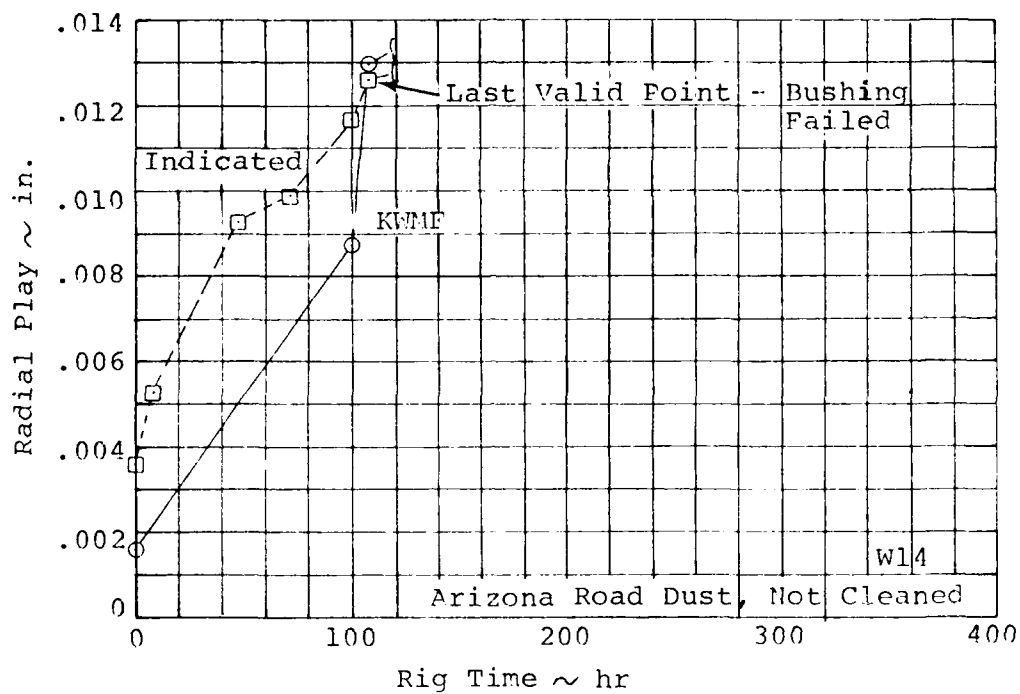


Figure 21. Radial Play vs. Rig Time - WIRE
Test Specimens W14 and W15.

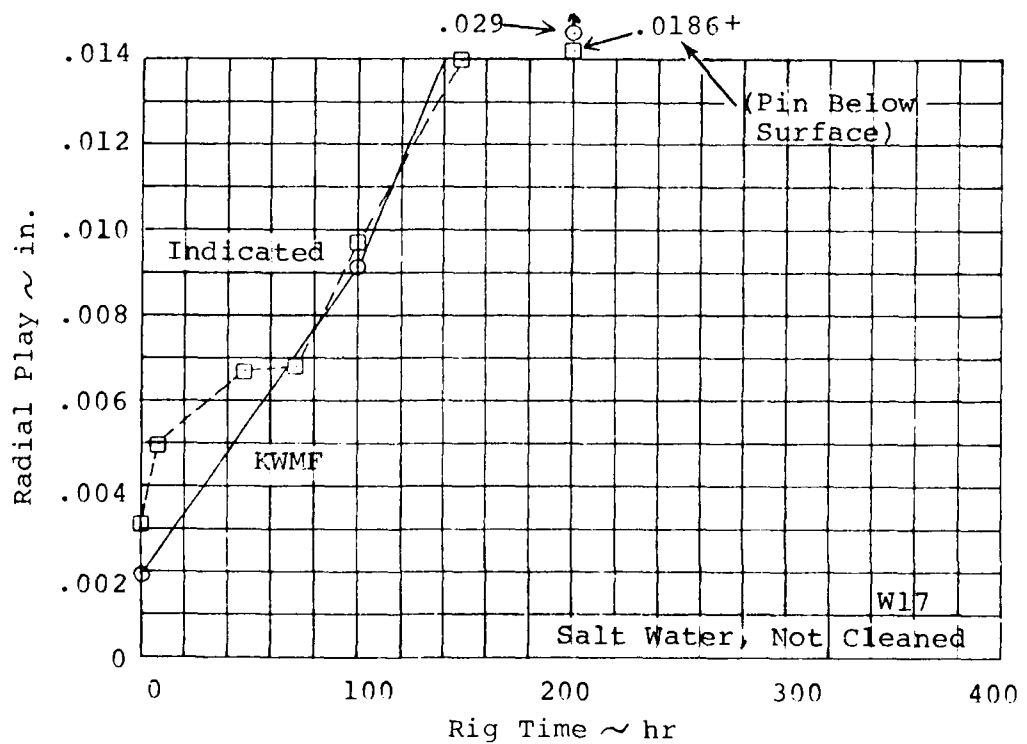
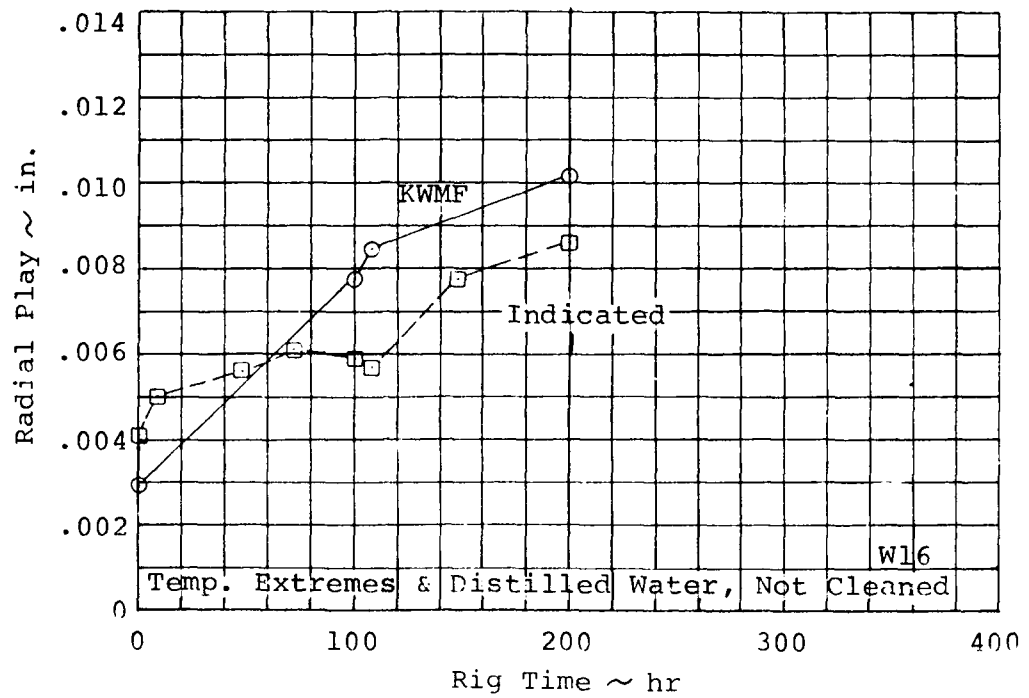


Figure 22. Radial Play vs. Rig Time - WIRE Test Specimens W16 and W17.

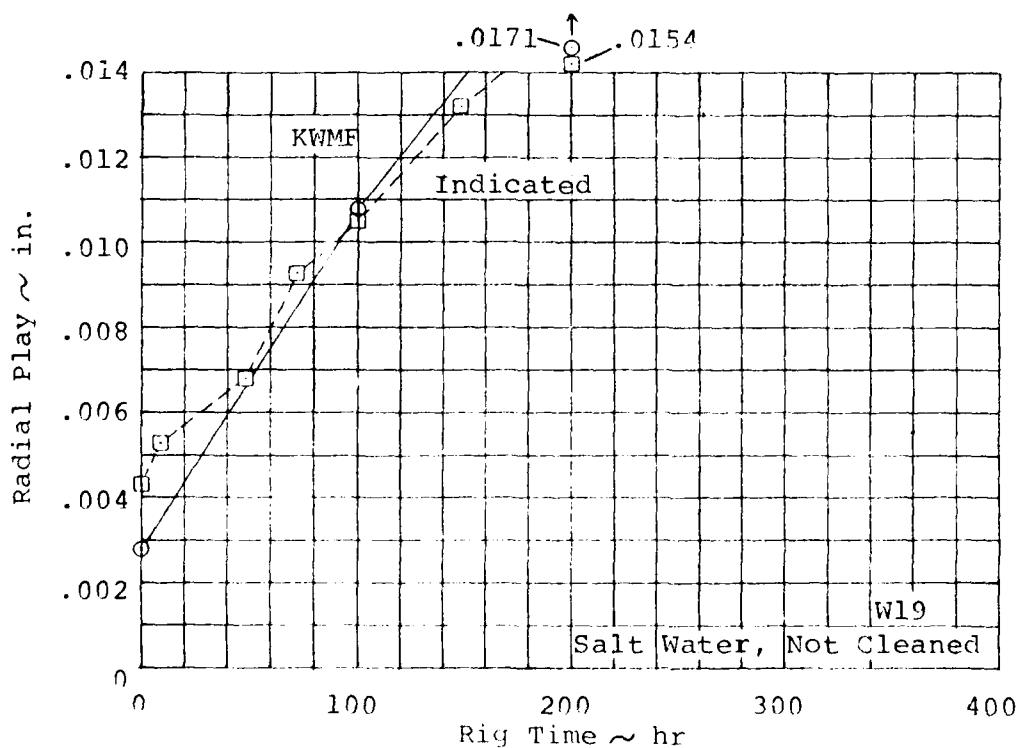
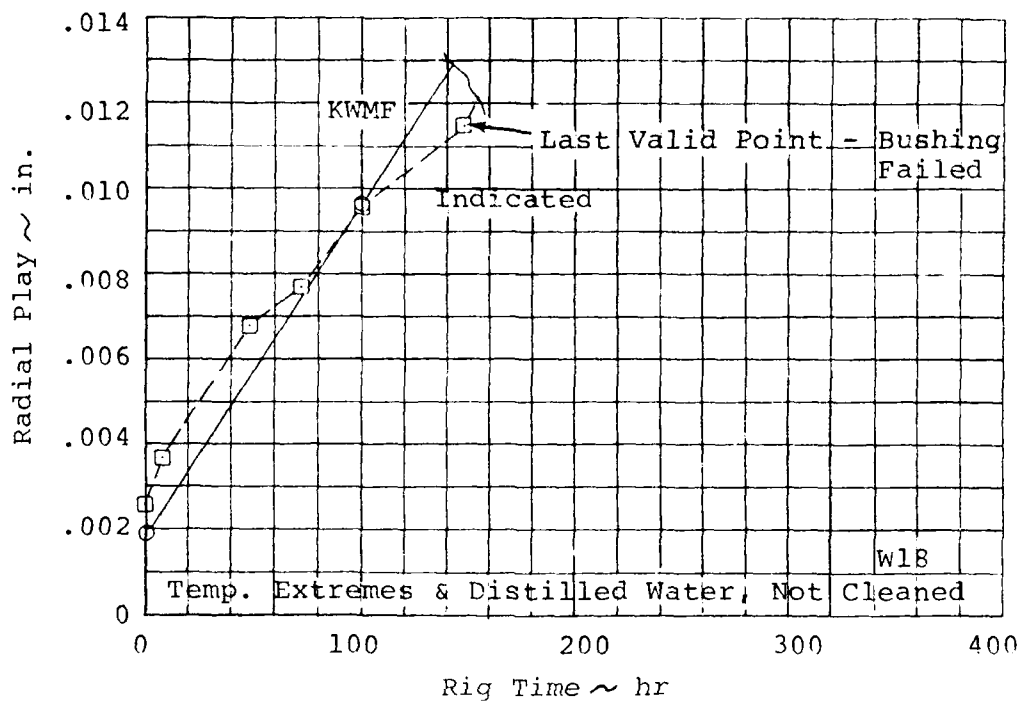


Figure 23. Radial Play vs. Rig Time - WIRE
Test Specimens W18 and W19.

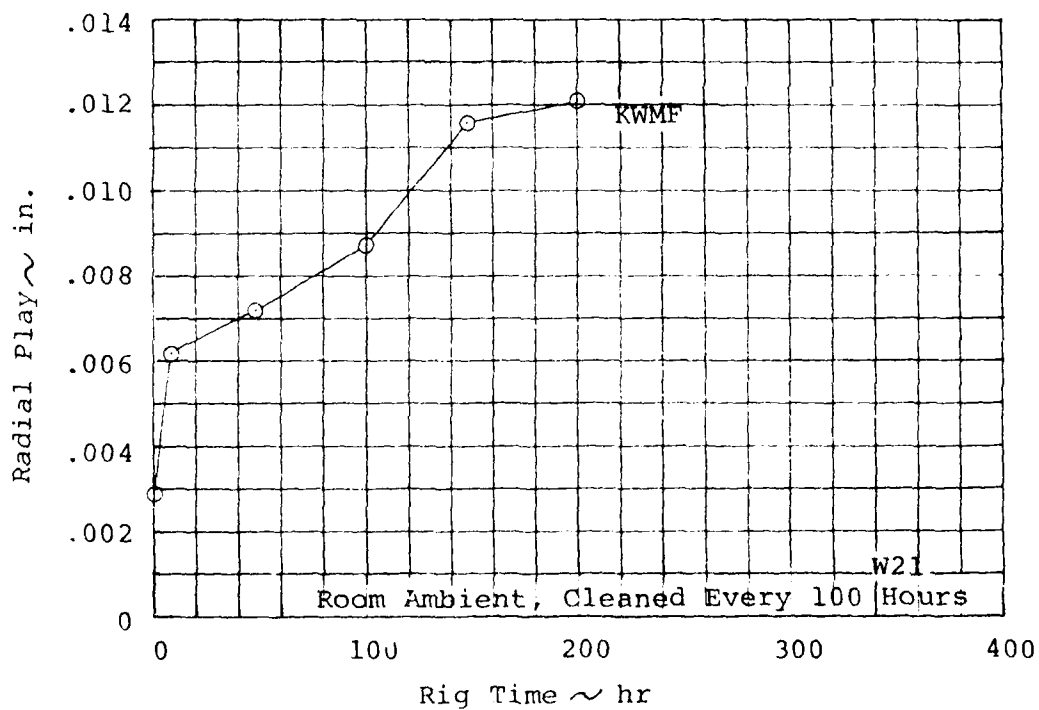
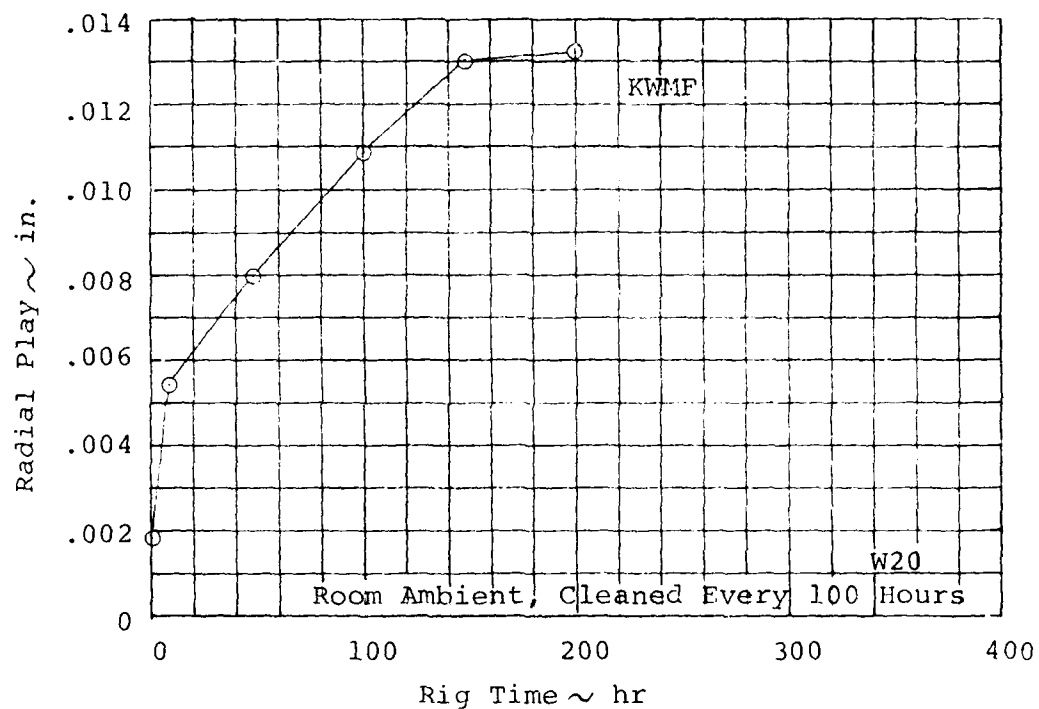


Figure 24. Radial Play vs. Rig Time - Standard Rod Ends W20 and W21.

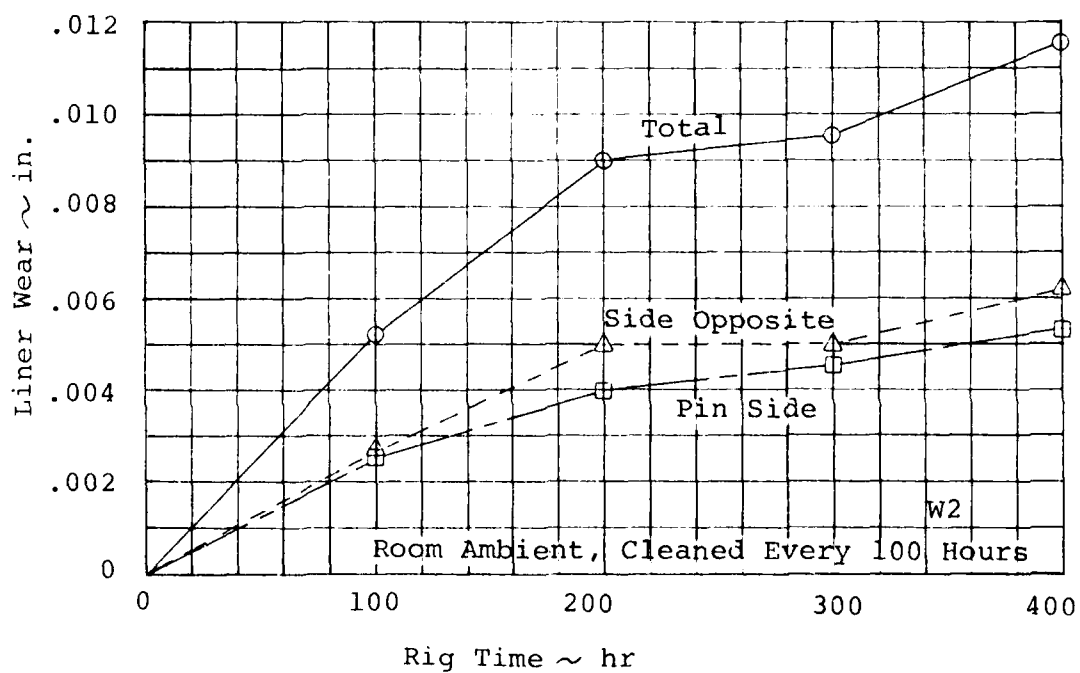
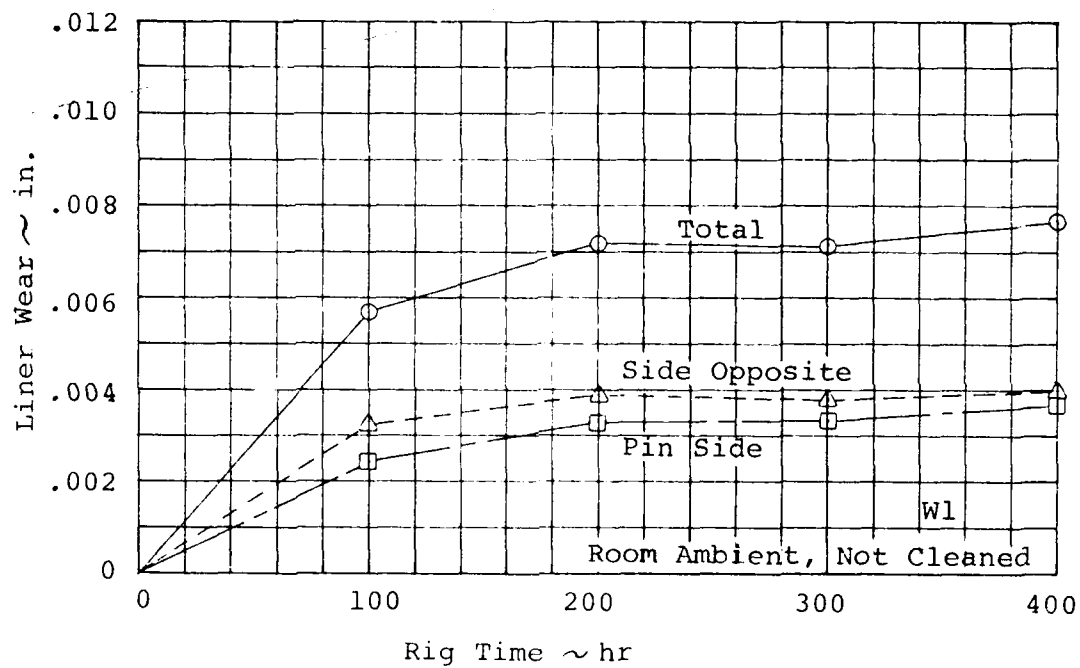


Figure 25. Liner Wear vs. Rig Time - WIRE
Test Specimens W1 and W2.

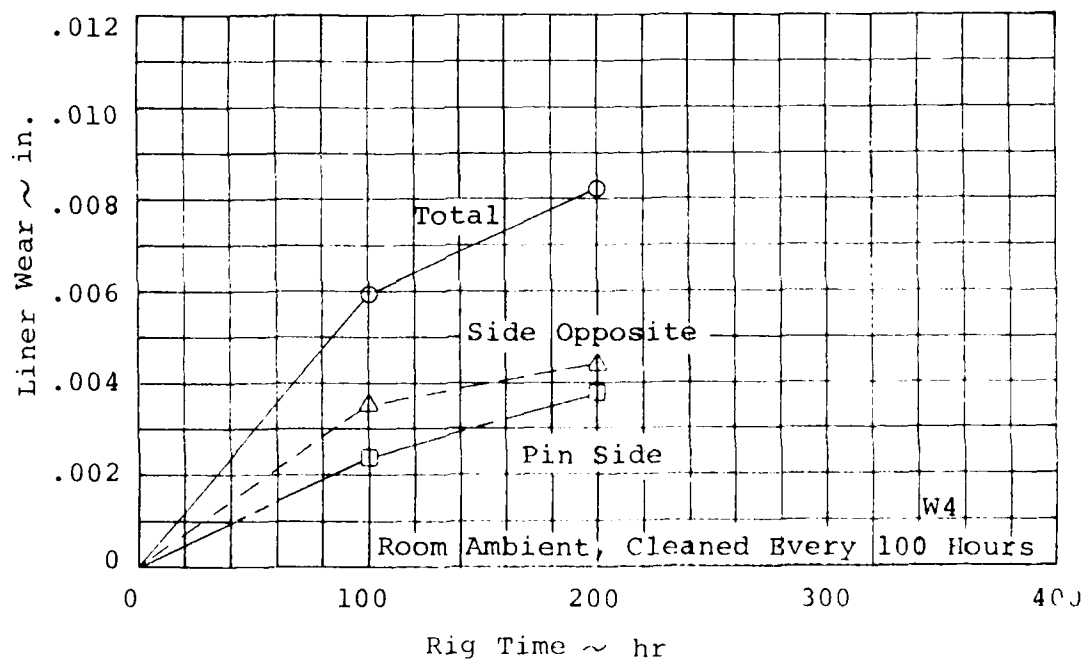
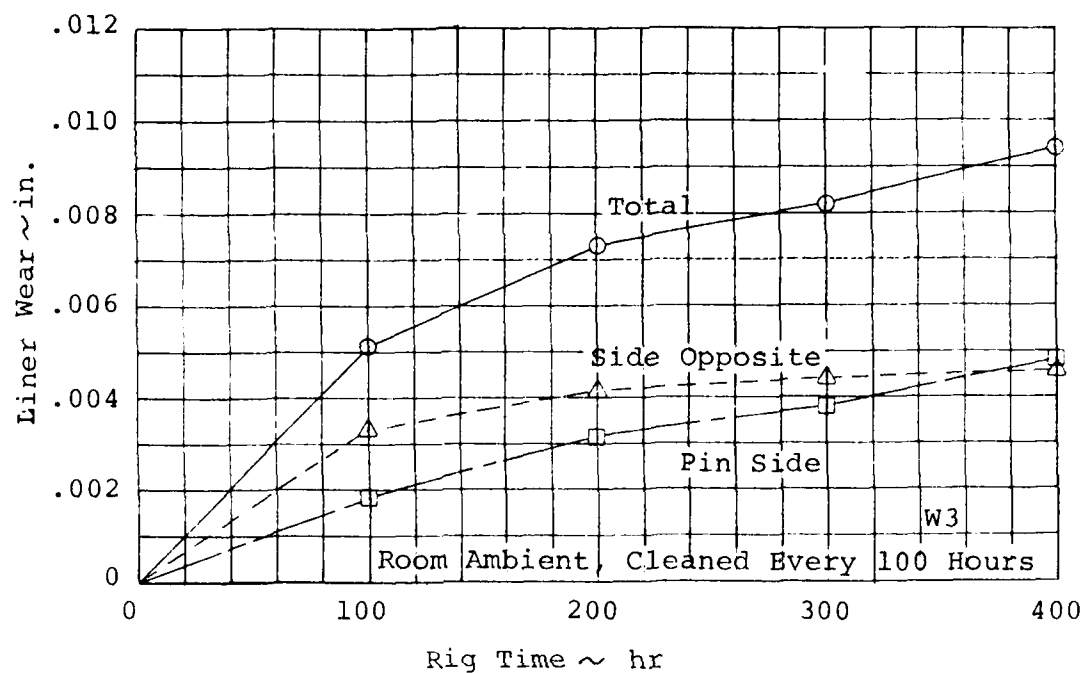


Figure 26. Liner Wear vs. Rig Time - WIRE Test Specimens W3 and W4.

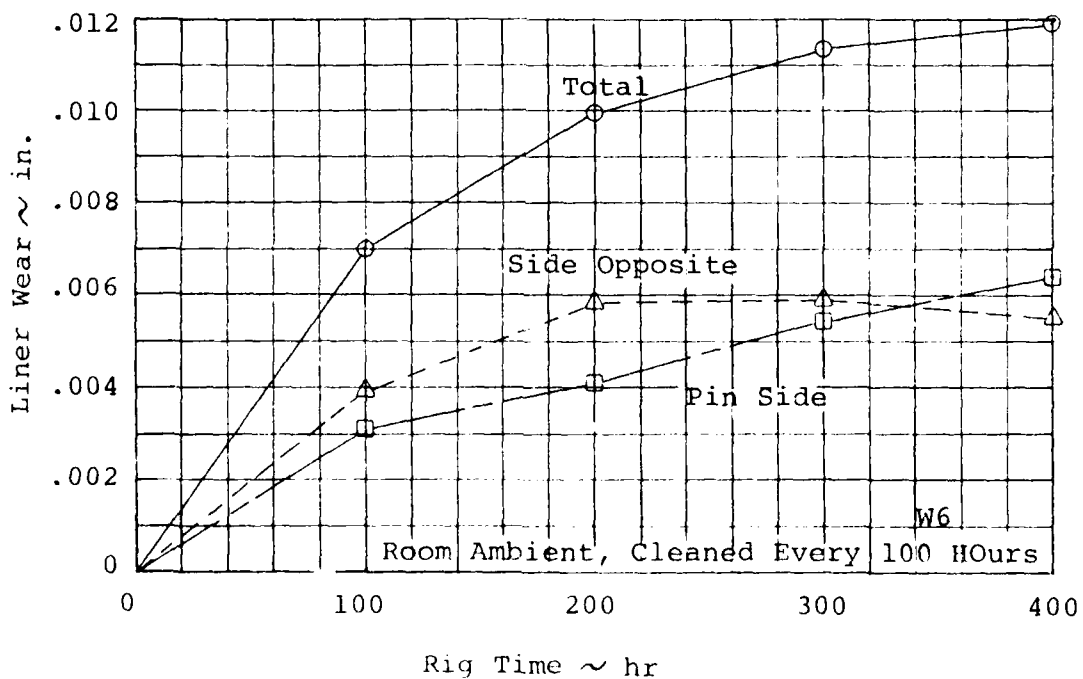
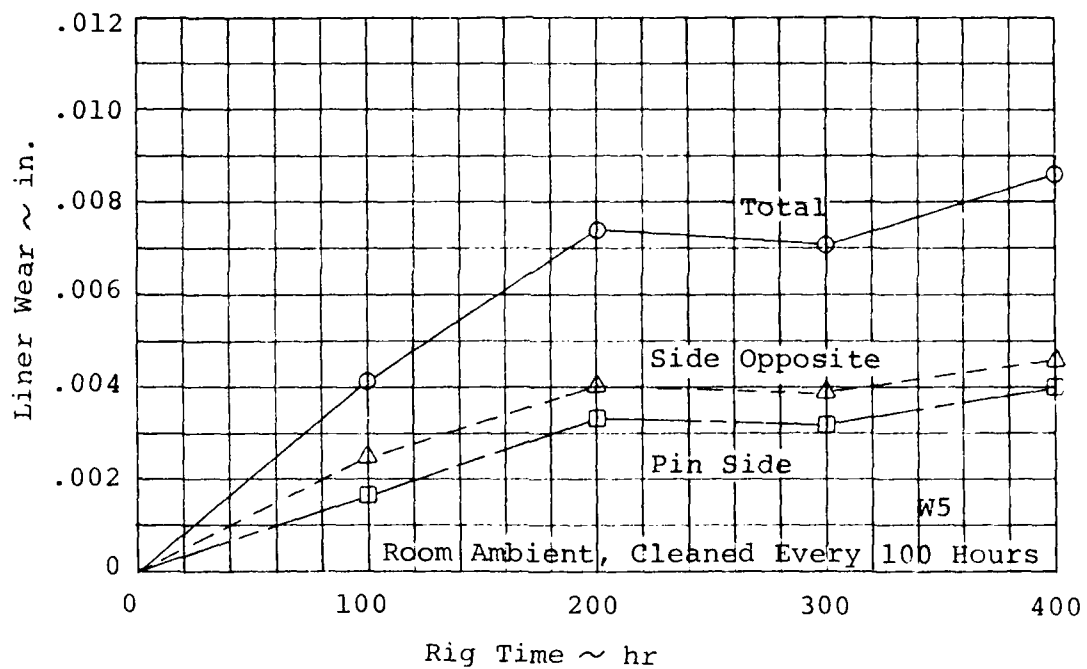


Figure 27. Liner Wear vs. Rig Time - WIRE
Test Specimens W5 and W6.

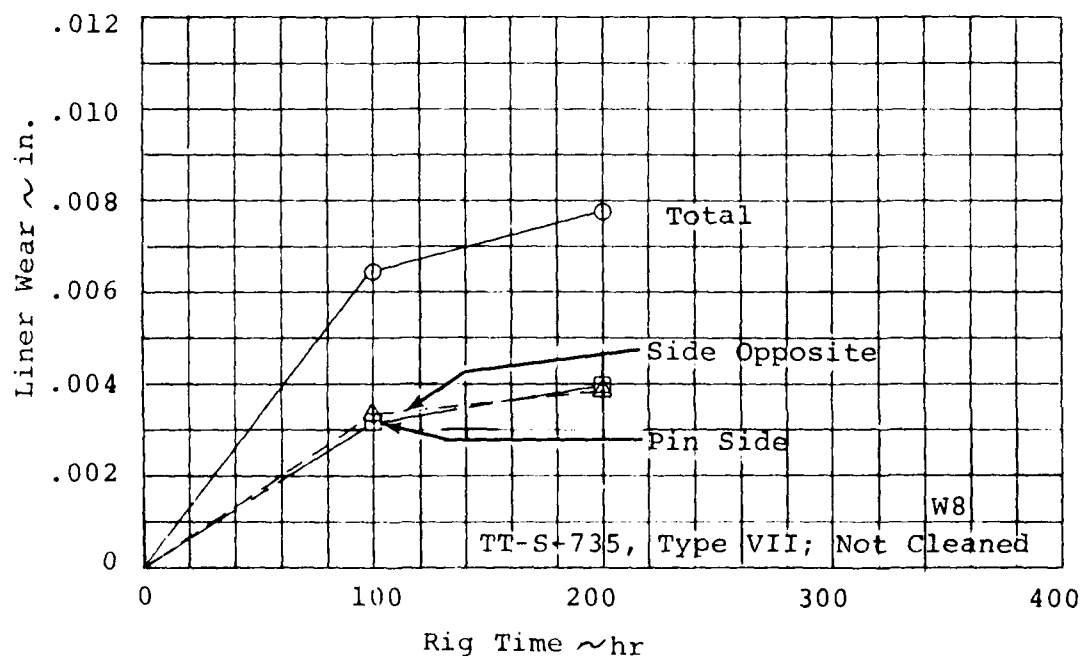
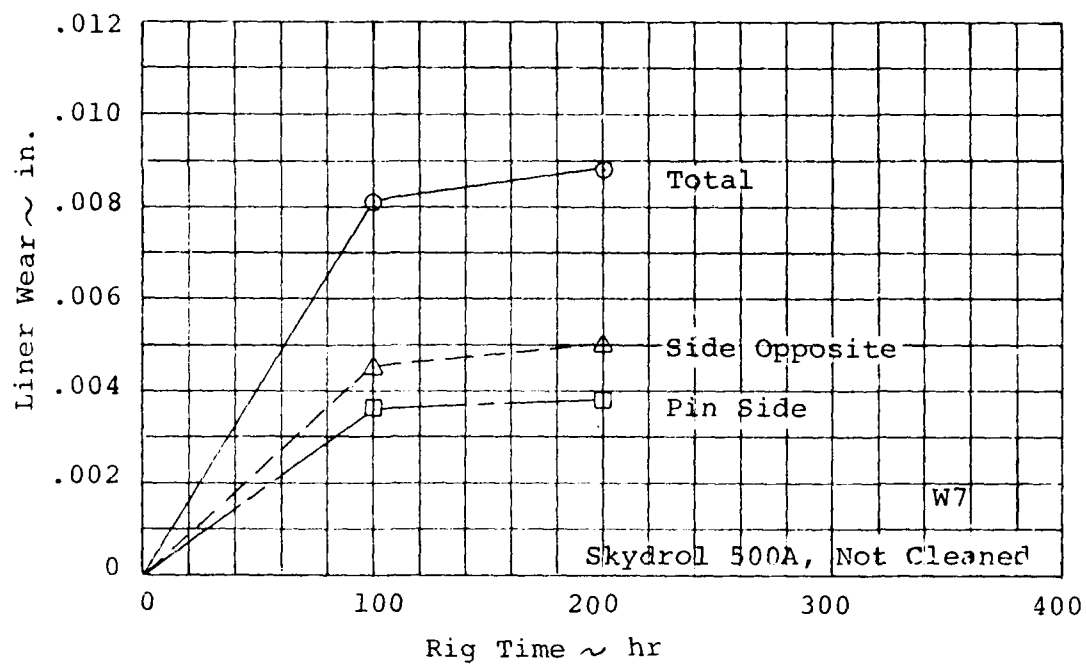


Figure 28. Liner Wear vs. Rig Time - WIRE Test Specimens W7 and W8.

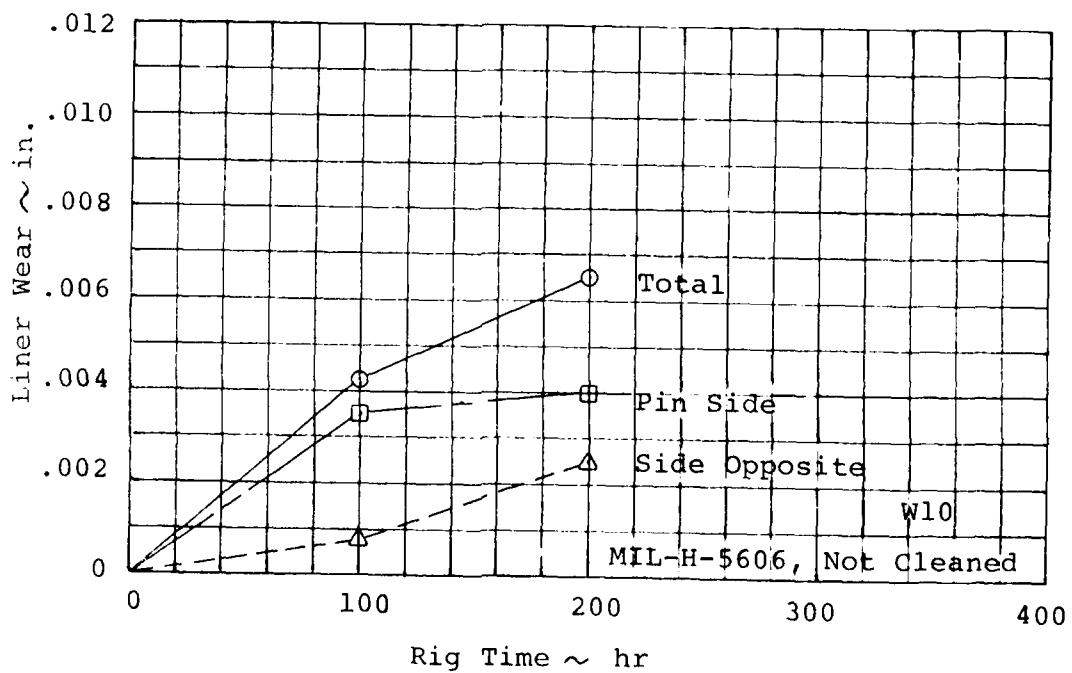
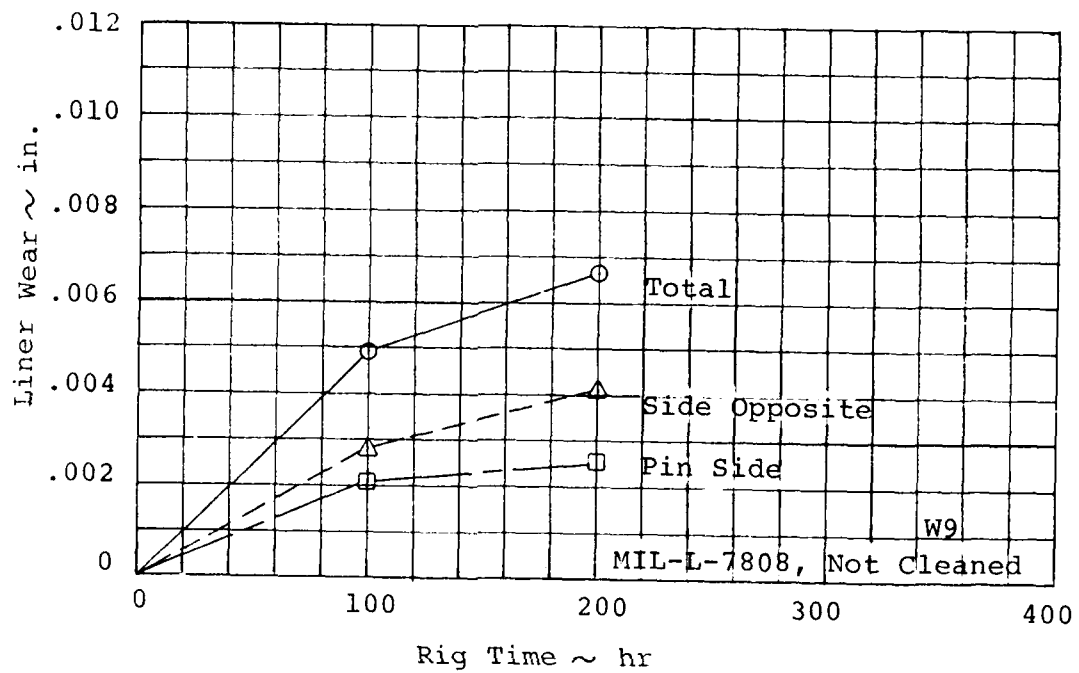


Figure 29. Liner Wear vs. Rig Time - WIRE
Test Specimens W9 and W10.

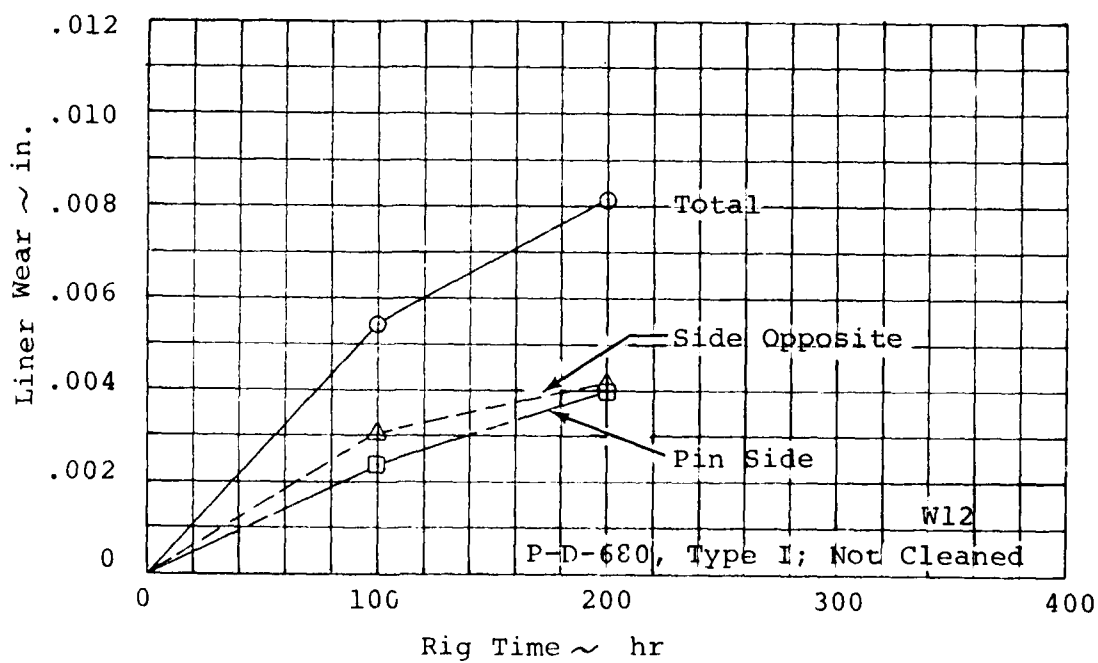
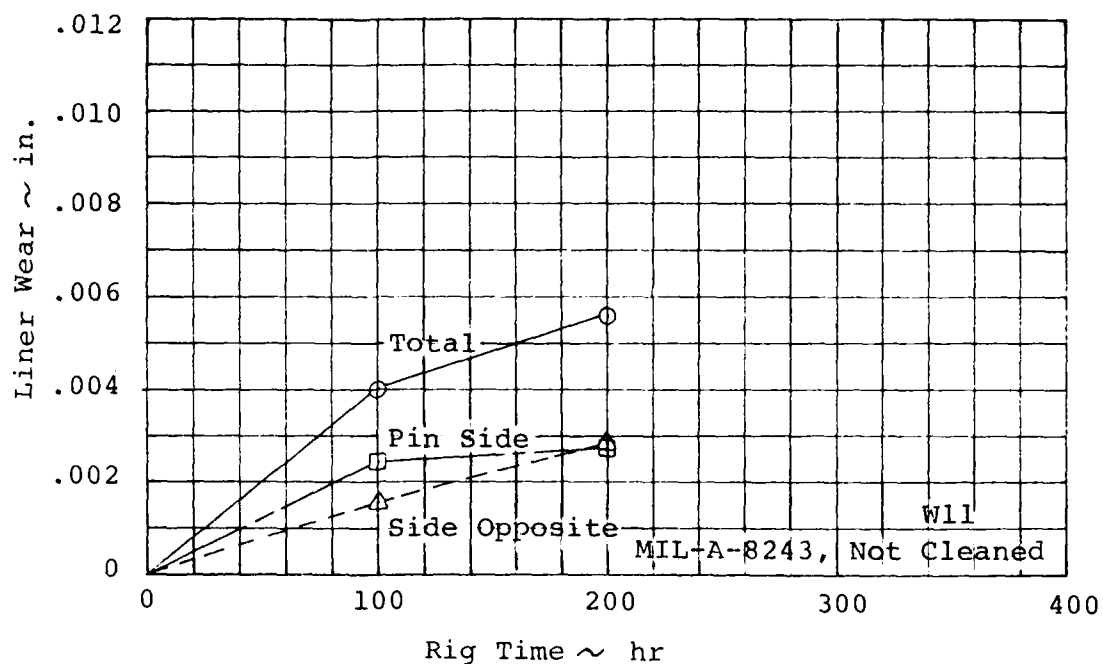


Figure 30. Liner Wear vs. Rig Time - WIRE
Test Specimens W11 and W12.

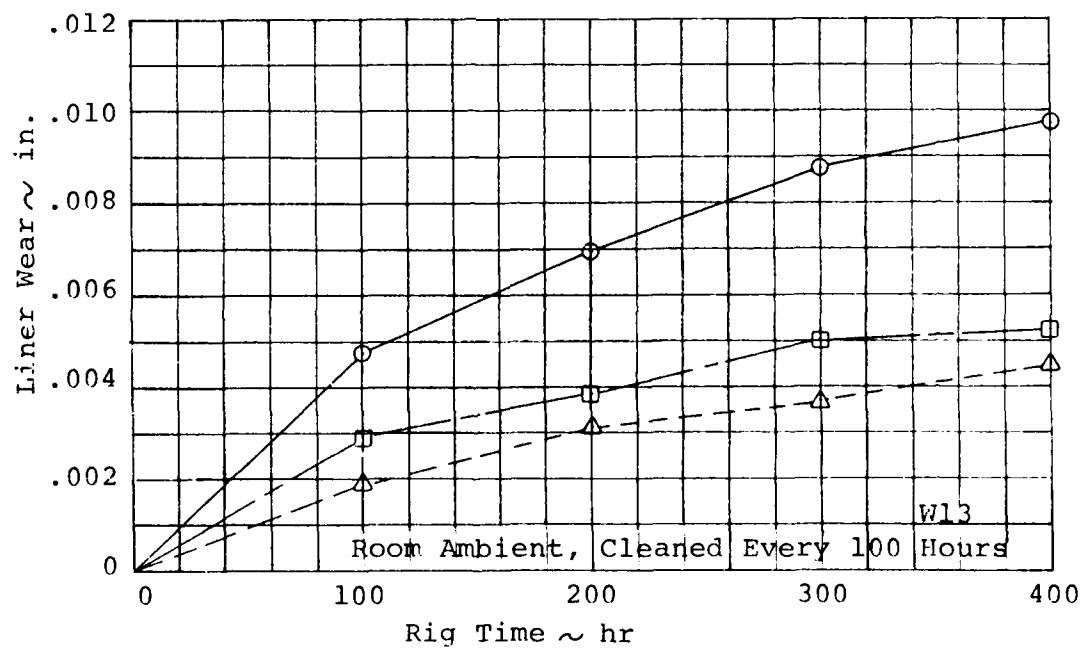


Figure 31. Liner Wear vs. Rig Time -
WIRE Test Specimen W13.

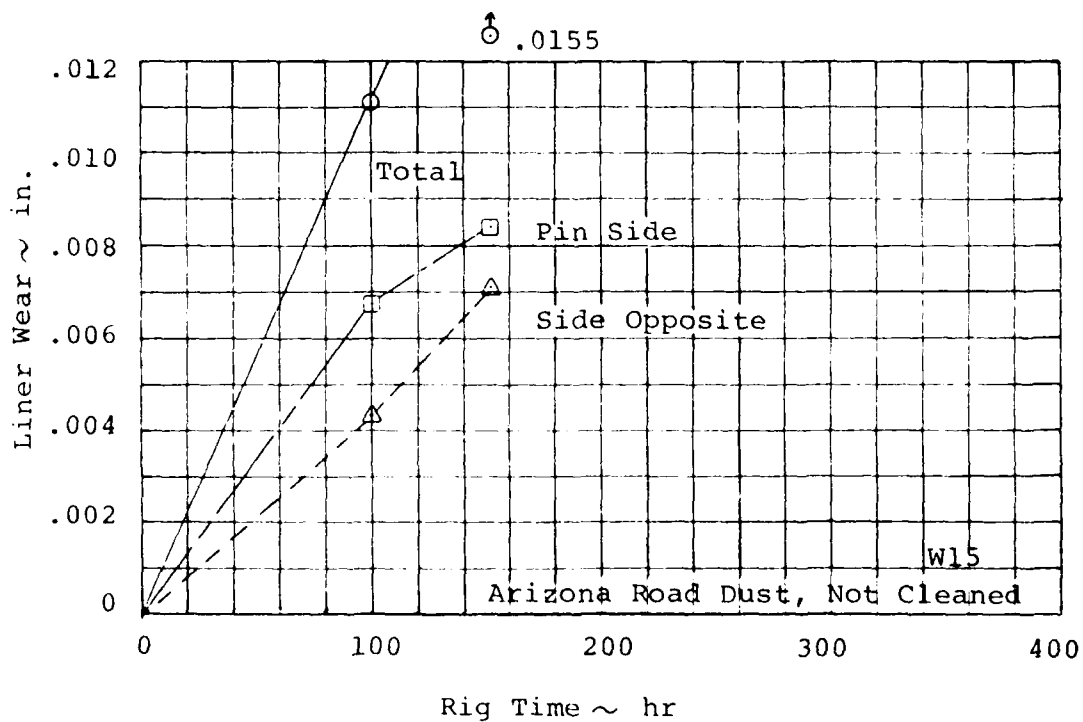
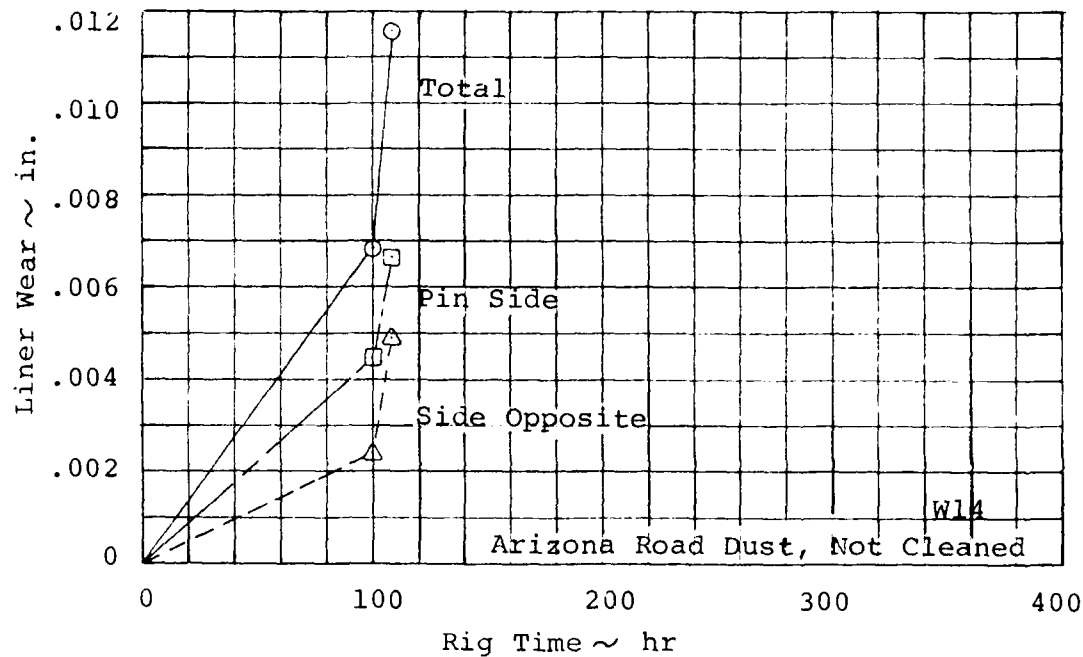


Figure 32. Liner Wear vs. Rig Time - WIRE Test Specimens W14 and W15.

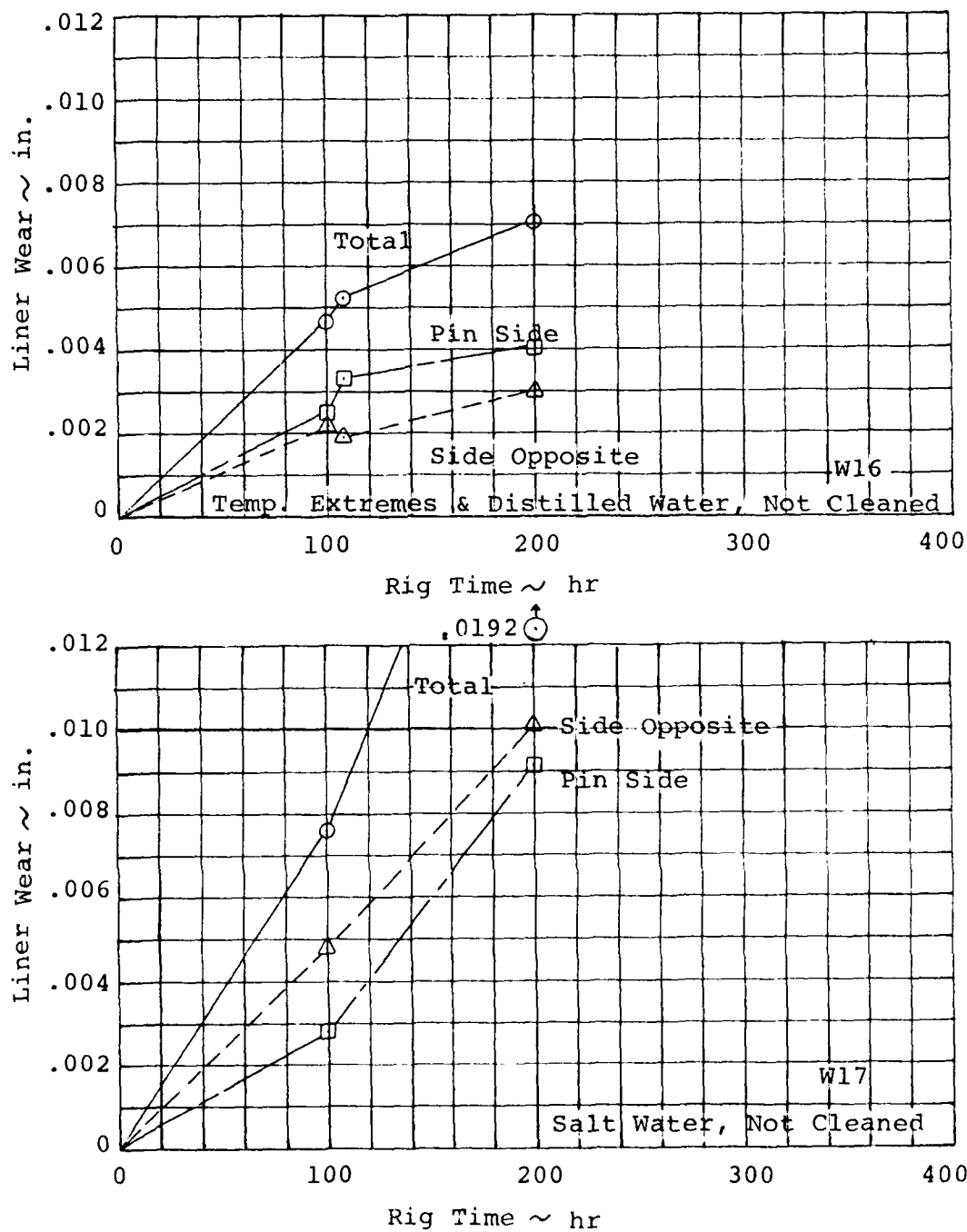


Figure 33. Liner Wear vs. Rig Time - WIRE Test Specimens W16 and W17.

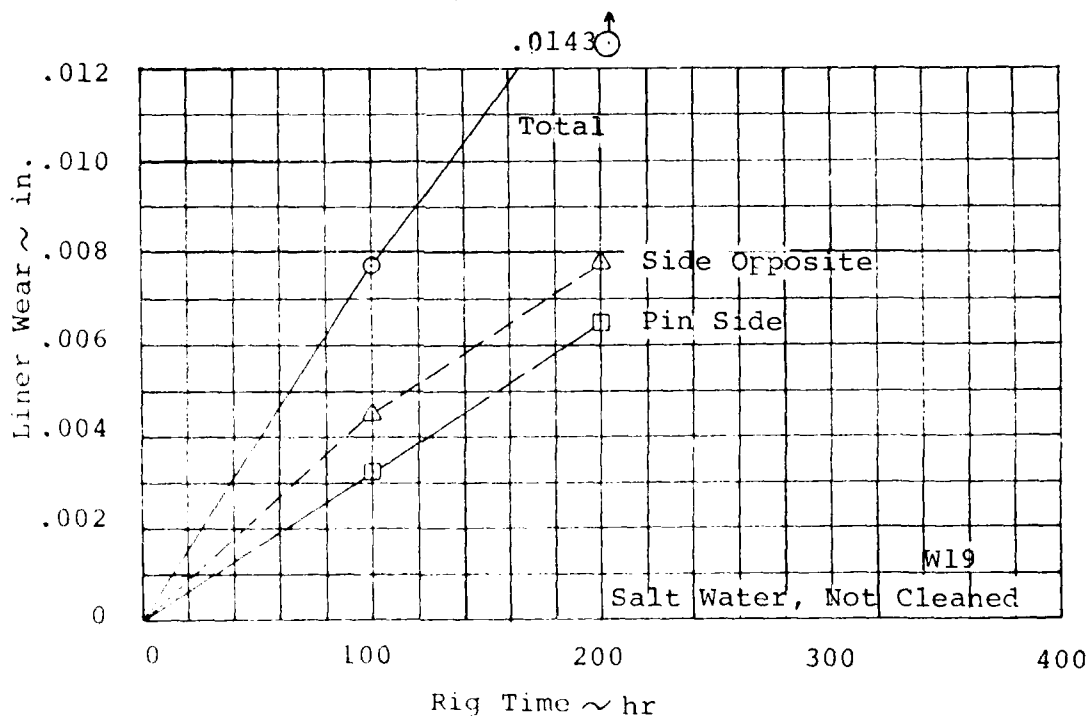
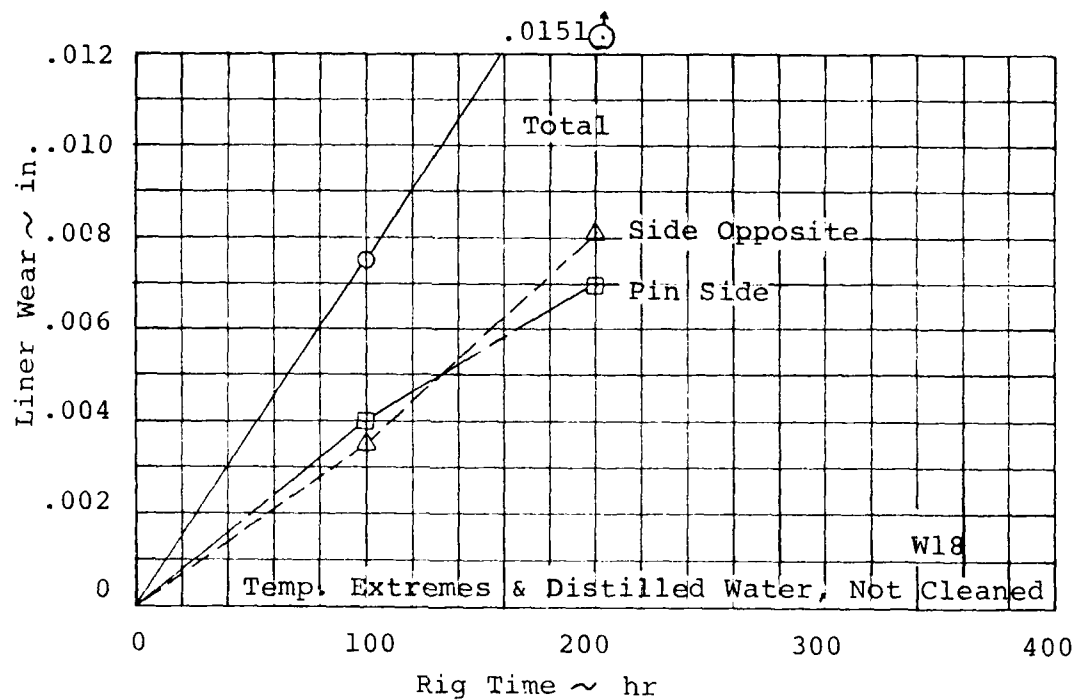


Figure 34. Liner Wear vs. Rig Time - WIRE
Test Specimens W18 and W19.

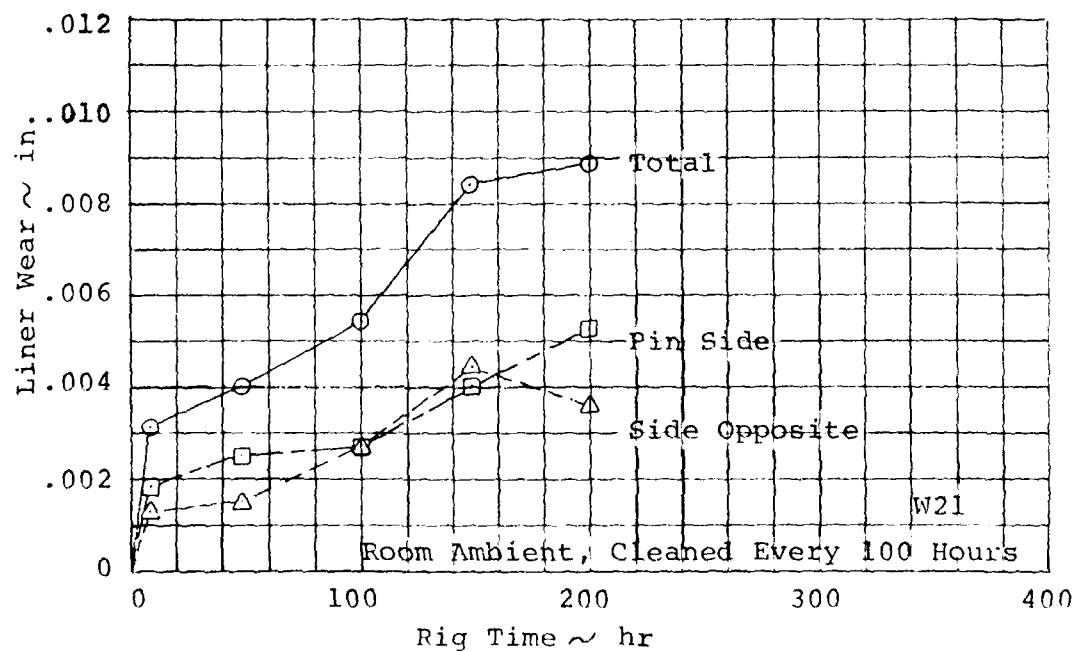
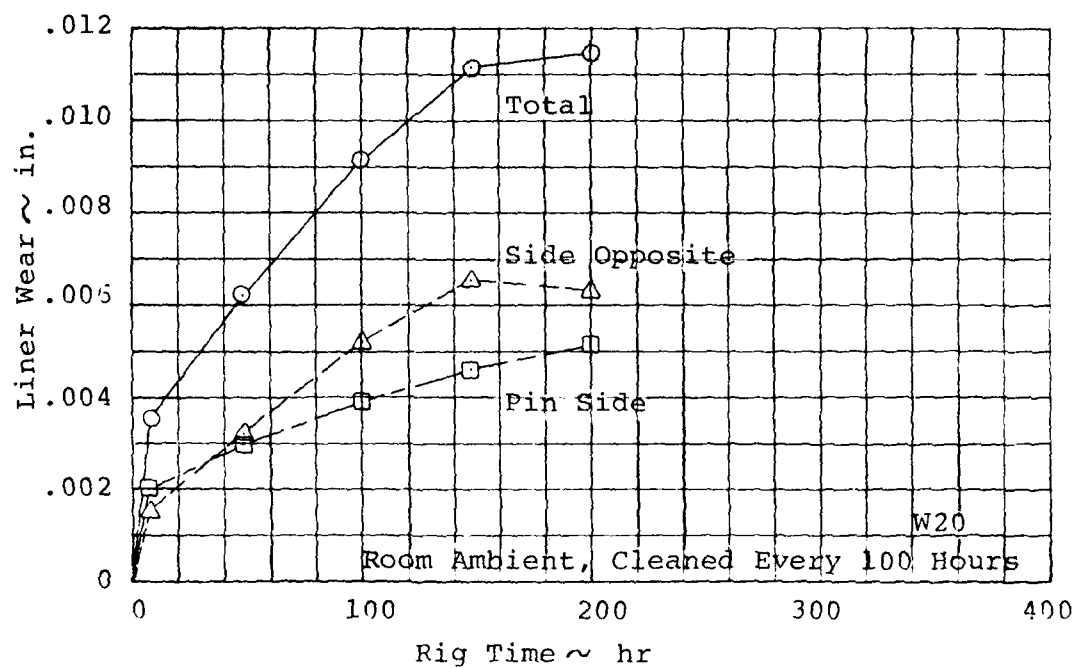


Figure 35. Liner Wear vs. Rig Time - Standard Rod Ends W20 and W21.

B. Fatigue Test

Two WIRE test specimens (F1 and F2) successfully withstanding in the fatigue test rig at an alternating radial ± 600 pounds for 30 million cycles. Two more specimens (F4) successfully withstood ± 800 pounds for 30 million cycles. The remaining two specimens (F5 and F6) successfully withstood 30 million cycles at ± 800 pounds plus an additional 30 million cycles at ± 1000 pounds. Specimen F5 and F6 were subsequently tested at ± 1200 pounds for 2.5 million cycles, at which specimen F6 failed in fatigue. Testing of specimen F5 at ± 1200 pounds with bearing F3 installed in place of specimen F6. A fatigue failure of specimen F3 occurred at 0.7 million cycles. Specimen F4 was installed in place of specimen F5 and testing at ± 1200 pounds resulted in a failure of specimen F4 after 14.0 million cycles.

Testing of specimen F4 continued at ± 1200 pounds with bearing F2 (and later bearing F1) installed in lieu of the failed specimen F5. Fatigue testing of specimen F4 at ± 1200 pounds was suspended after completion of 30 million cycles without failure. Specimens F1 and F2 accrued 11.2 and 8.1 million cycles, respectively, of fatigue loading at the ± 1200 -pound load level without a failure. Many bolt failures caused by bending fatigue were encountered during the entire fatigue program, as reported in Table 2.

TABLE 2. FATIGUE TEST SUMMARY

LOAD CONDITION (LB)	UPPER BEARING		LOWER BEARING		REMARKS
	S/N	CUMULATIVE FATIGUE CYCLES (MILLIONS)	S/N	CUMULATIVE FATIGUE CYCLES (MILLIONS)	
+600	F1	30.0	F2	30.0	Completion of Test Run
+800	F3	30.0	F4	30.0	Completion of Test Run
+800	F5	30.0	F6	30.0	Completion of Test Run (In- stall New Bolts in F5 & F6)
+1000	F5	44.2	F6	44.2	Failure of Bolt in Bearing F6 (Install New Bolts in F5 & F6)
+1000	F5	47.2	F6	47.2	Failure of Bolt in Bearing F6 (Install New Clevis and New Bolt for Bearing F6 Only)
+1000	F5	60.0	F6	60.0	Completion of Test Run (In- stall New Bolts in F5 & F6)
+1200	F5	60.7	F6	60.7	Failure of Bolt in Bearing F6 (Install New Bolt in F6 Only)
+1200	F5	61.4	F6	61.4	Failure of Bolt in Bearing F6 (Install New Bolts in F5 & F6. Interchange Positions of F5 and F6)

TABLE 2. FATIGUE TEST SUMMARY (Continued)

LOAD CONDITION (LB)	UPPER BEARING		LOWER BEARING		REMARKS
	S/N	CUMULATIVE FATIGUE CYCLES (MILLIONS)	S/N	CUMULATIVE FATIGUE CYCLES (MILLIONS)	
		F3		F5	
+1200		30.7	F5	63.2	Failure of Bearing F3 (In- stall F4 in Lieu of F3. New Bolt in F4. Old Bolt Re- mained in F5)
+1200	F4	30.05	F5	63.25	Failure of Bolt in F5. (In- stall New Bolt in F5 Only)
+1200	F4	33.0	F5	66.2	Failure of Bolt in F4. (In- stall New Bolt in F4 Only)
+1200	F4	40.8	F5	74.0	Failure of Bearing F5 (In- stall F2 in Lieu of F5. New Bolt in F2. Old Bolt Re- mained in F4)
+1200	F4	44.2	F2	33.4	Failure of Bolt in F2. (In- stall New Bolt in F2 Only)
+1200	F4	47.5	F2	36.7	Failure of Bolt in F2. (In- stall New Bolt in F2 Only)
+1200	F4	48.9	F2	38.1	Failure of Bolt in F2. (In- stall F1 in Lieu of F2. New Bolt in F1. Old Bolt Re- mained in F4)

TABLE 2. FATIGUE TEST SUMMARY (Continued)

LOAD (LB)	UPPER BEARING		LOWER BEARING		REMARKS
	CONDITION	CUMULATIVE FATIGUE CYCLES (MILLIONS)	S/N	CUMULATIVE FATIGUE CYCLES (MILLIONS)	
±1200	F4	49.0	F1	30.1	Failure of Bolt in F4. (In- stall New Bolt in F4 Only)
±1200	F4	51.0	F1	32.1	Failure of Bolt in F4. (In- stall New Bolt in F4 Only)
±1200	F4	52.2	F1	33.3	Failure of Bolt in F4. (In- stall New Bolts in F1 & F4. Interchange Positions of F1 & F4)
±1200	F1	39.9	F4	58.8	Increase Loading to ±1400 Lb
±1400	F1	40.2	F4	59.1	Increase Loading to ±1600 Lb
±1600	F1	41.1	F4	60.0	Increase Loading to ±2000 Lb
±2000	F1	41.2	F4	60.1	Stop Testing. F1 and F4 Were Both Very Hot.

C. Static Test

Specimen S3, which was a standard rod end, was installed in the Tinius Olsen testing machine. The tension load was slowly applied and was increased until the rod end failed. Figure 36 is a copy of the actual load-deflection plot which was automatically plotted by the Tinius Olsen machine and shows that specimen S3 failed at 8100 pounds tension.

Specimen S1, which was a wear-indicating rod end (WIRE), was loaded in the same manner and as shown in Figure 37 failed at a tension load of 6380 pounds. The failure occurred at the hole drilled for the wear-indicating bushing assembly (12 o'clock position), whereas specimen S3 had failed at the 4 o'clock position. Figure 38 is a photograph of these two failed specimens.

It is important to note that the load-deflection plots obtained from the Tinius Olsen machine and reproduced in Figures 36 and 37 are not usable for determining rod end deflections because the deflections plotted are summations of all the loading devices located between the upper and lower loading platens of the testing machine. Also, note the discontinuity in the load deflection plot of Figure 37 caused by slippage of the Tinius Olsen loading grips.

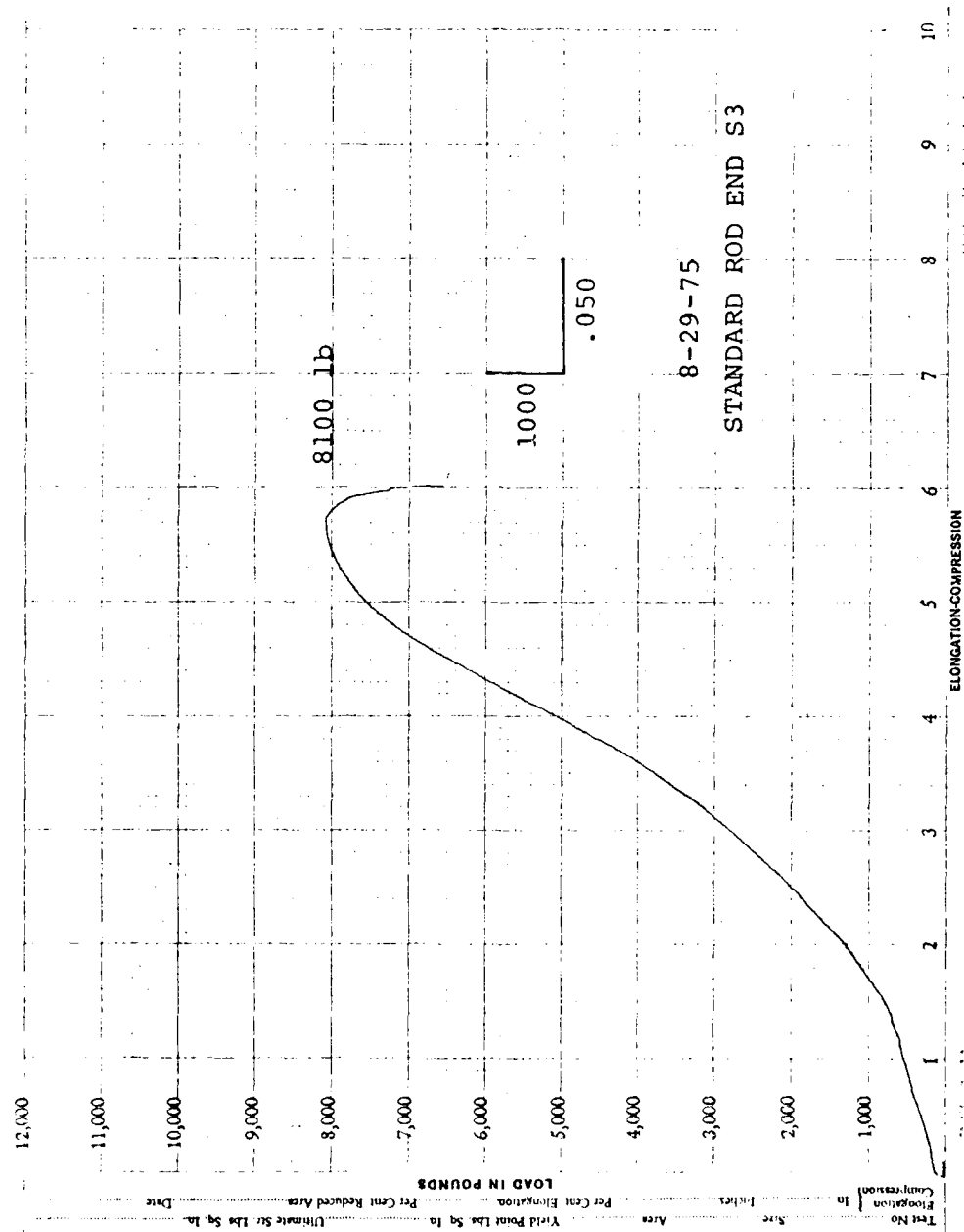


Figure 36. Load vs. Deflection - Standard Rod End S3.

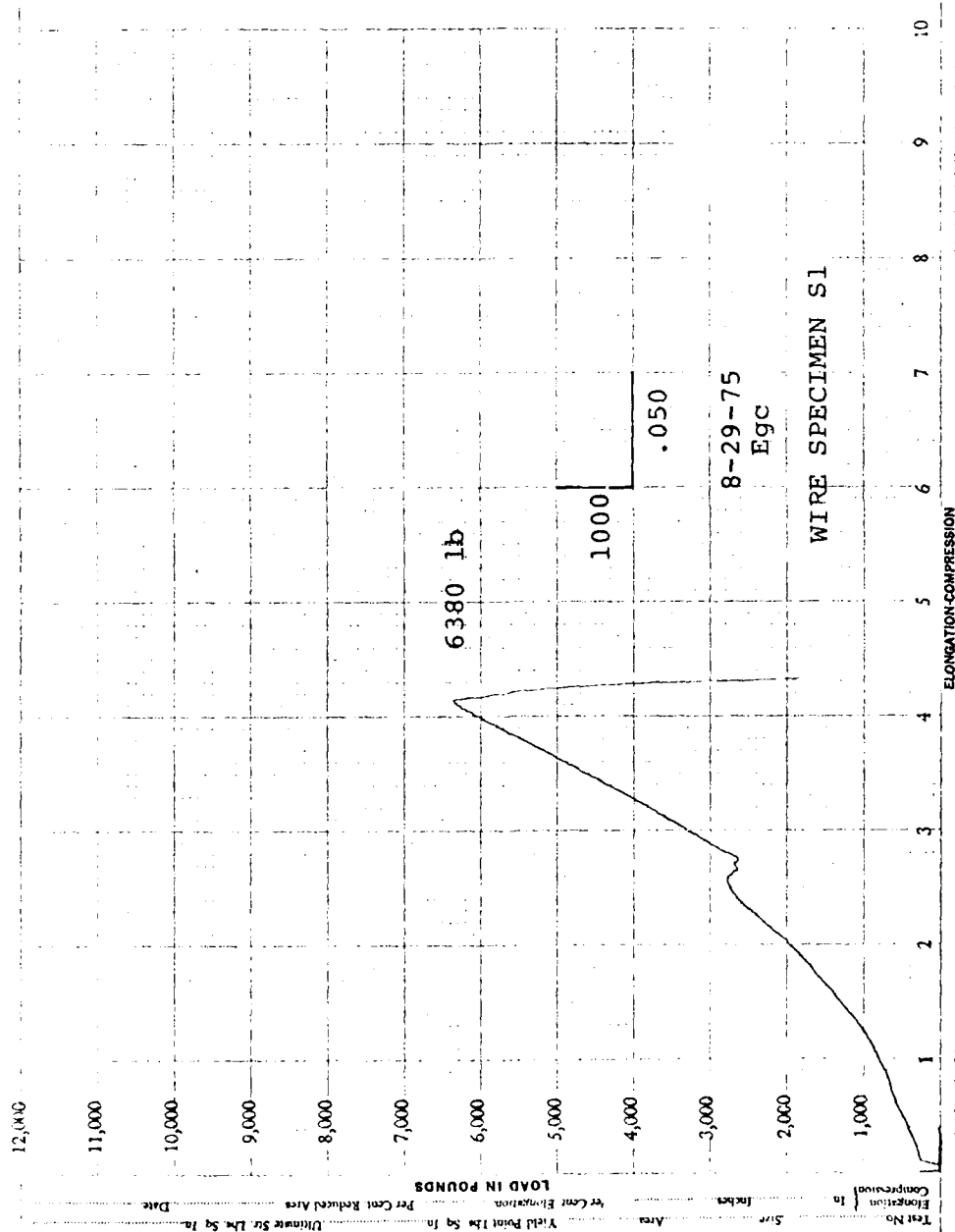


Figure 37. Load vs. Deflection - WIRE Test Specimen S1.

Wire, S1

Standard Rod End, S3

Section Cut
Out For Met-
allurgical
Evaluation

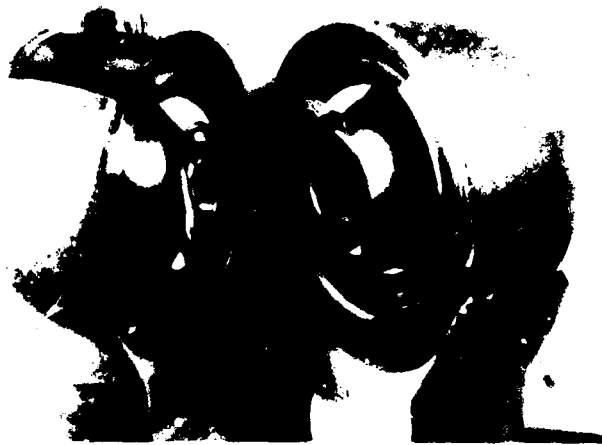


Figure 38. Photograph of Static Test Failures.

METALLURGICAL EVALUATION OF TESTED BEARINGS

LINER CONDITION AND BOND INTEGRITY

Specimens W1 through W21 were sectioned and examined for edge condition and setback, embedded contaminants, porosity, and tearing. Nothing of importance was found. All liners looked excellent in this respect. Also, all 21 of these bearings were inspected for defects in the liner bond. There were no voids or lack of liner bond noted in any of these. The area around the drilled hole showed no signs of distress, nor was there anything to be noted which would indicate a potential trouble area caused by the drilled hole.

DEBRIS RETENTION AND PIN HANG-UP

As shown in Table 3, the wear-indicating pins of all WIRE bearings except W2, W3, and W13 exhibited some tendency to hang up, with some bearings being worse than others. The sanitary bearings did not experience any hang-up until approximately 200 hours of testing, and even then the tendency to hang up was minimal. Fluid contaminants Skydrol 500A; TT-S-735, Type VII; P-D-680 Type I; salt water; and distilled water caused the most trouble with pin hang-up. The metallurgical evaluation showed that the debris cavities furnished by the design were filled to various degrees. Some of the worst cases were bearings W7, W8, W9, W10, W14, W15, W17, and W19. In each of these bearings, the wear debris had filled the circumferential debris cavity at the pin chamfer and had worked up along the shank of the measuring pin and also between the wear-measuring bushing O.D. and the I.D. of the drilled hole in the rod end. Bearing W7, which was contaminated with Skydrol 500A, had the worst debris problem. In this particular bearing, the debris was a black, gummy-looking material which resisted easy movement of the pin.

The pin hang-up phenomenon is considered to be a minor problem, in that operating personnel must be forewarned to reset the pin with an article more rigid than the fingernail. It was proven that the pin cannot be reset adequately with a fingernail. It is necessary to use something more rigid, such as a long bolt which can be gripped in the palm of the hand and used to apply a constant force with no impact.

TABLE 3. PIN HANG-UP SUMMARY

Rig Hours	ERROR CAUSED BY PIN HANG-UP (INCHES)							
	48	100	152	200	248	300	348	400
Bearing Designation								
W1	0	0	0	0	0	0	0.0006	0.0009
W2	0	0	0	0	0	0	0	0
W3	0	0	0	0	0	0	0	0
W4	0	0	0	0.0020				
W5	0	0	0	0.0010	0	0.0005	0	0
W6	0	0	0	0.0005	0	0	0	0.0006
W7	0.0120	0.0120	0	0				
W8	0	0.0050	0.0100	0.0110				
W9	0	0	0	0.0025				
W10	0	0.0010	0	0.0014				
W11	0	0.0010	0	0.0018				
W12	0	0.0080	0.0090	0.0090				
W13	0	0	0	0	0	0	0	0
W14	0	0.0006	?a					
W15	0	0.0023	?a					
W16	0.0007	0.0009	0.0010	0.0004				
W17	0	0.0037	0.0240	?b				
W18	0	0.0092	0.0110	?a				
W19	0.0005	0.0100	0.0130	0.0157				

a Bushing Movement Occurred

b Measuring Pin Below Surface

OUTWARD MOVEMENT OF WELDED BUSHING ASSEMBLIES

The wear-indicating bushing assemblies of bearings W14, W15, and W18 moved outward during the final 100 hours of testing. Figure 39 shows the displaced wear-indicating pin and bushing assembly of bearing W15. Bearing W14 was almost identical in appearance. Bearing W18 was significantly different and will be discussed later.

Bearings W14, W15, and W18 were sectioned through the pin hole and the welded zone. It was determined that no significant weld was obtained on W14 and W15. A weld depth of 0.050 inch before polishing had been specified for all the bearings.

In order to obtain more information on the weld depth, bearings W1, W16, S1, F3, S4, F5, and F6 were also sectioned. Table 4 lists the weld depths in addition to the banjo cross-sectional thickness for all these bearings. The average weld depth was approximately 0.010 inch with only specimen S1 having approximately 0.023 inch of weld penetration. Figures 40 and 41 are microphotographs of bearing W1, showing a typical welded bushing assembly.

FAILURE OF WEAR-INDICATING PIN FROM BEARING W18

The wear-indicating pin from bearing W18 was found broken off after removal from the wear test rig. The pin had just previously been used to obtain wear readings after the 200-hour test run. Also, as mentioned previously, the bushing assembly had displaced outward, but not in a symmetrical manner as had bearings W14 and W15. Figure 42 shows a horizontal crack through the welded area of bearing W18, which allowed the bushing to tip instead of moving out symmetrically as did W14 and W15. This tipping of the bushing assembly subsequently caused the wear-indicating pin to wear abnormally as shown in Figure 43. Also, unsymmetrical crimping of the locking tangs on the bushing assembly as shown in Figure 44 helped to cause a fatigue failure of the wear-indicating pin. Actually, only one tang was crimped inward and was forced against the pin in one local area, which caused a stress concentration and eventual failure origin.

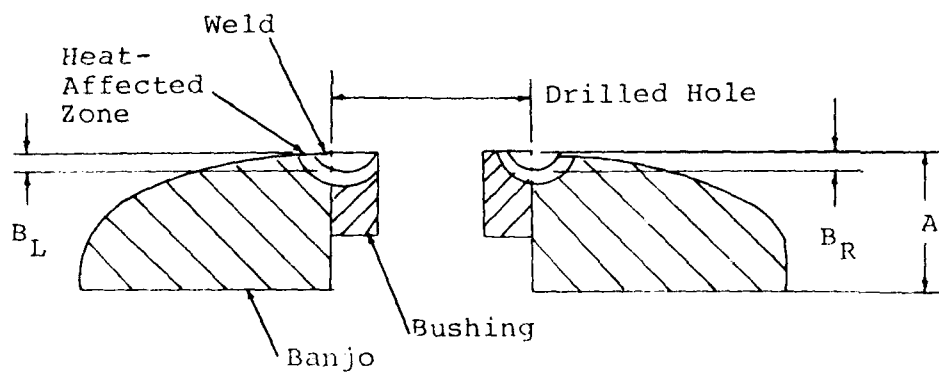


Figure 39. Displaced Bushing From Bearing W15.

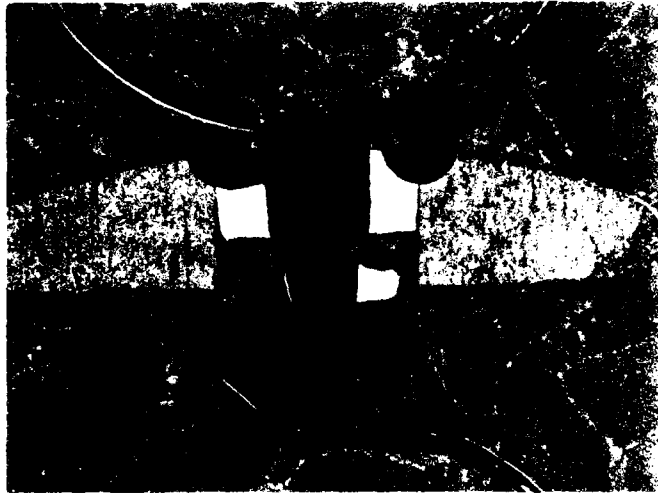
TABLE 4. MEASUREMENTS OF WELD PENETRATION

BEARING DESIGNATION	MEASUREMENTS (INCHES)		
	A	B _L	B _R
F3	0.082	0.013	0.013
F4	0.083	0.014	0.016
F5	0.085	0.006	0.009
F6	0.086	0.008	0.009
S1	0.087	0.026	0.022
W1	0.080	0.010	0.011
W14	0.083	0.000	0.000
W15	0.084	0.000 ^a	0.000 ^a
W16	0.072	0.008	0.007
W18	0.072	0.008	0.014
W21	0.090	--	--

^a Heat-Affected Zone Barely Visible



Mounting Clip (Not Part of Bearing)



8.33X

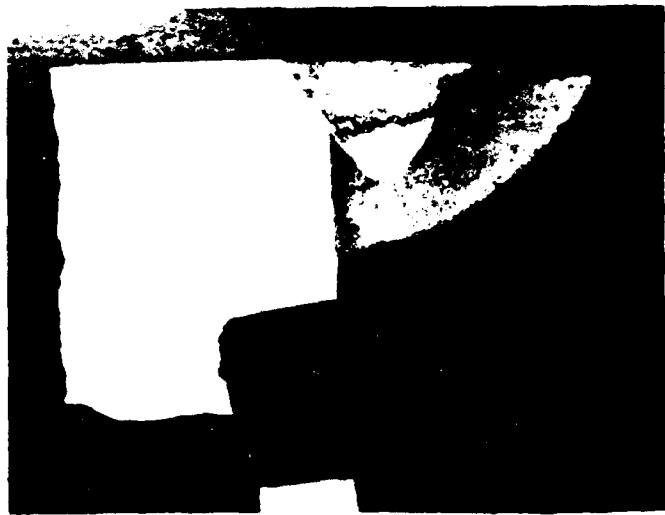
Mounting Clip (Not Part of Bearing)

Figure 40. Cross Section of Wl.



50X

Figure 41. Enlarged View of Electron Beam Weld on Bearing Wl.



50X

Figure 42. Cross-Sectional View of Failure of Beam

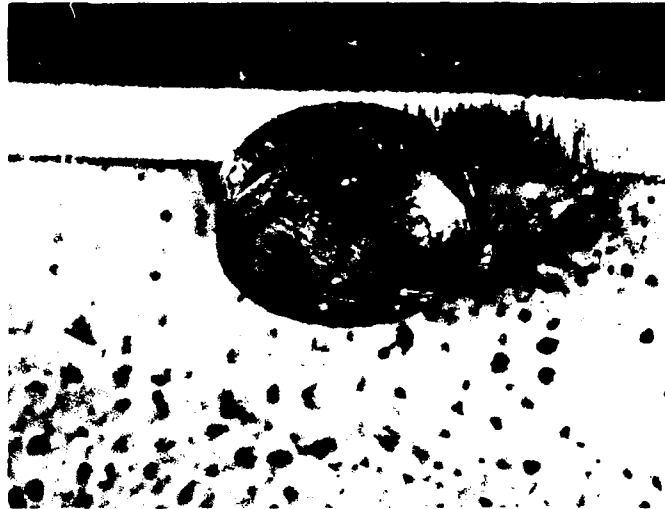


Figure 43. Abnormal Wear Pattern on Pin From

Failure Origin on
Fractured Surface
of Measuring Pin

Unsymmetrical C
of Locking Tang

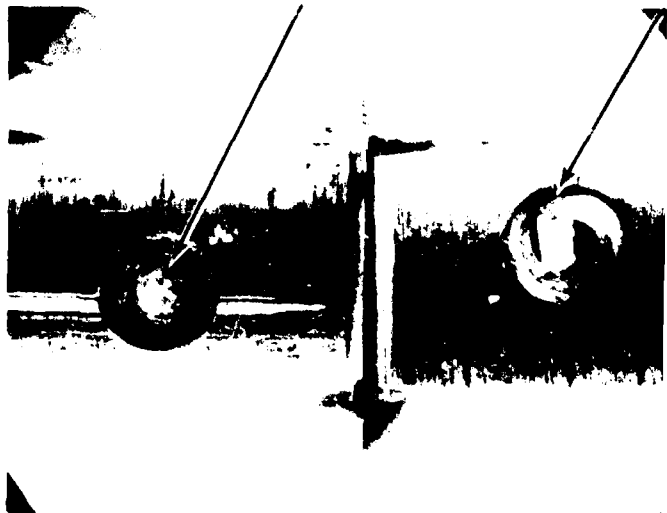


Figure 44. Failed Pin on Bearing W18.

FATIGUE FAILURES

As shown in Figure 45, bearing F3 failed through the hole drilled for the wear-indicating device at the 12 o'clock position. Two failure origins were located on the O.D. of the banjo adjacent to and on each side of the drilled hole. Even though there was considerable fretting visible on the I.D. of the banjo, the failure origins were located on the O.D. in the welded area.

Bearing F5 failed at both the 4:30 and 7:30 o'clock positions in the banjo. Each fracture had a failure origin located at the I.D. of the banjo at the half-width location and was coincident with fretting which had occurred at this location because of micromotion occurring between the I.D. of the banjo and the O.D. of the swaged-in spherical bearing. This failure is representative of the most common type of classical rod end fatigue failure.

Bearing F6 had three fractures, located at the 3 o'clock, 9 o'clock, and 12 o'clock positions. The failures at the 3 o'clock and 9 o'clock positions were fatigue failures in the aforementioned classical manner. The fatigue origins were associated with fretting at the I.D. of the banjo and were very similar to those described for bearing F5. The fracture at the 12 o'clock position was similar to the fracture described for bearing F3, but the fatigue progression was relatively small. The fatigue progression at 3 o'clock and 9 o'clock encompassed a larger portion of the failed cross section, thus indicating that the failures at the 3 o'clock and 9 o'clock positions had started first. There was a definite gunmetal blue discoloration localized around the fracture area at the 12 o'clock position, indicating that this region had been heated to a high temperature before eventual bearing failure.

Bearings F1, F2, and F4 were magnafluxed after completion of the fatigue tests, and no cracks were found. No material defects were noted for bearings F3, F5, and F6 which could have contributed to the failures. Bearings S1 and S3 were also inspected, and no defects were found which contributed to the static failures.

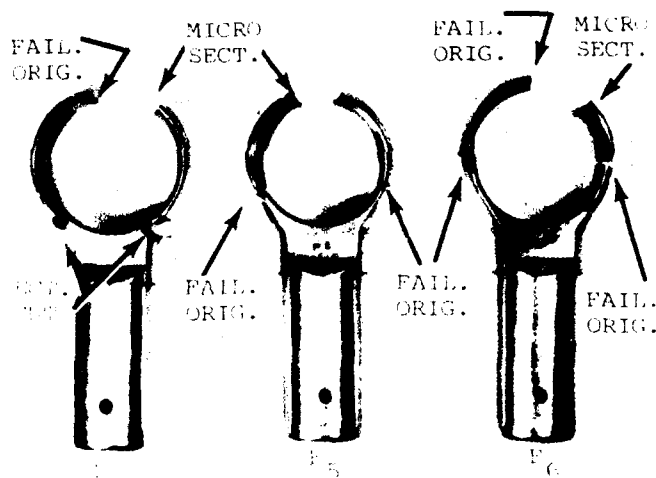


Figure 45. Fatigue Test Failure Locations.

ANALYSIS OF STATIC TEST AND FATIGUE TEST RESULTS

INTRODUCTION

To assess the ability of the WIRE to react measured UH-1 flight loads and to assess the effect of the device on a standard rod end, the following items were considered:

1. Results of static and fatigue tests performed.
2. Comparison of test results to flight loads measured in the UH-1H damper rod.

STATIC TEST RESULTS

One standard rod end, S3, and one WIRE test specimen, S1, were tested to failure in static tension loading. Bearing S3 failed at 8100 pounds at approximately the 4 o'clock position. Since bearing S1 failed at 6380 pounds through the wear-indicating pin location, it is obvious that the static strength of the modified rod end has been reduced by 21% based on this single test. The bolt connecting the rod end to the damper on the Bell UH-1B, D, and H models is an AN-174H15 close-tolerance 1/4-inch-diameter bolt having an allowable load in single shear of 3680 pounds. Because this is a limiting value of the damper rod load and is nearly half of the tested static strength, the WIRE specimen has adequate static strength.

FATIGUE TEST RESULTS

A. Determination of Mean Load-Cycle Curve

Six WIRE specimens were subjected to the fully reversed vibratory loads summarized in Table 5. The test results from these specimens were used in conjunction with the static test result from specimen S1 to obtain the mean load-cycle curve shown in Figure 46. The actual steps involved are described as follows:

1. Plot on semilogarithmic paper the bearing S1 static failure of 6380 pounds at one cycle and the conservative runout value of ± 1000 pounds, approximated from Table 5, at 30 million cycles. See Figure 46.
2. Through these two points, draw a curve which is parallel to a reference curve. This reference curve

TABLE 5. FATIGUE TEST LOAD-CYCLE SUMMARY

BEARING S/N	BUSHING	LOAD	CYCLES AT LOAD (MILLIONS)	CYCLES CUMULATIVE (MILLIONS)	RESULT
F1	PRESS	+600	30	30	No Failure
		±1200	9.9	39.9	
		±1400	0.3	40.2	
		±1600	0.9	41.1	
		±2000	0.1	41.2	
F2	PRESS	+600	30	30	No Failure
		±1200	8.1	38.1	
F3	WELD	+800	30	30	Failure
		±1200	0.7	30.7	
F4	WELD	+800	30	30	No Failure
		±1200	28.8	58.8	
		±1400	0.3	59.1	
		±1600	0.9	60.0	
		±2000	0.1	60.1	
F5	WELD	+800	30	30	Failure
		±1000	30	60	
		±1200	14	74	
F6	WELD	+800	30	30	Failure
		±1000	30	60	
		±1200	2.5	62.5	

DESIGN CONCEPT NO. 4

DESCRIPTION:

A single hole is drilled through the banjo and race. A pin and bushing are used as in Design No. 2. An elastomeric O-ring keeps the pin from falling into the bolt hole during functional inspection as in Design No. 1.

ADVANTAGES COMPARED TO DESIGNS NOS. 1, 2 AND 3:

1. Machining the banjo and race are greatly simplified by eliminating the counterbore.
2. The drilled hole can be ballized to produce a residual compressive layer adjacent to the hole, thus increasing fatigue strength if required.
3. Space is provided for debris accumulation adjacent to the pin/ball contact.

DISADVANTAGES COMPARED TO DESIGNS NOS. 2 AND 3:

1. The pin could be pushed into the ball bolt hole with a wire.
2. The pin is not well supported to react the out-of-plane loads caused by sliding at the pin/ball contact.

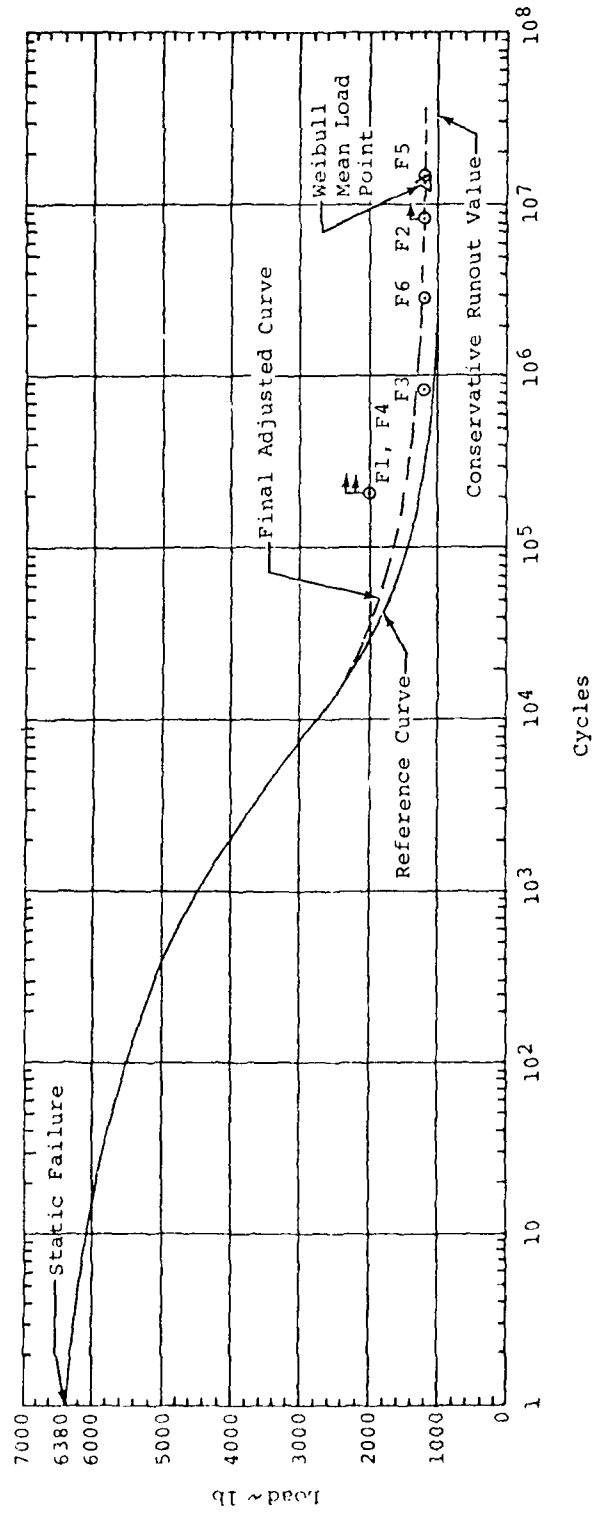


Figure 46. Load vs. Cycles.

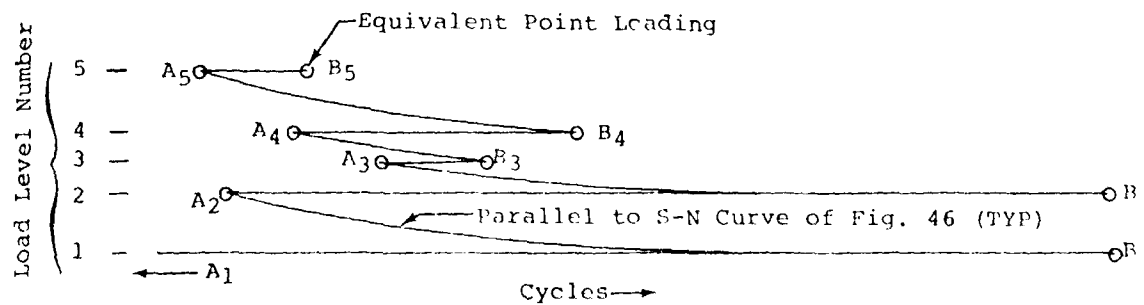
was taken from NACA TN 3866³ and represents an S-N curve for 4130 steel, 125,000 H.T., having a notch of $K_t = 2.0$. (The rod end banjo material is 4340 steel, 125,000 H.T. which has the same fatigue characteristics as 4130 steel. Figure 69 of Stress Design Factors⁴ was used to calculate a stress concentration factor, K_t , of 2.36 for the rod end banjo with a drilled hole. It was assumed that the differences in shape of the S-N curve for a notch of $K_t = 2.0$ and $K_t = 2.36$ are minimal and no correction were made.)

3. Reduce the spectra of Table 5 to one equivalent point loading for each specimen by the use of the previously plotted reference curve of Figure 46 in conjunction with commonly accepted cumulative damage techniques. Chapter 12 of Metal Fatigue⁵ describes the method of drawing curves parallel to the S-N curve in order to reach each new load level. Table 6 lists the data for each rod end as used for the cumulative damage analysis, together with a typical reduction of the loading spectra to one equivalent point. See Figure 46 for points plotted for specimens F1 through F6.
4. Perform a Weibull analysis as described in report PWA 3001⁶ for the six test specimens. Table 7 shows the ranking used and Figure 47 shows the three failure points plotted on a Weibull Probability Chart. The straight line drawn through the three points intersects 1.36×10^7 cycles at the 50% failure line. This indicates that the mean load-cycle curve to be determined must pass through the point representing 1.36×10^7 cycles and ± 1200 pounds of load.

-
- 3 Illg, Walter, Fatigue Tests on notched and unnotched sheet specimens of 2024-T3 and 7075-T6 Aluminum Alloy and of SAE 4130 Steel with special consideration of the life range from 2 to 10,000 cycles, NACA TN 3866, Dec. 1956.
 - 4 Peterson, R.E., Stress Concentration Design Factors, John Wiley and Sons, Inc., October 1953.
 - 5 Sines, George and Waisman, J.L., Metal Fatigue, McGraw-Hill Book Company, Inc., 1959.
 - 6 Mitchell, R.A., Introduction to Weibull Analysis, PWA 3001, 6 Jan. 1967.

TABLE 6. DATA FROM CUMULATIVE DAMAGE ANALYSIS

BEARING S/N	LOAD LEVEL NUMBER	LOAD (POUNDS)	CYCLES (MILLIONS) AT POINT A	CYCLES (MILLIONS) AT POINT B
F1	1	+600	0.000	30.000
	2	± 1200	0.068	9.970
	3	± 1400	0.330	0.630
	4	± 1600	0.195	1.095
	5	± 2000	0.110	0.210
F2	1	+600	0.000	30.000
	2	± 1200	0.068	8.168
F3	1	+800	0.000	30.000
	2	± 1200	0.130	0.830
F4	1	+800	0.000	30.000
	2	± 1200	0.130	28.930
	3	± 1400	0.330	0.630
	4	± 1600	0.195	1.095
	5	± 2000	0.110	0.210
F5	1	+800	0.000	30.000
	2	± 1000	0.310	30.310
	3	± 1200	0.325	14.320
F6	1	+800	0.000	30.000
	2	± 1000	0.310	30.310
	3	± 1200	0.325	2.820



Typical Reduction of the Loading Spectra
to one Equivalent Point

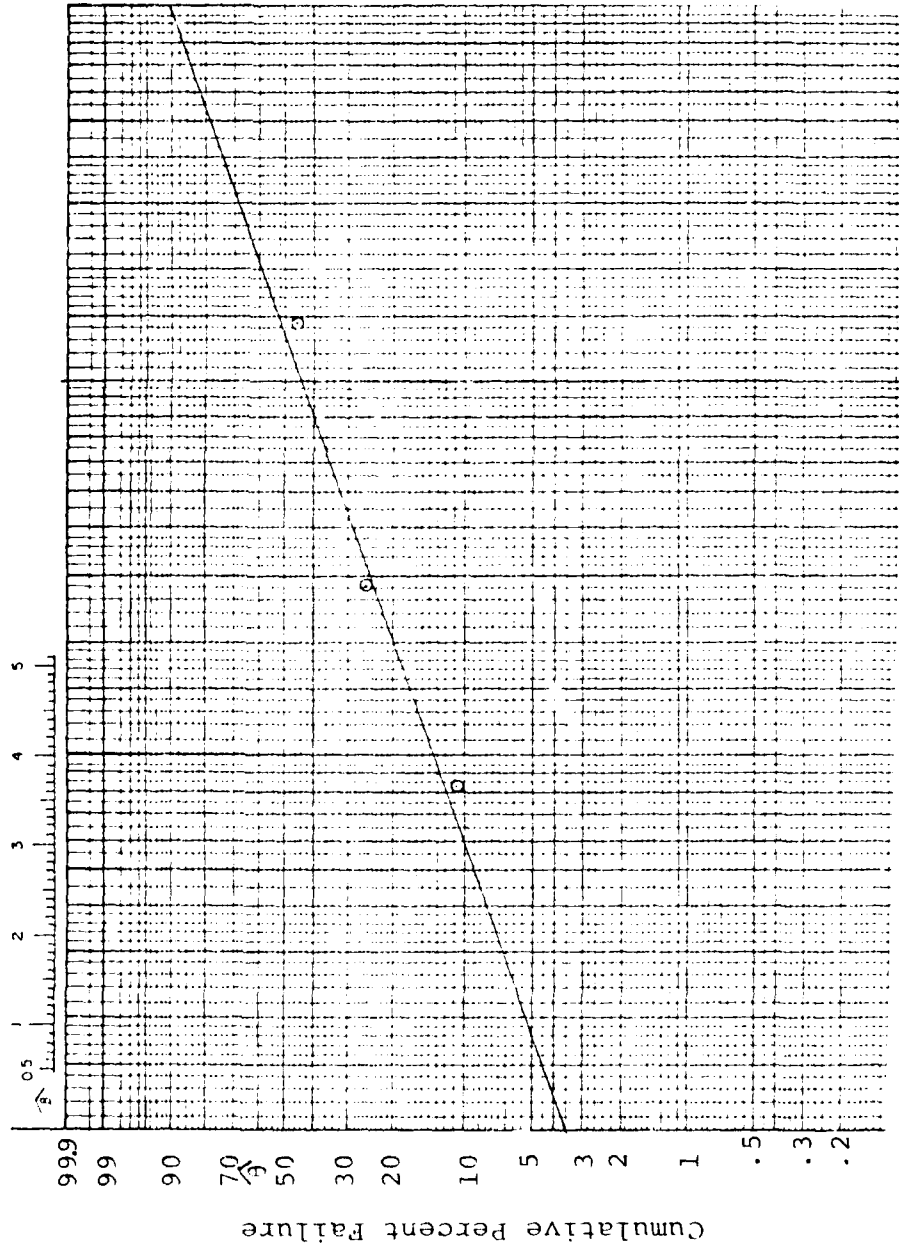
TABLE 7. WEIBULL ANALYSIS

ORDER NUMBER	BEARING S/N	CYCLES (MILLIONS)	TEST RESULT	RANK ORDER NUMBER	MEDIAN RANK
1	F3	0.830	Failure	1	10.9
2	F6	2.820	Failure	2	26.4
3	F2	8.168	Suspension		
4	F5	14.320	Failure	3.25	46.0
5	F1	9.970*	Suspension		
6	F4	28.930	Suspension		

*Note: Specimen F1 has the equivalent of at least 15×10^6 cycles at the ± 1200 pound load level when the testin at the ± 1400 , ± 1600 , and ± 2000 pound levels is considered.

WEIBULL PROBABILITY CHART

ESTIMATION POINT ③	PREPARED BY	DATE	DATA SOURCE	ITEM NAME
	REMARKS	ITEM NUMBER		



5. Draw the final adjusted curve through the static failure point and the point obtained from the Weibull analysis.
6. Consider the final adjusted curve to be the mean load-cycle curve of the WIRE specimens based on the test data for six fatigue test specimens.

B. Endurance Limit

The endurance limit of the WIRE specimens (assuming a life of 30×10^6 cycles defines the endurance limit) as read from the final adjusted load-cycle curve of Figure 46 is ± 1190 pounds.

C. Discussion

It can be seen from Figure 46 that the six test points (three failures and three suspensions) all fall within a very reasonable scatter band of values. There is no indication from the test point positions of Figure 46 that two separate modes of failure are present. In addition, the three WIRE fatigue test failures exhibited mixed modes of failure even with both modes occurring simultaneously on specimen F6. Thus, it is obvious that the addition of the wear-indicating device has created a second location of possible fatigue failure (12 o'clock) with essentially the same strength level as the classical rod end fatigue failure location (3 to 5 and 7 to 9 o'clock).

D. Comparison of Test Results and Measured Loads

The in-flight vibratory loads measured in the damper rod are presented in Appendix C. The highest load measured was ± 38 pounds and was obtained in a 45° banked turn. This maximum vibratory load was measured under steady-state conditions. For other maneuvers not flown, it is conservatively estimated that transient vibratory loads of twice the ± 38 -pound load can be obtained. For proper helicopter control design, the fatigue strength of a given part should be at least 3 times the measured high-speed level-flight loads or 1.5 times the measured maneuver loads on that part. It follows that the vibratory design load on the damper rod should be:

$$(\pm 38 \text{ pounds}) (2) (1.5) = \pm 114 \text{ pounds}$$

This value is well within the demonstrated fatigue strength of the WIRE of ± 1190 pounds.

CONCLUSIONS

The results of the static test show a 21% reduction in strength in the WIRE compared to the standard rod. However, the attachment bolt through the rod end limited the load to 3680 pounds in single shear and probably limited bending of the bolt. The static test strength of 6380 pounds, is almost twice this value and is satisfactory by comparison. The results of the fatigue test show that the WIRE has essentially the same strength as the rod end.

The WIRE is considered to be structurally adequate for both the static and fatigue requirements of the UH-1H helicopter.

CONCLUSIONS

Wear testing of the 19 WIRE test specimens and 2 standard ends demonstrated the following:

1. The wear endurance of the rod end has not been prejudiced by incorporation of the WIRE device.
2. The wear-indicating device gives relatively good and reliable indications of the radial play of the rod end.
3. The wear-indicating device will operate properly even though the rod end has been contaminated with fluids, dust, or salt water.
4. The wear-indicating pin will hang up and give erroneous results if the finger nail is used to reset the pins.

Fatigue testing of the six WIRE test specimens proved the basic fatigue strength of the rod end has not been reduced by addition of the WIRE device.

Static testing indicates that the ultimate strength of end has been reduced by approximately 20%. This reduced ultimate static strength is not considered to be significant for a rod end bearing. These bearings normally fail by wear or fatigue. In addition, the reduced rod end static strength greatly exceeds the strength of the mounting bolt.

RECOMMENDATIONS

The reported program has successfully met the initial designing, fabricating, and testing a wear-indicating device. The testing performed can not be considered sufficient for application qualification of the wear-indicating rod end shape formed on operational helicopters.

The electron beam welding procedure should be investigated in order to obtain better weld depth and more consistency.

APPENDIX A

EVALUATION OF SEVEN PRELIMINARY DESIGNS

DESIGN CONCEPT NO. 1

DESCRIPTION:

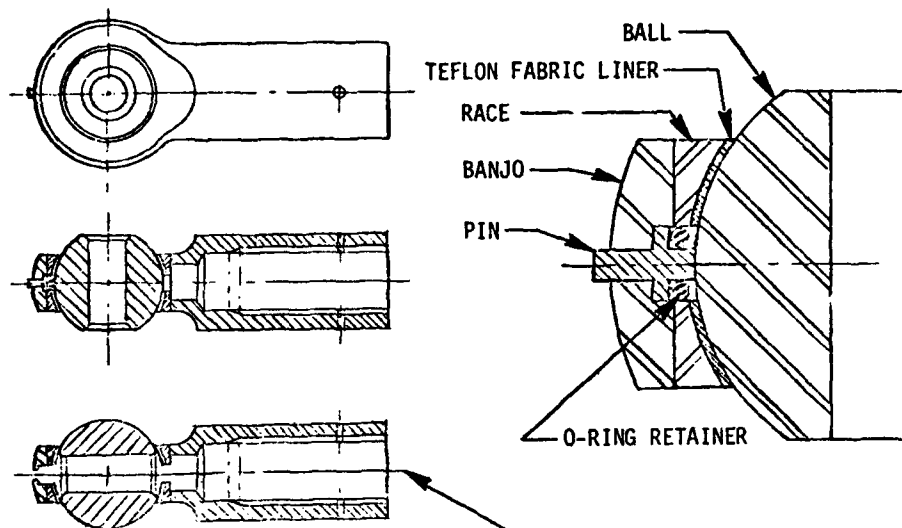
The indicating pin is trapped with a hole counterbored into the housing. The arrangement for machining is illustrated as a machining detail. The pin is made of beryllium copper. In the galvanic series, beryllium copper is very close and slightly anodic to both 410C stainless steel (race) and 440C stainless steel (ball). The pin hardness is RC20, which is less than the race (RC30-40) and the ball (RC58). Thus, the pin will wear, not the ball or the housing. The pin material does not gall or sieze when sliding on stainless steel. An elastomeric O-ring retainer surrounds the pin below the flange. This retainer is intended to prevent the pin from falling into the bolt hole when the ball is positioned as shown on the machining detail. The ball will be so positioned by anyone checking whether the pin is free to move.

ADVANTAGES:

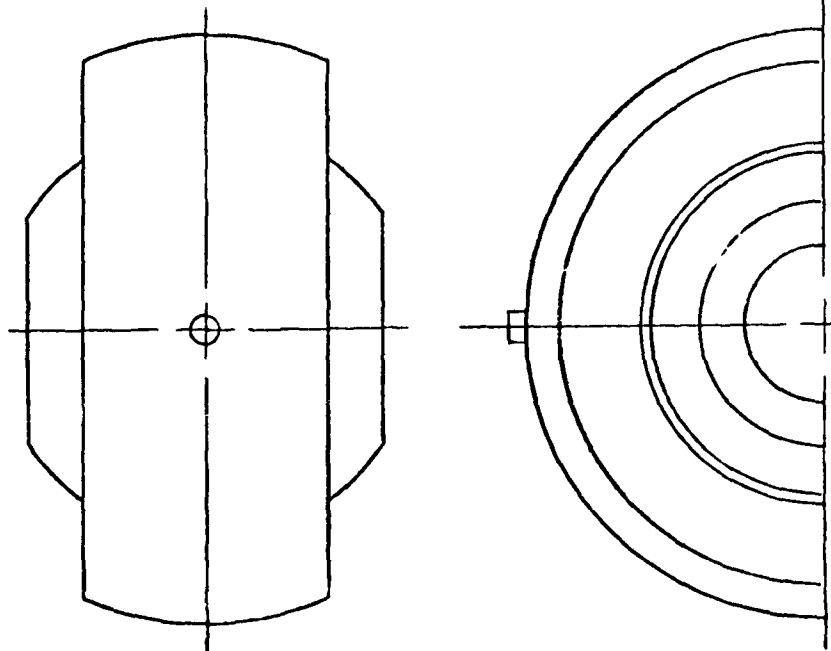
1. The pin is the only accurately machined new part.
2. The rod end external geometry has the least change.
3. Space is provided for debris accumulation adjacent to the pin/ball contact.

DISADVANTAGES:

1. Machining the cavity is difficult and must be accurate.
2. Liner material is removed on the side opposite the pin.
3. The pin could be pushed into the ball bolt hole with a wire.
4. The pin is not well supported to react out-of-plane loads caused by sliding at the pin/ball contact.



MACHINING DETAIL - COUNTERBORE THRU SHANK



DESIGN CONCEPT NO. 1

DESIGN CONCEPT NO. 2

DESCRIPTION:

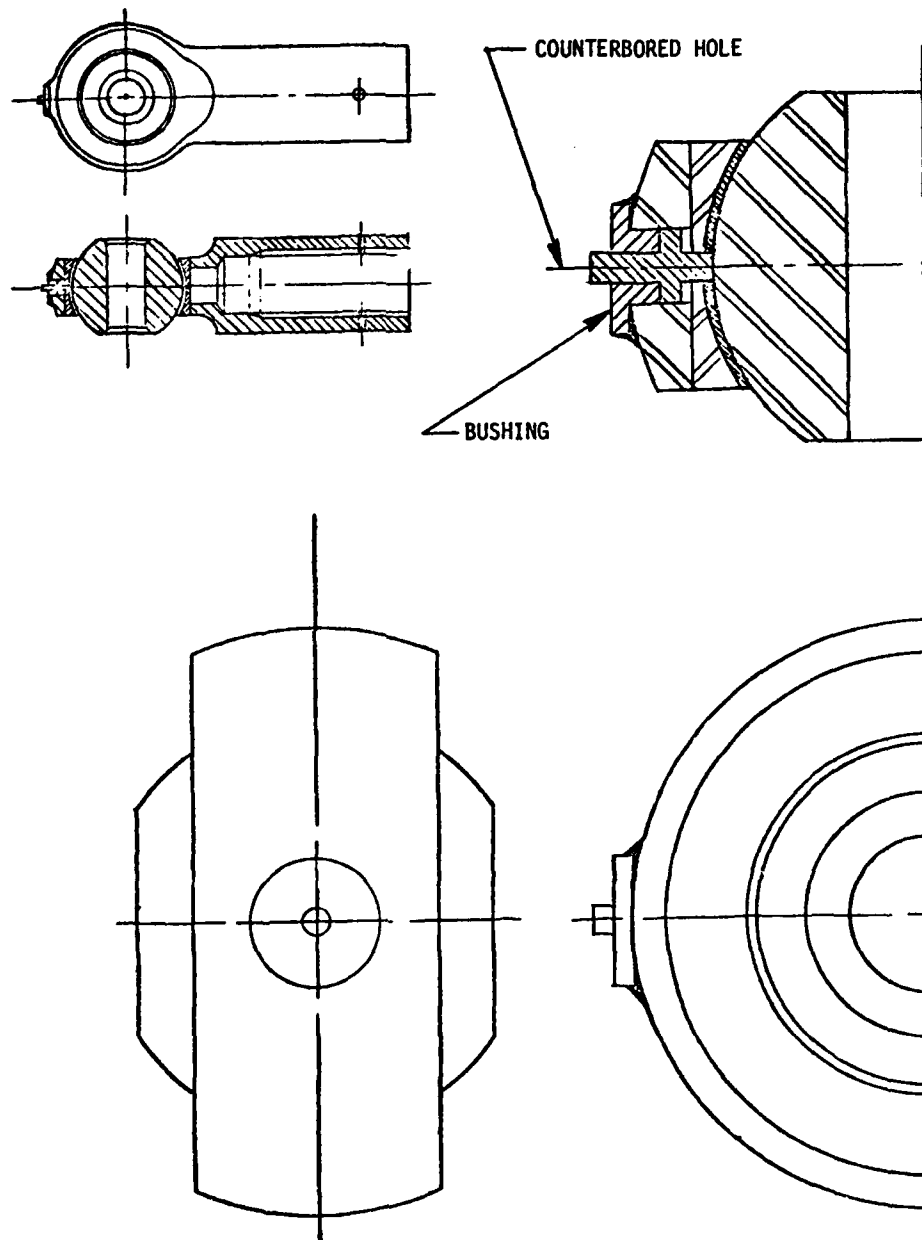
A small hole is drilled through the banjo and race. A larger counterbored hole is made through the banjo only. The pin is trapped in place by a bushing which is bonded in place. Pin material is beryllium copper.

ADVANTAGES COMPARED TO DESIGN NO. 1:

1. The pin cannot be lost.
2. The bushing flange is a good reference surface to measure wear against.
3. Machining the cavity is easier.
4. The pin is forced into firm contact with the ball by the pressed-in bushing.
5. The pin is well supported to react the out-of-plane loads caused by sliding at the pin/ball contact.

DISADVANTAGES COMPARED TO DESIGN NO. 1:

1. Two close-tolerance parts are required.
2. No space is provided for debris accumulation adjacent to contact.



DESIGN CONCEPT NO. 2

DESIGN CONCEPT NO. 3

DESCRIPTION:

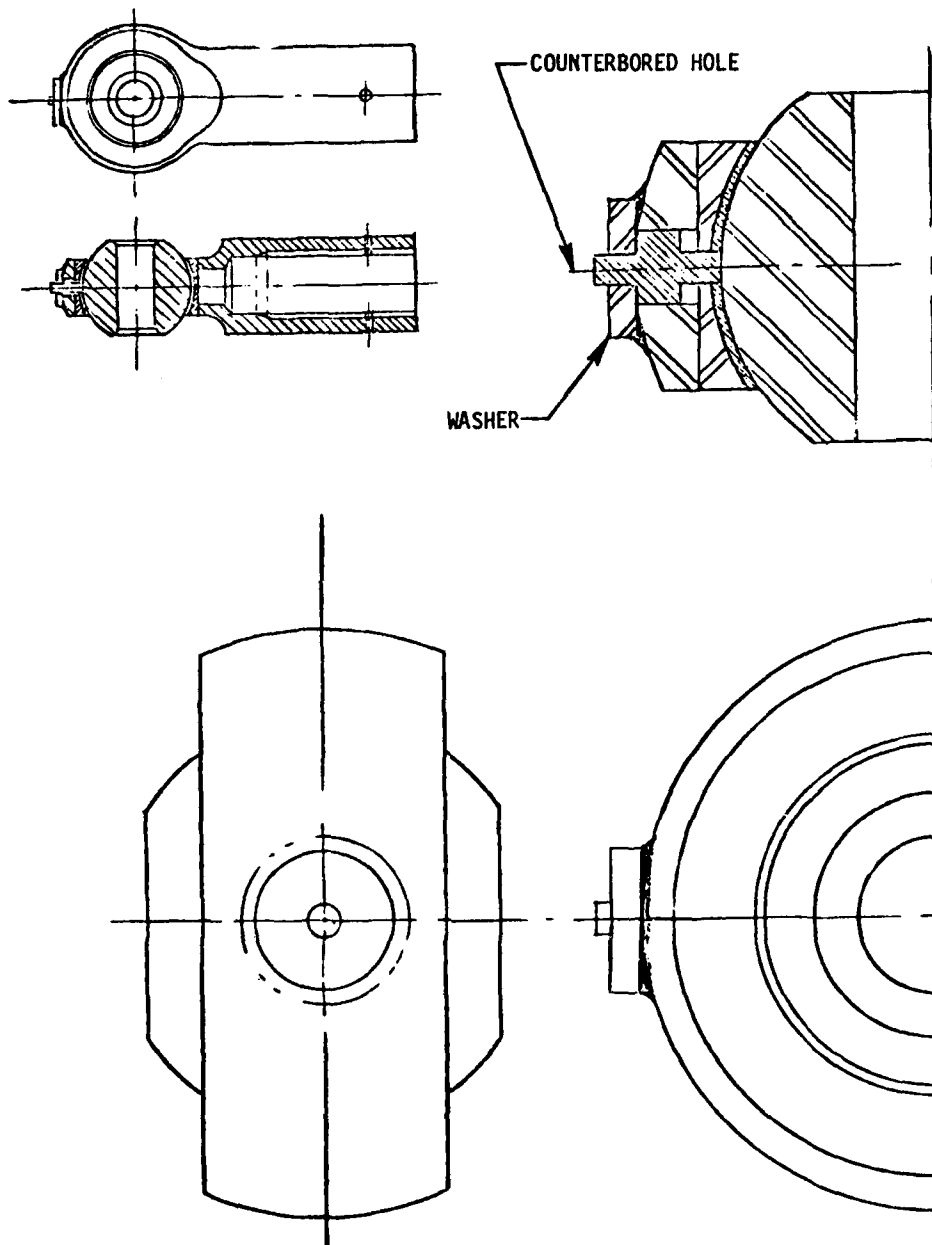
Same cavity formation as Design No. 2. The pin has a thicker flange than Design No. 2. The pin is retained by a washer bonded in place, rather than the bushing used in Design 2.

ADVANTAGES COMPARED TO DESIGN NO. 2:

1. The pin flange is thicker.
2. The pin is the only accurately machined new part.

DISADVANTAGES COMPARED TO DESIGN NO. 2:

1. Load toward the pin is reacted only by the bond which holds the washer in place. The bond may creep under sustained load.



DESIGN CONCEPT NO. 3

DESIGN CONCEPT NO. 4

DESCRIPTION:

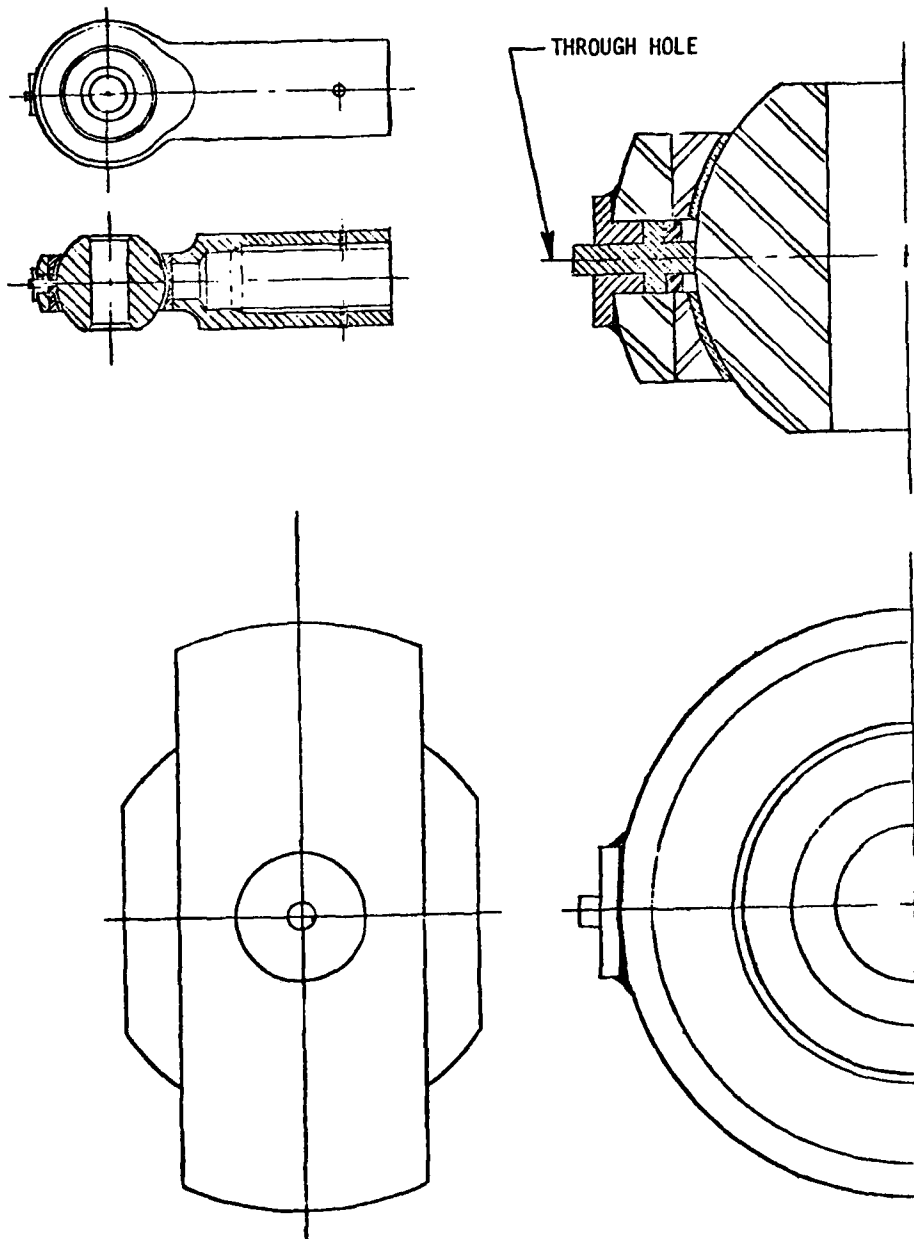
A single hole is drilled through the banjo and race. A pin and bushing are used as in Design No. 2. An elastomeric O-ring keeps the pin from falling into the bolt hole during functional inspection as in Design No. 1.

ADVANTAGES COMPARED TO DESIGNS NOS. 1, 2 AND 3:

1. Machining the banjo and race are greatly simplified by eliminating the counterbore.
2. The drilled hole can be ballized to produce a residual compressive layer adjacent to the hole, thus increasing fatigue strength if required.
3. Space is provided for debris accumulation adjacent to the pin/ball contact.

DISADVANTAGES COMPARED TO DESIGNS NOS. 2 AND 3:

1. The pin could be pushed into the ball bolt hole with a wire.
2. The pin is not well supported to react the out-of-plane loads caused by sliding at the pin/ball contact.



DESIGN CONCEPT NO. 4

DESIGN CONCEPT NO. 5

DESCRIPTION:

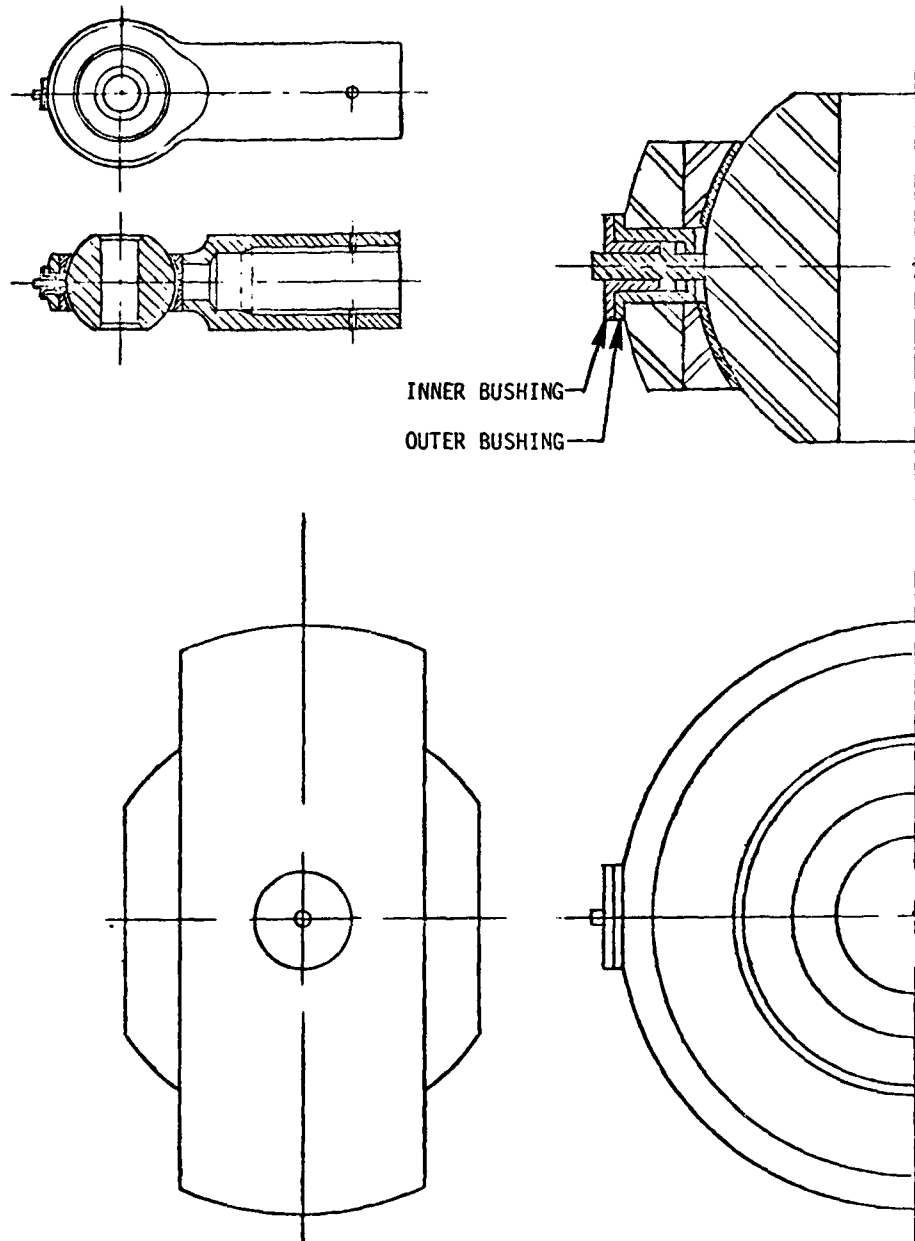
The pin is retained and positioned by a bushing within a bushing. A hole is drilled through both the banjo and the race. The hole is larger in diameter than required in Design No. 4 because the outer bushing is used.

ADVANTAGES COMPARED TO DESIGNS NOS. 1 THROUGH 4:

1. Machining the rod end is simplified compared to Designs Nos. 1, 2 and 3.
2. The drilled hole can be ballized.
3. The pin is retained.
4. The pin is well supported to react the out-of-plane loads caused by sliding at the pin/bail contact.
5. Space is provided for debris accumulation adjacent to the pin/ball contact.

DISADVANTAGES:

1. The hoop strength of the banjo is less than that of Designs Nos. 1 through 4 because a larger hole is required by the outer bushing.
2. Three close-tolerance machined parts are required.



DESIGN CONCEPT NO. 5

DESIGN CONCEPT NO. 6

DESCRIPTION:

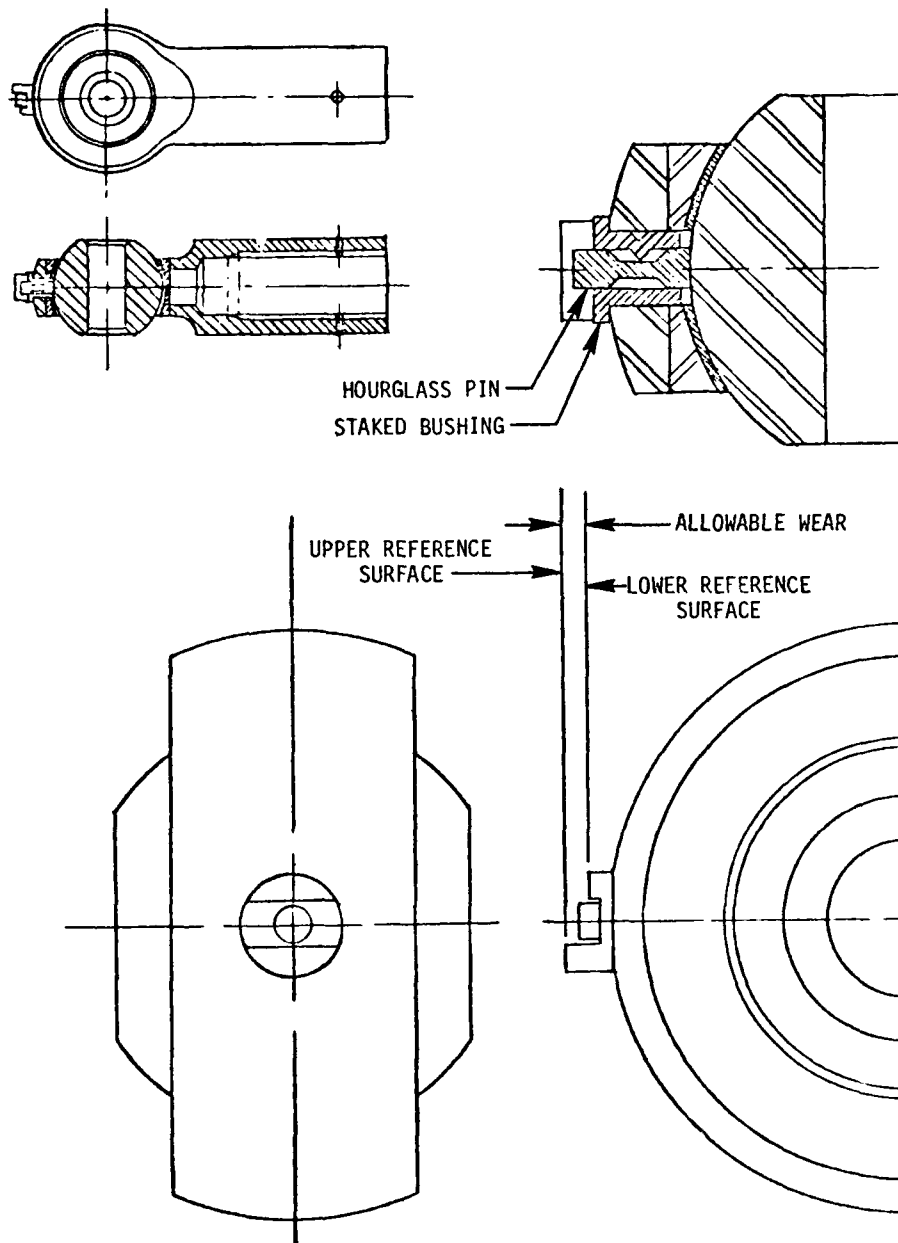
The pin is hourglass shaped and is retained by a staked bushing. The pin is magnetized to induce firm contact with the ball. The firm contact is intended to prevent debris from entering between the pin and the ball. The face of the pin has a baked-on Teflon coating. The bushing has two reference surfaces. Each surface location defines allowable wear in one direction. Total allowable radial wear is the distance from the upper surface to the lower surface. The pin material is 440C stainless steel.

ADVANTAGES COMPARED TO DESIGNS NOS. 1 THROUGH 5:

1. The advantages of the through hole are retained.
2. The raised reference surface protects the pin.
3. The out-of-plane loads are insignificant because wearing away of the pin is not required.
4. Space is provided for debris accumulation adjacent to the pin/ball contact.

DISADVANTAGES COMPARED TO DESIGNS NOS. 1 THROUGH 5:

1. The measurement works if the wear is equal in both directions. The pin could not indicate wear accurately if all the wear took place on the top or the bottom of the bearing.
2. Measurement is more complicated because ball load must be reversed and pin location assessed twice.



DESIGN CONCEPT NO. 6

DESIGN CONCEPT NO. 7

DESCRIPTION:

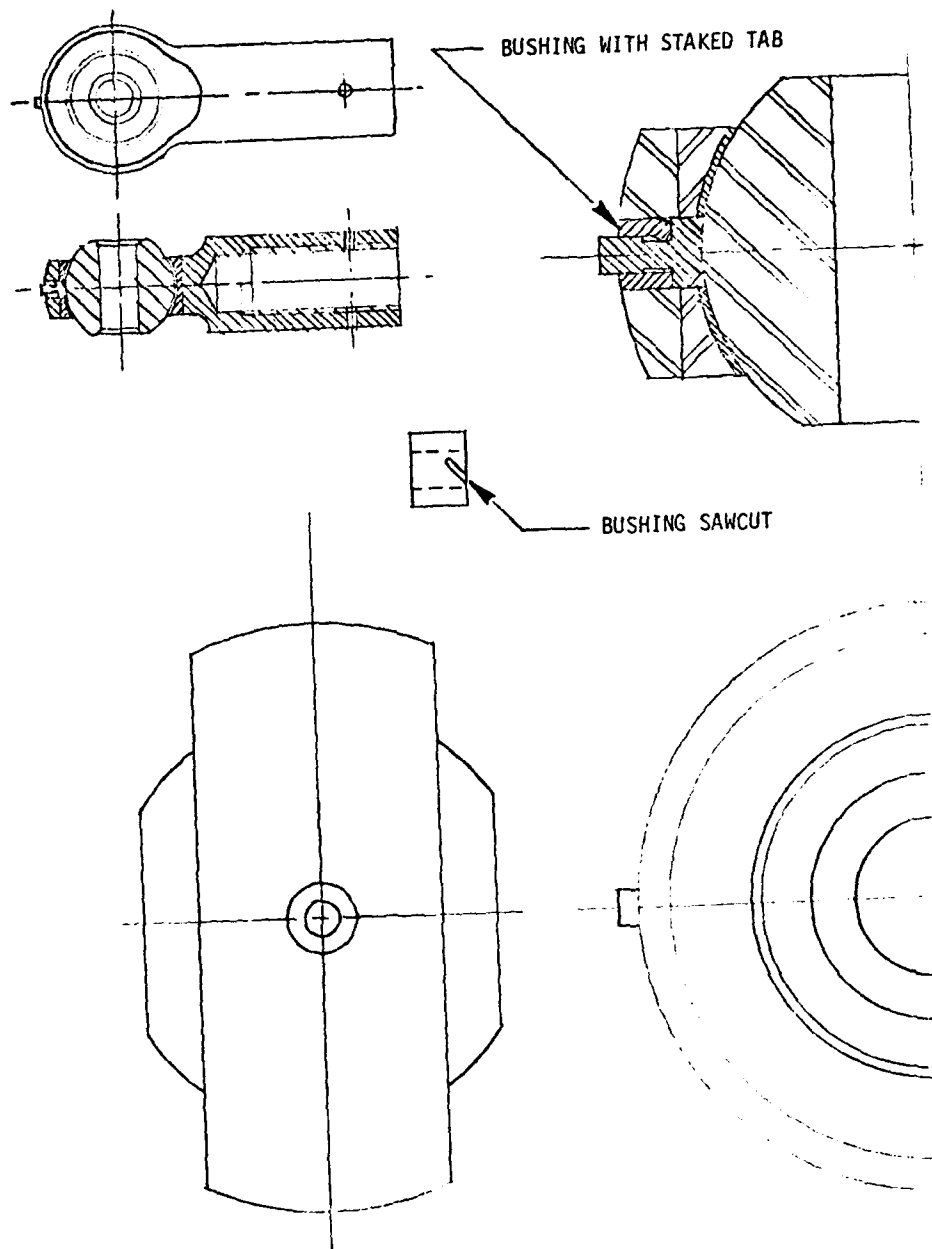
A single hole is drilled through the banjo and race. The pin has a recessed annular groove immediately above the pin flange. The bushing has a sawcut which forms a tab. The tab is staked into the pin groove, thus keeping the pin from falling into the bolt-hole during functional inspection. The bushing is machined flush with the rod end after installation.

ADVANTAGES:

1. The advantages of the through hole are retained.
2. The pin is positively retained.
3. The pin is well supported to react the out-of-plane loads caused by sliding at the pin/ball contact.
4. Space is provided for debris accumulation adjacent to the pin/ball contact.

DISADVANTAGES:

1. The pin is more difficult to machine than the other design concepts.



DESIGN CONCEPT NO. 7

RATING^a OF DESIGN CONCEPTS

Evaluation Factors	<u>Design Number</u>						
	1	2	3	4	5	6	7
Relative Difficulty of Machining	10	8	6	2	10	2	4
Effect on Banjo Strength	4	6	6	2	8	2	2
Murphy-proof Pin Retention	4	2	2	4	2	2	2
Debris Cavity Adjacent to the Pin/Ball Contact	2	4	4	2	2	2	2
Possible Mechanical Failure	4	4	8	4	4	2	2
	weak pin support	no debris trap	creep, no debris trap	weak pin support	weak-est banjo		
Possible Misinterpretation	4	2	2	2	2	10	2
TOTAL	28	26	28	16	28	20	14
Total Without Machining	18	18	22	14	18	18	10

a Equal weight is used for all factors. The range is 2 minimum to 10 maximum in steps of 2. Lowest score is best.

APPENDIX B

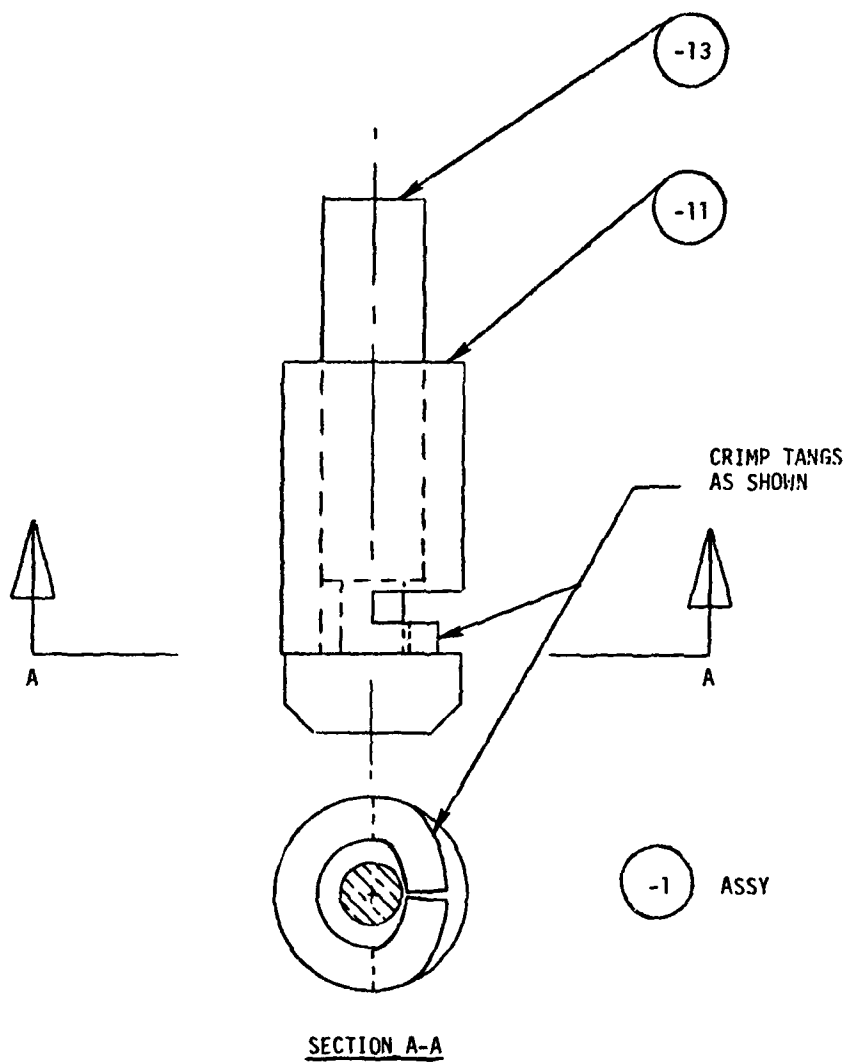
WIRE MANUFACTURE

Manufacturing Notes for SK24-410 Pin and Bushing Assembly:

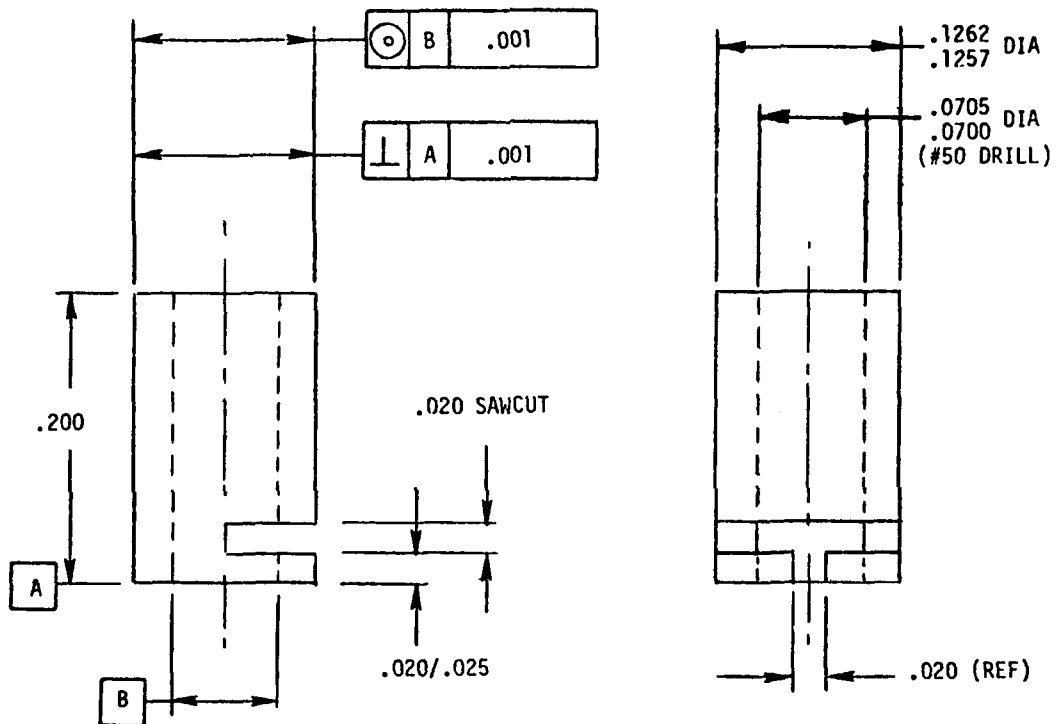
1. -11 Bushing to be made from .188 diameter x .06 wall thickness x .25 inch length of 410 Cres. Steel Rod per material specification AMS 5613.
2. -11 Bushing to be heat treated to 133,000 psi minimum tensile strength, Rockwell C28-36, per KPS 219, Class II.
3. -13 Pin to be made from .125 diameter x .38 length of beryllium copper rod per material specification CA173, Condition H.
4. -13 Pin to be heat treated to 112,000 psi minimum tensile strength, Condition H.
5. Magnetic particle inspect per KPS 208 rating "B".

Manufacturing Notes for SK24-411 Wear Indicating Rod End Indicator Installation:

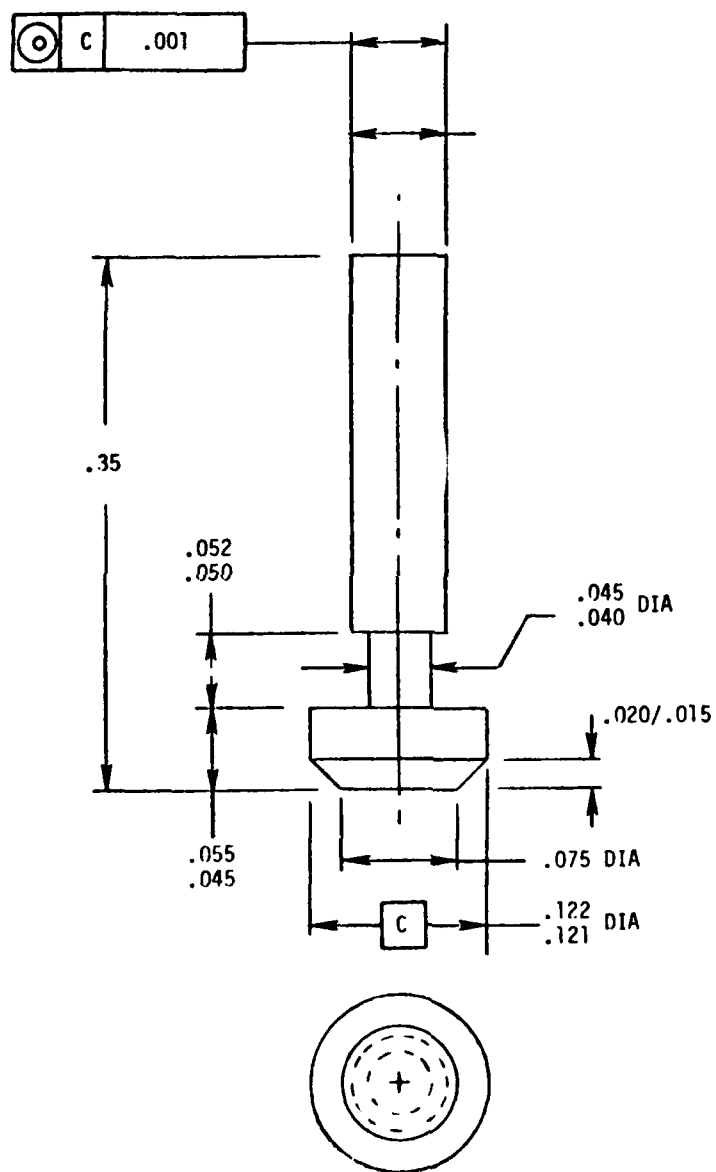
1. Brush cadmium plate per Spec. QQ-P-416.
2. Extreme care should be taken to maintain ball cleanliness each time the ball is rotated out-of-plane, thus eliminating possible contamination of the bearing.
3. Final cleaning (ultrasonically) to be performed with ball rotated as shown in Step V. Subsequent soak in air circulating oven at 160°F + 10°F for one hour before rotating ball back to position shown in Step I. (Manufacturing Steps I thru VI are given on following pages.)



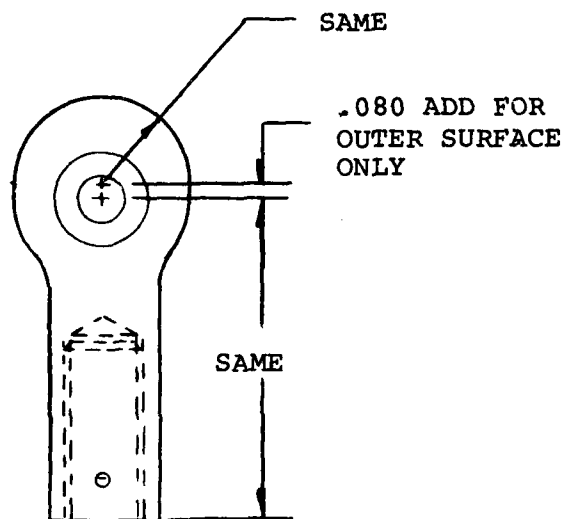
Pin and Bushing Assembly



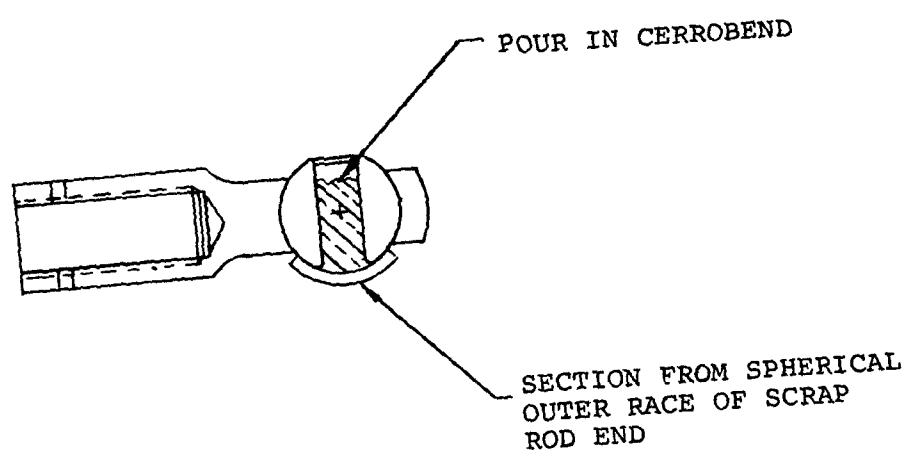
DETAIL - 11 Bushing



DETAIL -13 Pin

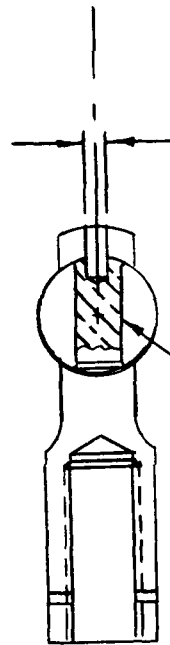


BELL NO. 47-140-252-3
FSN 3120-269-4453 ROD END
RECOMMENDED DESIGN CHANGE FOR NEW MFG.



STEP I

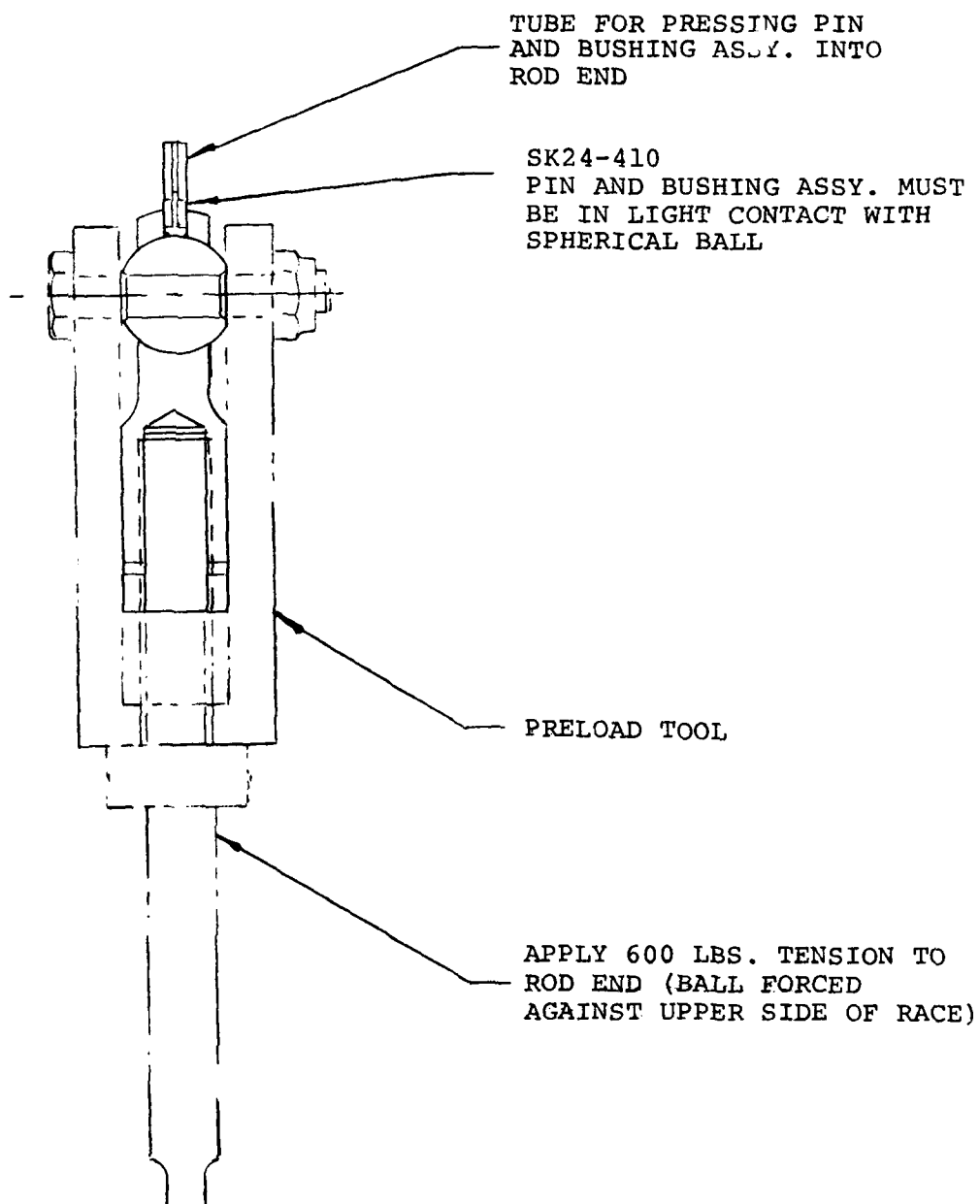
ROTATE BALL TO ALIGN CERROBEND
SLUG WITH CENTERLINE



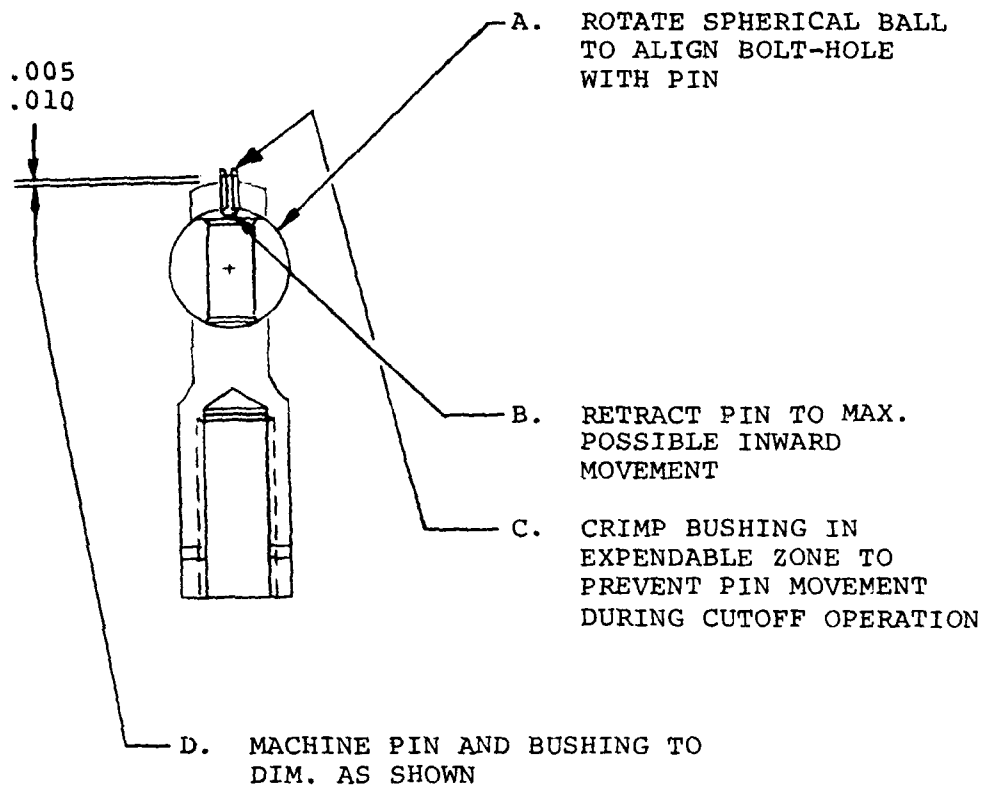
.1255
.1250 DIA. THRU OUTER RACE

CERROBEND SLUG BACK UP
FOR DRILLING. AFTER
DRILLING, CLEAN ULTRASONICALLY,
ROTATE BALL AND REMOVE CERRO-
BEND SLUG

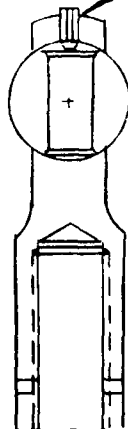
STEP II



STEP III



STEP IV



ELECTRON BEAM WELD ALL
AROUND BUSHING .050
DEPTH PER MIL-W-46132.
WITH PIN RETRACTED,
FILL CRACK BETWEEN
PIN & BUSHING WITH
WAX. MASK OFF BALL.
MAKE SURE DEBRIS IS
EXCLUDED FROM INTERIOR
WEAR SURFACE.

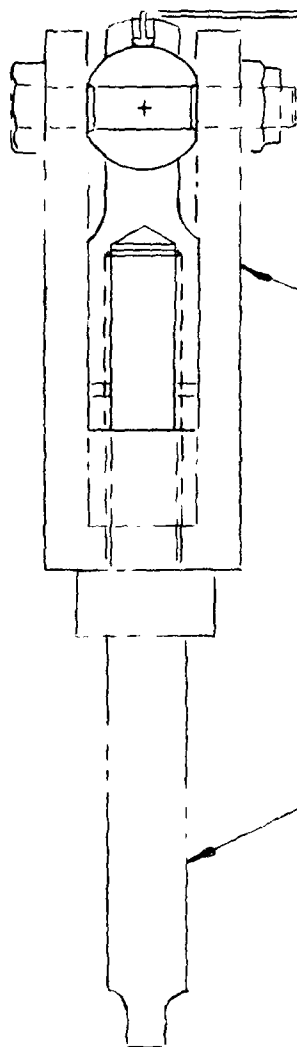
POLISH SMOOTH SO PIN
AND BUSHING ASSY. BLEND
WITH OUTER SURFACE.

BRUSH CADMIUM PLATE OUTER
SURFACE PER NOTE #1 WHILE
SUPPORTING THE ROD END WITH
THREADED SHANK UP. REMOVE
SEALER FROM BETWEEN PIN &
BUSHING. REMOVE BALL MASKING.

STEP V

MACHINE PIN HEIGHT EQUAL TO
ALLOWABLE WEAR AFTER APPLYING
TENSION

.012 INCH FOR FSN 3120-269-4453
CLEAN PER NOTE #3



PRELOAD TOOL

APPLY 600 LB. TENSION TO
ROD END (BALL FORCED
AGAINST UPPER SIDE OF
RACE)

STEP VI

APPENDIX C

FLIGHT TEST LOADS

Damper rod flight loads were obtained, during flight, on a UH-1H helicopter for conditions of climbs and descents, constant altitude coordinated banked turns, and airspeed sweeps. The various test conditions were flown at gross weights of 8250 and 9500 pounds with a mid-range center of gravity, approximately fuselage station 138. Climbs and descents to autorotation were conducted at 70 knots indicated airspeed at the lighter gross weight. Coordinated banked turns were flown at both gross weights at airspeeds of 50 and 90 knots. Airspeed sweeps, ranging from in-ground-effect hover to approximately 120 knots, were flown at both gross weights.

Prior to the start of testing, a deadweight calibration of the damper rod was performed in increments of 20 pounds to a maximum of 200 pounds tension. The calibration was fed through the same signal conditioning and recording channels as those used for the flight tests. Pre-flight and post-flight calibrations were conducted using a 100,000-ohm one-tenth of one percent precision calibration resistor. Inter-connecting wiring between the rotor system and airframe utilized a 164-channel slip ring and support shaft mounted in the main rotor shaft. The damper rod strain gages were wired to a B & F Instruments Model 24-200 balance box using a Trygon PS12-900F bridge power supply. The balance box, utilized as a signal conditioning unit, had its output wired to an onboard Pulse Code Modulation (PCM) encoder. The PCM signal was then transmitted from the test helicopter to the ground station via an L-band telemetry link. Figures C-1, C-2, and C-3 show the subject damper rod, the main rotor slip ring installation, and the onboard instrumentation package, respectively. The testing was conducted at the Kaman Aerospace Corporation Experimental Flight Test Facility by Kaman personnel between 21 August 1975 and 10 October 1975, involving 6 flights covering 5.4 hours of rotor time.

Figure C-4 presents plots of damper rod load in \pm pounds versus bank angle and airspeed. Figure C-5 is a plot of damper rod load versus rate of climb (descent) in feet per minute.

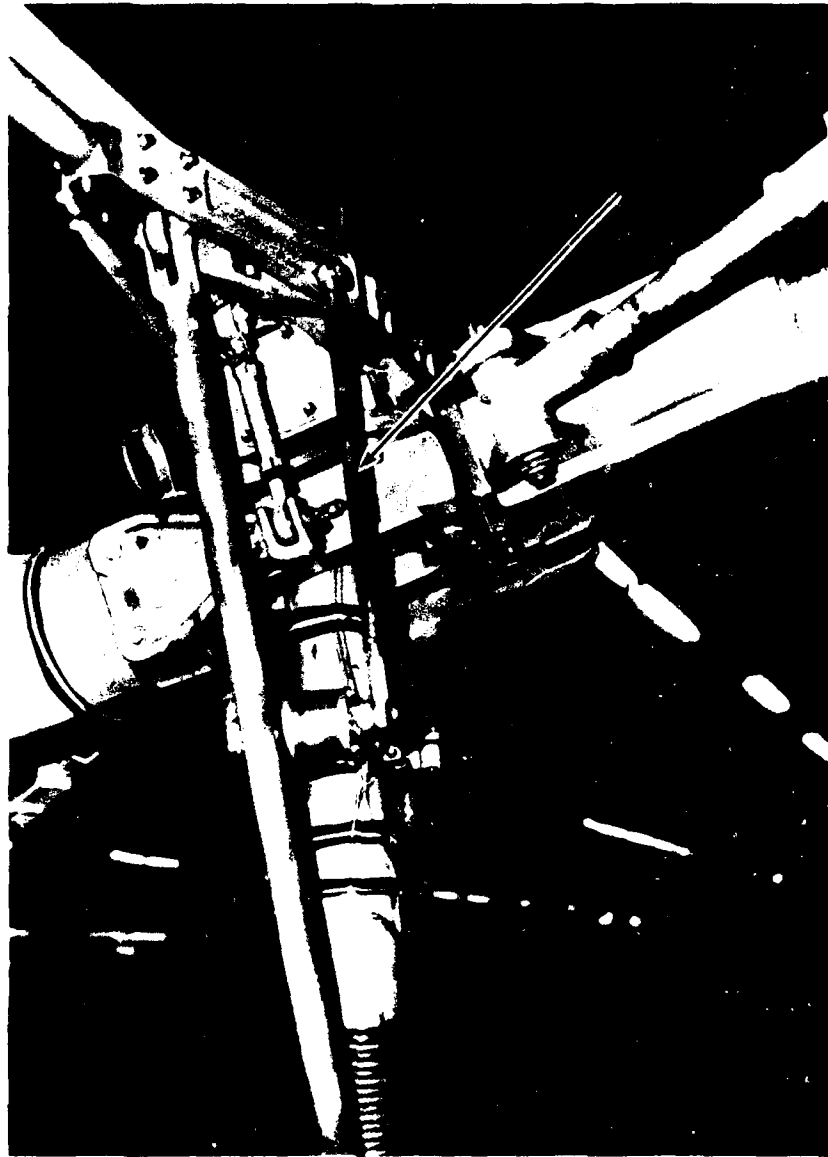


Figure C-1. Damper Rod Installation
on a UH-1H Helicopter.

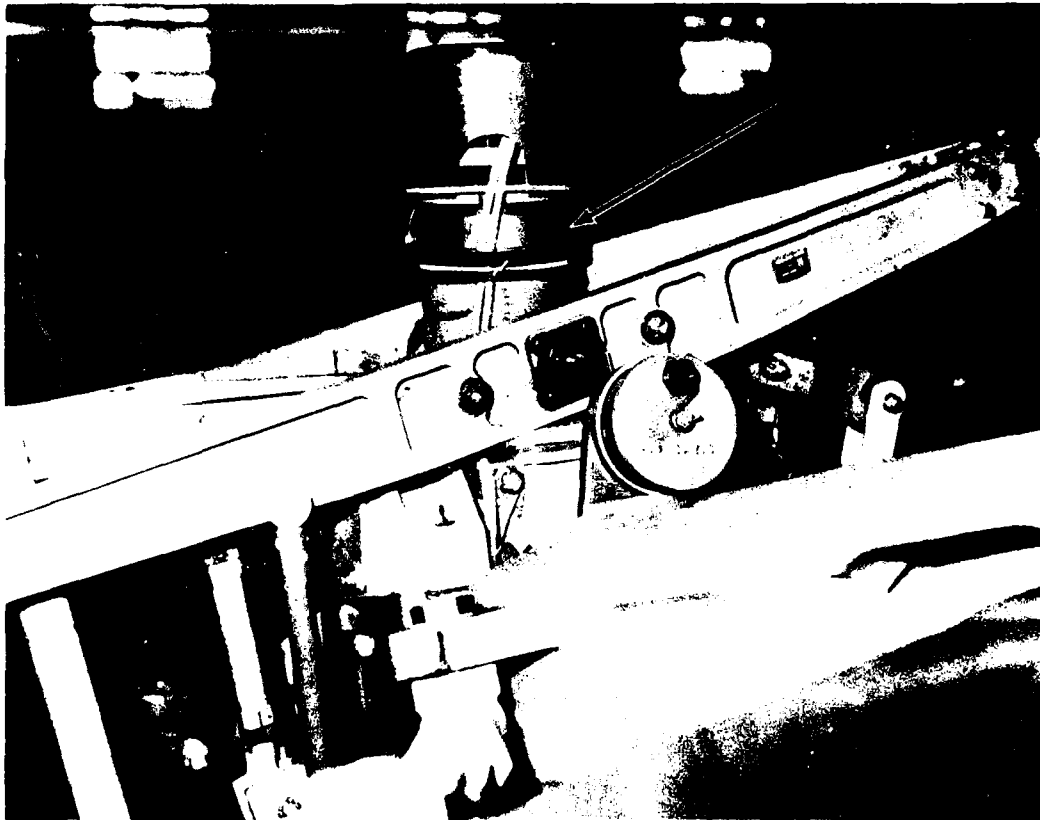


Figure C-2. Main Rotor Slip Ring
Installation on Rotor
Shaft.



Figure C-3. Onboard Instrumentation
Package as Seen From Left
Side of Helicopter.

UH-1H A/C S/N 66-1093

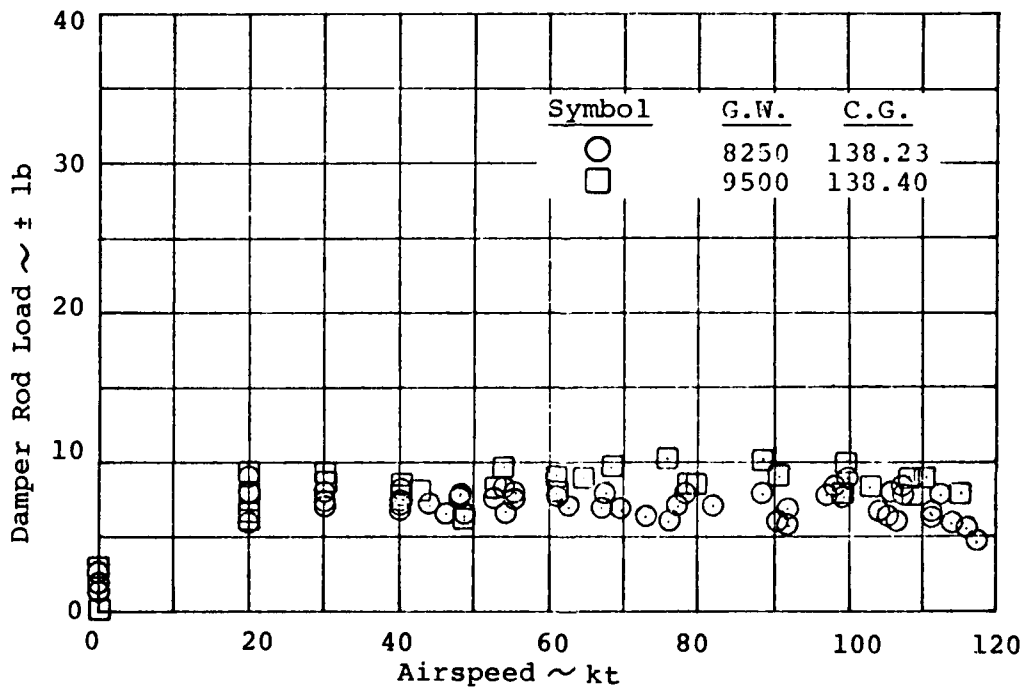
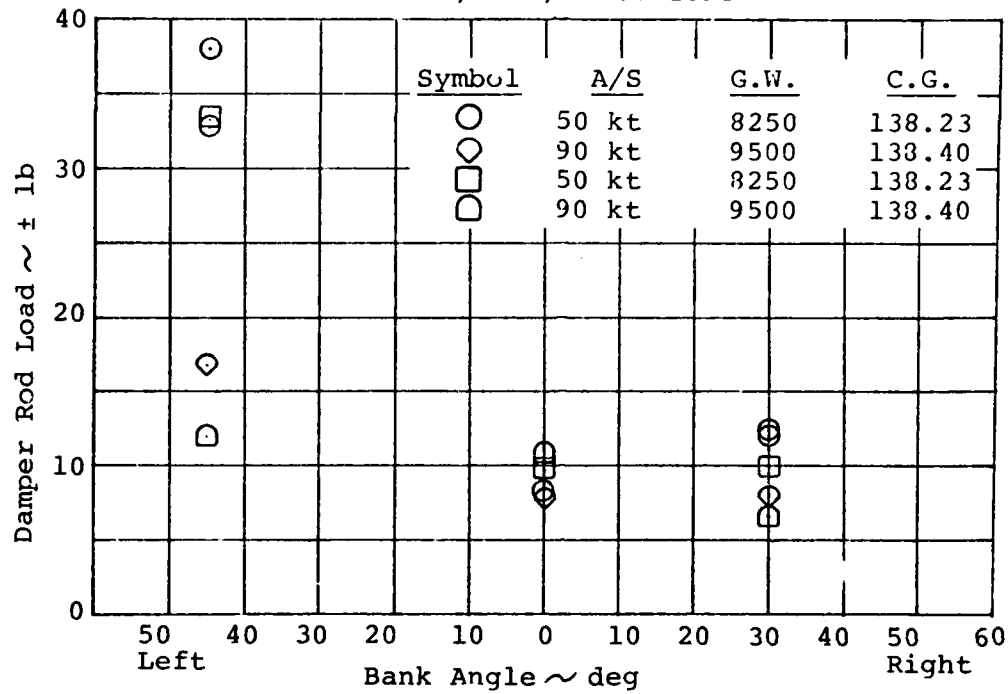


Figure C-4. Damper Rod Load vs. Bank Angle and Airspeed.

UH-1H Aircraft S/N 66-1093

<u>Symbol</u>	<u>A/S</u>	<u>G.W.</u>	<u>C.G.</u>
○	70 KT	8250	138.23
□	Indicates Autorotation		

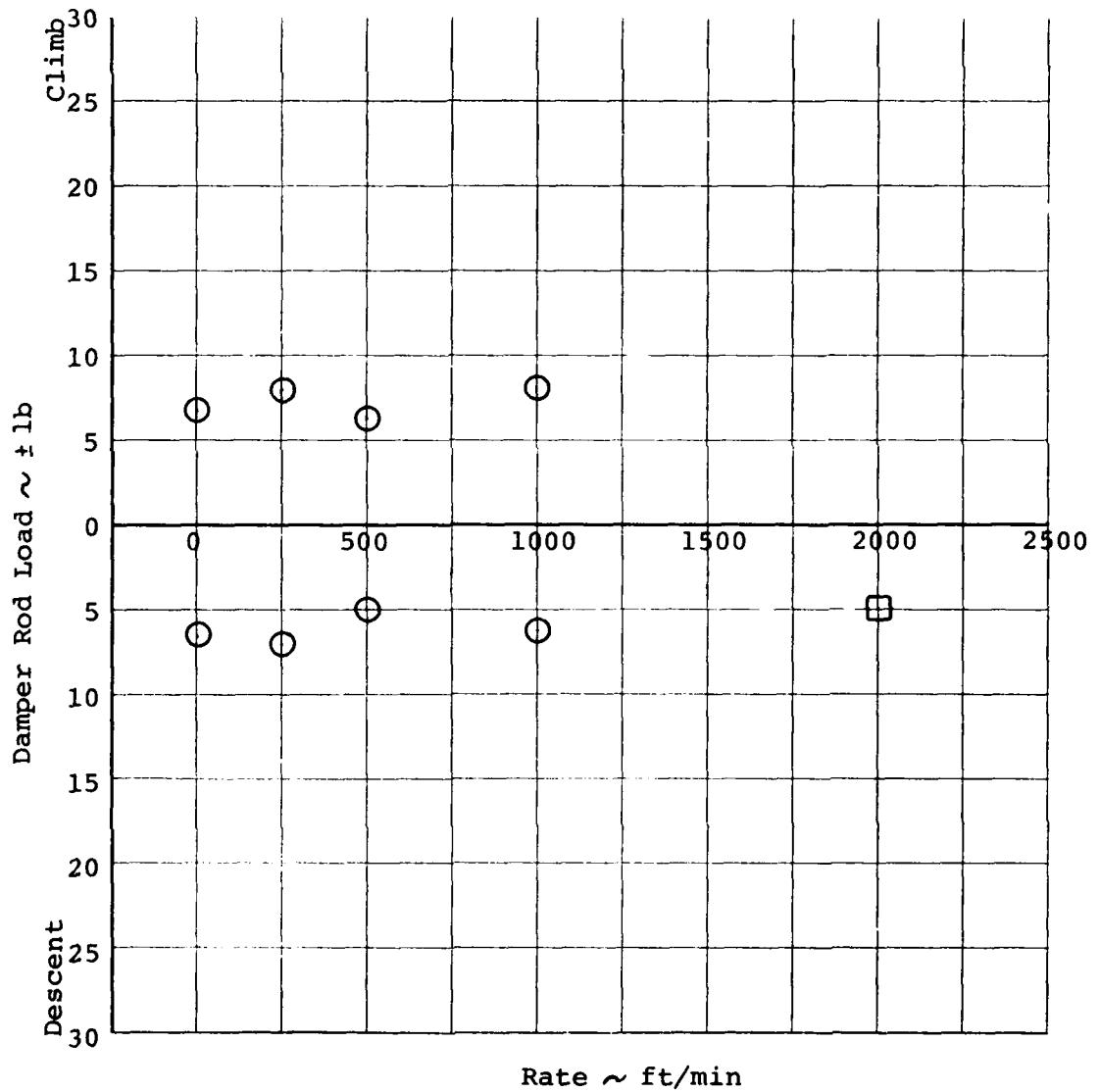


Figure C-5. Damper Rod Load vs. Rate of Climb (Descent).

APPENDIX D

WEAR MEASUREMENTS

Kamatics Wear-Measuring Fixture

Figures D-1 and D-2 are photographs of the Kamatics Wear-Measuring Fixture (KWMF) which was used to measure the actual liner wear and also radial play for the 21 bearings tested in this program. As shown in Figure D-2, each test bearing to be measured was installed in the fixture such that the spherical ball of the bearing was rigidly held in a fixed position by a bushing-bolt stackup. The shank of the rod end to be measured had a spring loading adapter attached by the tension loading rod. The dial indicator measured displacement of the banjo to the nearest 0.0001 inch with respect to the fixed ball. (Note that the dial indicator had a machined adapter threaded onto the stem, and this adapter rested on the banjo in a circular area immediately adjacent to the wear-indicating bushing assembly. This adapter allowed measurements to be taken from a reference surface on the banjo which would not be affected by measuring pin changes or movement of the wear-measuring bushing assembly.)

The subject rod end was loaded to 50 pounds compression by turning the handwheel and moving the loading ring up until the spring had been compressed 0.280 inch (previously determined by calibration in the Tinius Olsen test machine that the spring must be compressed 0.280 inch to develop 50 pounds of load). While the spring remained compressed 0.280 inch, the subject rod end was loaded to 50 pounds tension by attaching the load tray (shown in Figure D-1) to the tension rod and adding deadweight to the tray until the weight of tray and added weights totaled 100 pounds. (By adding only 50 pounds total weight, the rod end could be loaded to zero pounds.)

Readings on the dial indicator were taken at the following conditions:

1. Zero load (compression spring loose and loading tray disconnected).
2. 50 pounds tension (compression spring loose and 50 pounds of weight attached to tension rod).

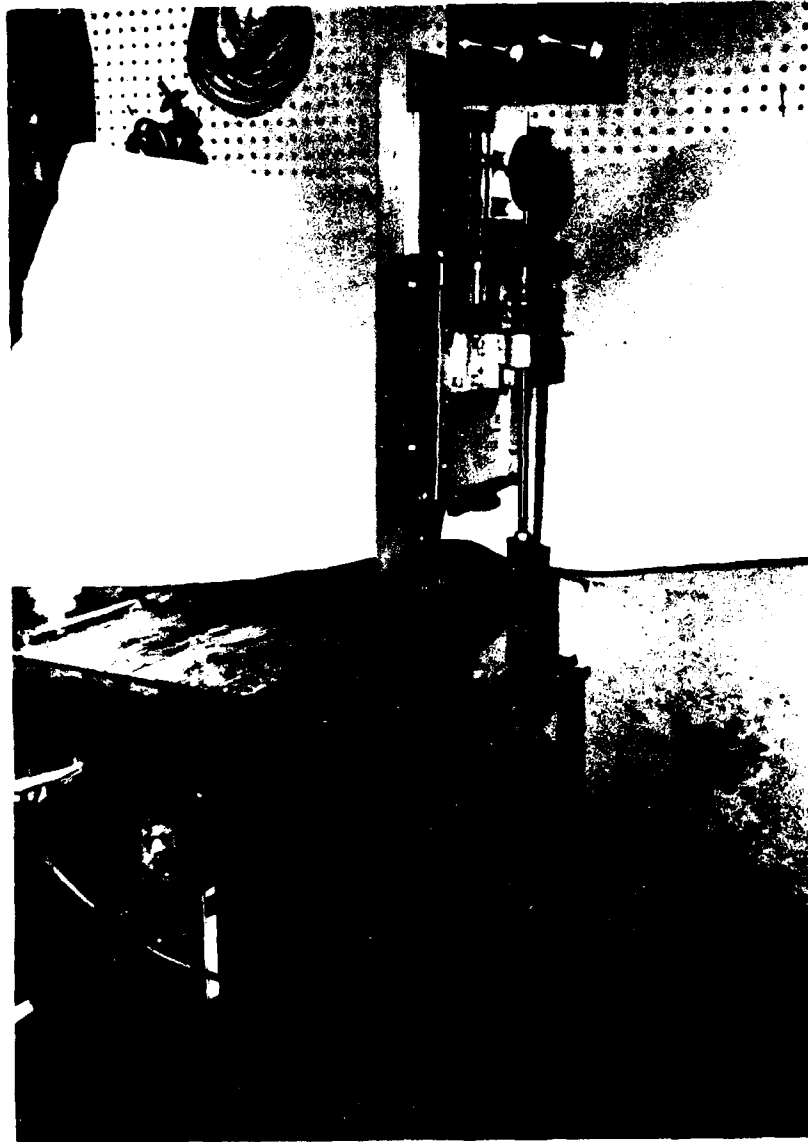


Figure D-1. Kamatics Wear-Measuring Fixture (KWMF).

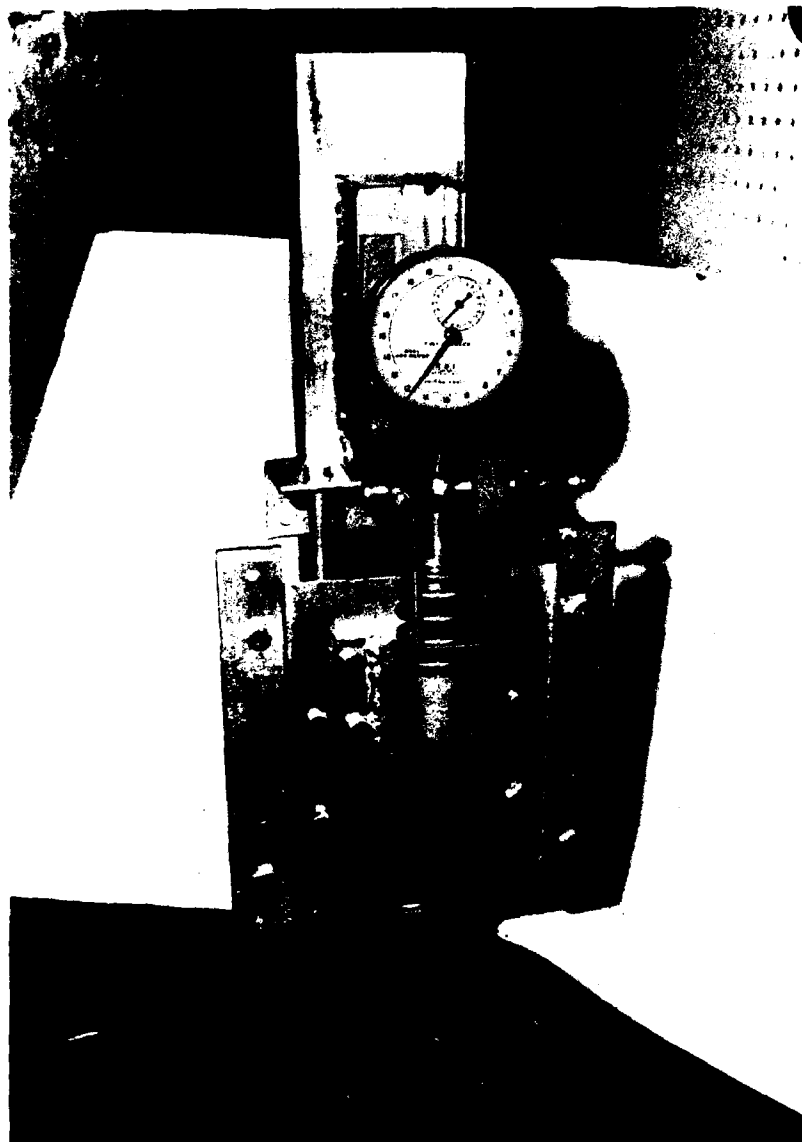


Figure D-2. Close-up of KWMF, Showing Wire Test Specimen Installed for Measurement.

3. 50 pounds compression (compression spring compressed 0.280 inch and loading tray disconnected).
4. Zero load (compression spring compressed 0.280 inch plus 50 pounds of weight attached to tension rod).
5. 50 pounds tension (compression spring compressed 0.280 inch plus 100 pounds of weight attached to tension rod).
6. 50 pounds compression (return to condition 3 for recheck).
7. Zero load (return to condition 1 for recheck).

Either the dial indicator readings from steps 2 and 5 and also from steps 3 and 6 checked within 0.0001 inch, or a rerun of the data was performed.

Dial indicator readings from steps 3 and 6 were used to determine the wear of the liner on the side opposite the wear-indicating pin, and those from steps 2 and 5 were used to determine the liner wear on the indicating pin side of the liner. A summation of the two wear readings was the actual radial play of the bearing.

Standard rod end specimen S2, which had been used for hole drilling experiments and therefore was unsatisfactory for use as a test specimen, was installed in the KWMF eight different times throughout the test program to check measuring consistency. These times were picked to coincide with the following:

1. 8/27/75 - Tare measurement of W13 prior to start of W13 wear testing.
2. 9/6/75 - Tare measurement of W1 prior to start of W1 wear testing.
3. 9/19/75 - Wear measurement of W1 after 100 hours of wear testing.
4. 10/13/75- Wear measurement of W1 after 200 hours of wear testing.
5. 10/27/75- Wear measurement of W1 after 300 hours of wear testing.
6. 11/11/75- Wear measurement of W1 after 400 hours of wear testing (100 hours on W20 and W21).
7. 11/17/75- Wear measurement of W20 and W21 after 148 hours of wear testing.

8. 12/2/75 - Wear Measurement of W20 and W21 after 200 hours of wear testing.

The radial play of bearing S2 measured 0.00180, 0.00170, 0.00160, 0.00160, 0.00165, 0.00155, 0.00185, and 0.00165 inch. respectively, at the eight measuring times mentioned above. Thus, bearing S2, used as a measuring control, showed that the KWMF gave radial play readings which did not vary more than 0.0003 inch.

Wear Test Rig

Radial play measurements from the wear-indicating pin of each test specimen were obtained in the wear test rig while the test bearing was installed in the test rig. This closely simulates the actual condition where the WIRE will be checked for wear by a mechanic while the bearing is installed and in place on the flight vehicle. As shown in Figure C-3, the subject rod end was placed in compression, and depth micrometer readings were taken on the pin and also on the bushing adjacent to the pin (2 readings 180° opposite each other). The depth micrometer rested on the rig bearing pillow blocks which provided a good solid measuring reference surface.

The difference between the average of the two bushing readings and the pin reading was recorded as the radial play of the bearing. Any play or wear in the rig bearings was cancelled by use of this measuring system.

Initially, two loads were used; namely, 50 pounds and 600 pounds. However, the 50-pound load was eventually eliminated because the 50-pound radial play readings were not consistent. It was obvious that the friction in the multiple lever system on the wear rig was causing inconsistent loading of the rod ends.

Each subject rod end was also loaded to 600 pounds tension and the three depth mike readings were taken. The difference between the average of the two bushing readings and the pin reading resulted in a value for each rod end which remained essentially constant throughout the test program.

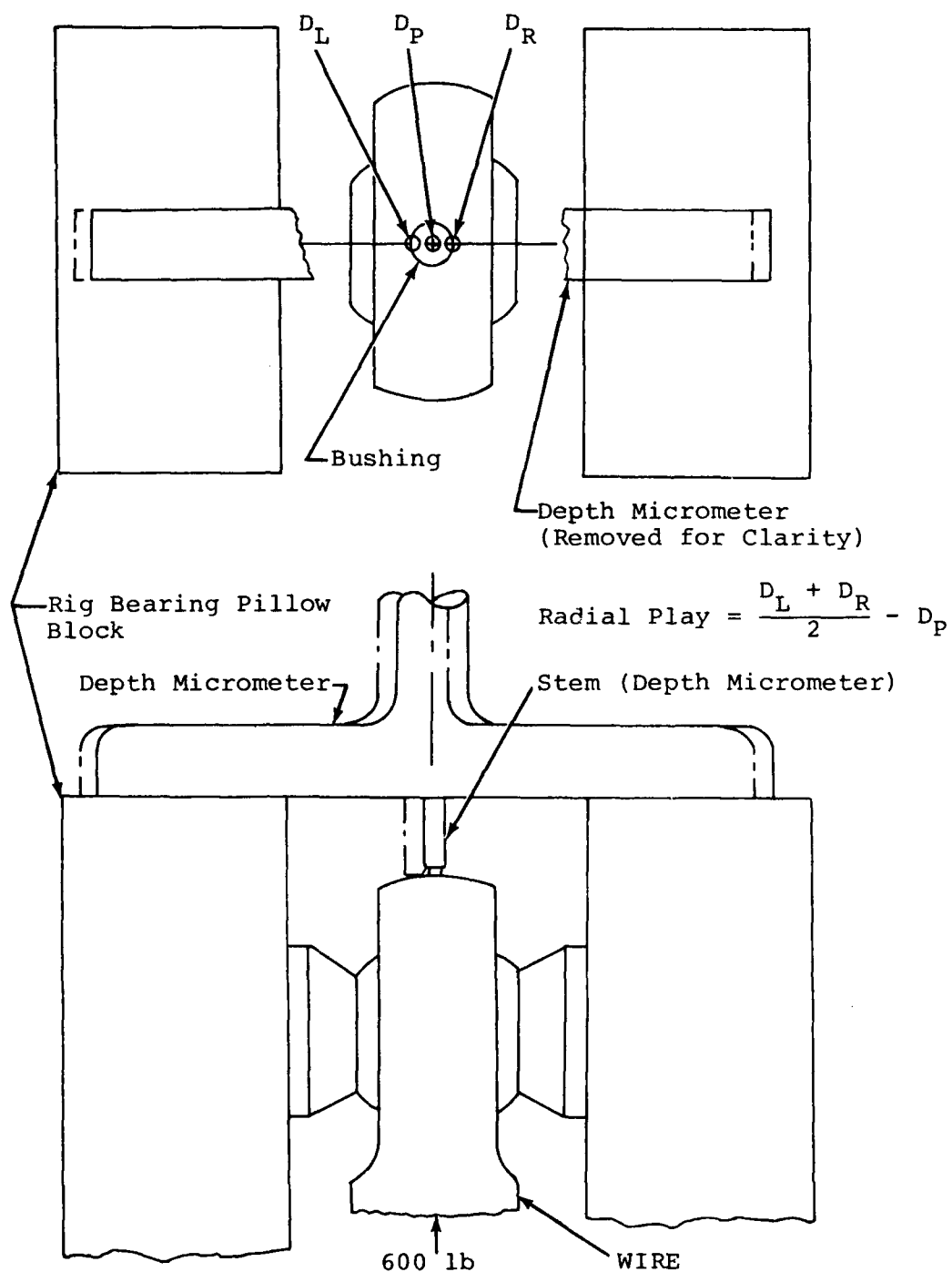


Figure D-3. Depth Micrometer Measuring System.